EXPERIMENTAL STUDY ON THE BEHAVIOR OF A PRESTRESSED NINETEEN PARALLEL WIRE STRAND (PWS) IN SUSPENSION BRIDGES UNDER HYDROCARBON POOL FIRES

by

Kerem Bulut İldan

B.S., Civil Engineering, Yeditepe University, 2014

Submitted to the Institute for Graduate Studies in
Science and Engineering in partial fulfillment of
the requirements for the degree of
Master of Science

Graduate Program in Civil Engineering

Boğaziçi University

2018

EXPERIMENTAL STUDY ON THE BEHAVIOR OF A PRESTRESSED NINETEEN PARALLEL WIRE STRAND (PWS) IN SUSPENSION BRIDGES UNDER HYDROCARBON POOL FIRES

APPROVED BY:

Assoc. Prof. Serdar Selamet (Thesis Supervisor)	.....
Prof. Gülay Altay (Thesis Co-supervisor)	.....
Assist. Prof. Sami And Kılıç	.....
Assoc. Prof. Kutay Orakçal	.....
Prof. Nesrin Yardımcı	.....

DATE OF APPROVAL: 31.05.2018

ACKNOWLEDGEMENTS

I would like to thank my mum and my father. Without their moral and financial support this thesis would not have been possible. Words cannot express the feelings I have for my mum for her constant unconditional support both in my study and my career as well. My father's guidance helped me to stay positive throughout the process. No words can properly express my love and gratitude, I can only say thank you, Mum, Dad and Brother, for everything that you have done for me and continue to do for me. A special thanks to Kazım Dayı, who became a friend of mine and a source of sage advice. Thank you again, for your help during test instrumentation.

My deep appreciation goes out to Vicdan Kaya who has had a huge impact on my life. I do not exaggerate when I writing "on my life". Without her supports I could not afford to pursue my post graduate program and further I could not able to continue my business carrier. I will never ever forget what she did for me.

I would like to thank my thesis advisor Associate Prof. Serdar Selamet for his role in this project. His calm demeanor and constant reassurance kept me grounded and on track during this process. I am very grateful for his guidance in this project and in my professional life. I am grateful to my thesis co-advisor Prof. Gülay Altay and I am extremely grateful for her mentorship. I would like to thank to Prof. Nesrin Yardımcı. As a result of her expertise and guidance, I have a much deeper understanding of engineering approach. Her words and encouragement have provided me with confidence and undoubtedly helped shape my career path.

I owe great thanks to Ahmet Fazıl Kara and Oğuz Şenkardeşler for their help and guidance during the test instrumentation, an experimental testing. Cem Tura and Ömer Aygün were extremely helpful during the design and drawing process of the steel test frame. I also would like to acknowledge İsmail Yalın not only providing me engineering background but also for my professional development when designing and manufacturing the socket holding system.

I would like to thank the department secretary Ayşe Aydın and staff at Lab. Hasan Şenel and Hamdi Ayar all took interest in my research and provided support. Most of all, I would like to express my special thanks to my schoolmates Tülay Ercan, Navid Abediasl, Serap Hanbay, and Saad Mohammad for the academic support, friendship and encouragement they have given me throughout my studies. A separate thanks to Tülay Ercan for her support sharing that helped power my way through graduation process.

And lastly to Nur Güneş, who has been by my side all the way through this MSc, living every single day of it, and without whom, I would not have had the courage to take firm steps forward on this journey.

I've undoubtedly missed some people, and if you're one of them, I apologize.

This study was supported by SPONSORS which are listed below in alphabetic order along with their contribution to the project. Without their technical and sincerely supports this experimental study would not have been possible. I am especially grateful to these people for believing in me and my research project.

(i) GÜNEY ÇELİK (Adana) ⇒ Hamza MENEMENCİOĞLU, Yılmaz YILDIRIM
- Supplied items: High-strength galvanized steel wire (150 kg), Zinc ingot (10kg), Socket materials

(ii) USTAOĞLU ÇELİK (İstanbul) ⇒ Burak USTAOĞLU, Ömer AYGÜN
- Supplied Items: Steel Test Frame steel members (total weight: 1000 kg).
- Supplied Services: Custom manufactoring of test frame including scraping, welding, painting.

(iii) ÖZEN METALURJİ (İstanbul) ⇒ Mustafa BAŞ, Talha Furkan BAŞ
- Supplied Items: Pure copper (250gr), Clay.
- Supplied Services: Zinc alloy preparation and foundry work at Boun Lab.

(iv) DORA METAL (İstanbul) ⇒ Aykut TAŞKIRAN
- Supplied Items: Grade St52.3, 50mm thickness sheet plates (total weight 1250kg) for test frame.

- Supplied Services: Plasma cutting for sheet plate.

(v) ALC MAKİNA (İstanbul) ⇒ Ali ALUÇ, İsmail YALIN

- Supplied Items: Socket holding system material (25kg), Mild steel bar (50kg) for socket locker, all required bolt, nut and washer.
- Supplied Services: Power lathe work, Cnc milling, Machining work for socket material, socket holding system and steel plates (30mm thickness) for test frame.

(vi) ASİL ÇELİK (Bursa) ⇒ Abdi AYDOĞDU

- Supplied Items: Socket raw material.

(vii) PROCHEM (İstanbul) ⇒Levent BERK, Meysun BERK

- Supplied Items: Chemical agents (caustic soda 10kg, flux cleaner 10kg).

(viii) BOĞAZİÇİ KRİSTAL (İstanbul) ⇒Necati HARMAN, Mehmet ATAK, Emrah ŞAMİLOĞLU

- Supplied Services: Wire EDM (electrical discharge machining) cutting for Socket Locker material.

(ix) C.H. ROBINSON (İstanbul) ⇒ Gökalp ERTUĞRUL

- Supplied Services: Transportation of the Steel Test Frame (2500kg) (from Eyüb to Tuzla).

(x) METKO HÜTTENES-ALBERTUS ⇒ Erdem ERDOĞAN

- Supplied Items: Klebepaste SB (30 kg).

(xi) EFES YALITIM (İstanbul) ⇒ Derya AYHAN, Erhan ÇORAP

- Supplied Items: Ceramic fibre blanket density: 128kg/m^3 (three roll).

(xii) EGEBANT (Kocaeli) ⇒ Serdar DEMIREL

- Supplied Items: 3M Scotch Bi-Directional Filament Tape 8959 (two pieces).

(xiii) NORM BAĞLANTI (İstanbul) ⇒ İsmet BAYASLAN

- Supplied Items: Heavy duty pipe clamp (50 pieces).

(xiv) SMY ⇒ Kanber SEZGİN, Savaş SEZGİN

- Supplied Services: Power lathe work, Machining work for socket lockers (3 pieces).

(xv) NURGAZ (İstanbul) ⇒ Hüseyin İLERİ

- Supplied Items: Welding and soldering tools supply for zinc alloy foundry work.

(xvi) SPANZET MAKİNA (İstanbul) ⇒ Hasan ASLI

- Supplied Items: Ratchet strap tie down 1 ton (2 pieces).

ABSTRACT

EXPERIMENTAL STUDY ON THE BEHAVIOR OF A PRESTRESSED NINETEEN PARALLEL WIRE STRAND (PWS) IN SUSPENSION BRIDGES UNDER HYDROCARBON POOL FIRES

Modern suspension bridges are constructed by increasing use of high performance tension members in which parallel wire strand (PWS) type, has been used as a suspender (hanger) cable for long-span suspension bridges. The main cables of a suspension bridge system support the total bridge deck load through these suspender cables. This study focuses on the special effects of open-air hydrocarbon type pool fires which may possibly outcome of a freighter truck crash or sabotage ever since the quantity and flammability of its contents poses one of the worst-case threats to a nearby abovementioned suspender cables. Most of the research on bridge fires is based on the theoretical finite element models whose validity has not been checked experimentally. In this thesis, experimental testing was built to have a full understanding in the behavior with regard to tensile strength and ductility of PWS system which was subjected to in-service stresses and fire loading. Each specimen contains 19 galvanized wires with 1860 Mpa grade of 5.1 mm diameter and 4 meter length in between socket ends. The program includes static loading tests at ambient temperature and transient elevated temperature tests while specimens held at constant load level at 45% of ultimate load capacity. The specimens exposed to UL-1709 standard fire and a realistic gasoline pool fire scenario until the rupture. Thus, for the insulated specimen static test after cooling was conducted. It is shown through these test results that the high-strength bridge wires are very susceptible and critical tension components when exposed to a pool fire load and these results can be used as an actual data for developing relevant design strategies for mitigating fire hazard in suspension bridges.

ÖZET

ASMA KÖPRÜLERDE HİDROKARBON HAVUZ YANGININA MARUZ KALAN ÖNGERİLMELİ ONDOKUZ ADET PARALEL TEL DEMETİNİN (PWS) DAVRANIŞINA DAYALI DENEYSEL ÇALIŞMA

Modern asma köprülerde yüksek performanslı taşıyıcı elemanı olan askı kabloları için paralel tel halat (PWS) sistemi tercih edilmektedir. Asma köprü sisteminde, tabliyelerin toplam yükü bu askı kabloları vasıtası ile ana kabloya aktarılır. Bu tez çalışması, yukarıda bahsi geçen askı kablolarının yakınında tanker kazası veya terör eylemi gibi durumlardan kaynaklanabilecek açık hava hidrokarbon tipi havuz yangınlarının özel etkilerine odaklanmaktadır. Bu durumda oluşabilecek ısı miktarı askı kablolar için olabilecek en ciddi tehditlerden birisidir. Günümüzde asma köprü yangınları üzerindeki araştırmaların çoğu, geçerliliği deneysel olarak kontrol edilmeyen veya edilemeyen teorik sonlu eleman modellerine dayanmaktadır. Bu tez çalışmasında, PWS sisteminin çekme mukavemeti ve süneklik üzerindeki yangının etkisi incelenmiştir. PWS numunesi 5.1 mm çapında 4 metre nominal uzunluğu olan yüksek mukavemetli (1860 Mpa) 19 adet galvanizli tel ile tellerin her iki ucuna sabitlenmiş soketlerden oluşmaktadır. Program, oda sıcaklığında yapılan statik testlerin yanı sıra yüksek yangın testlerini içermektedir. Yangın testi için yalıtımsız numuneler azami yük kapasitesinin 45%'i kadar yükte sabit tutularak UL Standart yangını ve tanker patlaması ile oluşan bir yangın senaryosu teller kopana kadar uygulanmıştır. Ayrıca, yangın izolasyonlu numune için yangın testi sonrasında teller oda sıcaklığına düştükten sonra statik test uygulanmışır. Test sonuçlarına göre havuz yangınına maruz kalan yüksek mukavemetli köprü tellerinin hassas ve kritik çekme elemanları olduğu anlaşılmıştır. Ayrıca asma köprülerde yangın tehlikesini azaltmak için bu araştırma çalışmasında elde edilen veriler ilgili tasarım yöntemlerin geliştirilmesi için kullanılabilir.

TABLE OF CONTENTS

LIST OF FIGURES

LIST OF TABLES

LIST OF SYMBOLS

A_{strand}	Area of one strand
C_r	Chromium
E	Young's modulus
fu, k	Tensile Strength (Minimum)
h_{eff}	Effective part of the strand socket
J	Charpy absorbed energy
P_r	Entire ring tension
Si	Silicon
T	Strand force
t_a	Average thickness of the strand socket
β	Slope of the conical cavity within the socket
ρ	Specific weight
σ	Stress
Φ_{wire}	Diameter of one wire

LIST OF ACRONYMS/ABBREVIATIONS

ASTM	American Society of Testing and Materials
CFD	Computational Fluid Dynamics
FE	Finite Element
FEM	Finite Element Method
FRR	Fire Resistance Rating
PBSFSC	Performance-based Structural Fire Safety Concept
PEEQ	Equivalent Plastic Strain
PPWS	Pre-fabricated Parallel Wire Strand
PWS	Pre-fabricated Wire Strand
CALTRANS	California Department of Transportation
CEN	European Committee for Standardization
FHWA	US Department of Transportation, Federal Highway Administration
NFPA	American National Fire Protection Association
SAIC	Science Applications International Corporation
MUTS	Minimum Ultimate Tensile Strength
TS	Tensile Strength
TC	Thermocouple
S#	# of the specimen

1. INTRODUCTION

This thesis study focuses on the special effects of open-air hydrocarbon pool fires which may possibly outcome of a freighter truck crash or sabotage ever since the quantity and flammability of its contents poses one of the worst-case threats to a nearby a suspender cable on suspension bridge. Therefore, this thesis presents the results of an experimental investigation for the tensile properties of a nineteen (19) parallel wire strand with socket heads at elevated temperature when held at constant stress level. Further, the program also includes static test after cooling.

In this chapter the motivation for research is presented as well as the contribution to state-of-the-art and scope of the project.

1.1. Motivation for Research

The bridges are constructed to serve a variety of drivers and to resist for about 100 years. Thus, bridges are exposed to extreme natural events such as wind storms, fire, and earthquake events all through their service life. Recently, bridge fires turn into a spreading concern for engineering community as a result of fast development of ground transportation and enhanced shipping of hazardous materials such as flammable and spontaneously combustible materials (FHWA, 2012; Garlock *et al.*, 2012). Since most bridges are freely accessible; they are susceptible to vandalism or sabotage that can generally give rise to explosions and fires. As fire is a catastrophic force in nature, flames may threaten structural integrity of a bridge and lead to over-costing of maintenance and repair service, notable delay to marine and road traffic flow and even potential loss of life.

There have been various fire incidents in bridges which have been recorded in the literature (Garlock *et al.*, 2012; Bai *et al.*, 2006; Astaneh *et al.*, 2009; SAIC, 2002). More detailed literature review about recent bridge fire incidents and corresponding research provided in Chapter 2.3 - Fire Hazards in Bridges. Generality of these scenarios

have begun by crash of vehicles, for instance fuel tankers, freight trucks and multiple car collisions either with vehicles or bridge members. In some cases, fires may induce significant deterioration of capacity of structural members, due to loss of strength and stiffness properties of constituent materials, which often lead to partial or full collapse of bridges (Paya *et al.*, 2012; Davis *et al.*, 2008; Guthire *et al.*, 2009). Even in the case of minor fire incidents, where no collapse occurs, proper investigation, inspection and maintenance, in the aftermath of a fire incident, is required before the bridge is opened to traffic. Shutting down a bridge for maintenance would require traffic detouring to nearby routes which can impose significant traffic delays in the affected region. Eventually, this would stress the flow of traffic and affect the commuters' pattern in the surrounding highway networks (CALTRANS, 2012).

Fire hazard in the bridges can be overcome to a certain extent through provisions of appropriate fire resistance to structural members, such as cables, cable anchorages, girders, prestressed concrete beams and decks. Fire resistance is defined as the time duration at which a structural member exhibits adequate performance in terms of integrity, stability and temperature transmission to the unexposed side. In general, fire resistance is achieved via proper design, selection of materials and detailing of the structural members. Unfortunately, at present, there is no standardization or common approach to designing for fire resistance of structural members in suspension bridges, especially for the cables and cable anchorages. This is based on the rationale that bridges are open structures and fire safety measures are not needed in the event of fire. While structural building designs for fire have been codified and are under constant scrutiny and analysis, the literature concerning bridge design standardization for fire is nonexistent. Although bridges are open structures, extreme fire events indeed occur as localized fires if enough flammable materials or hydrocarbon fuels are present. These incidents result in fire plumes where a building fire is usually considered as a confined compartment fire (Gross and Cauffman, 2011).

Moreover, the fire conditions for bridge systems vary greatly from those of building structures. This has been associated to the fact that collisions occur at high velocities because burning of petrol based fuels, which have comparably low flash points, in

an open environment. Hence, bridge fires may reach remarkably high temperatures (in the range of 800-900^{o}C) within the first several minutes of fire initiation and increasing to 1000^{o}C or more in the first thirty minutes (Shutt, 2008; Stoddard, 2004)- all while releasing a greater amount of heat energy. Such fires are categorized as hydrocarbon fire in fire engineering research field. Figure 1.1 shows that the hydrocarbon curve experiences a more rapid rise to a higher maximum temperature by comparison with the E119 curve for building fires. The severity of such vehicular fires may produce high thermally induced forces in the critical components of structural elements and cause reductions in material properties, and, in some cases, over-costing losses such as loss of a wiring in cables of suspension bridges.

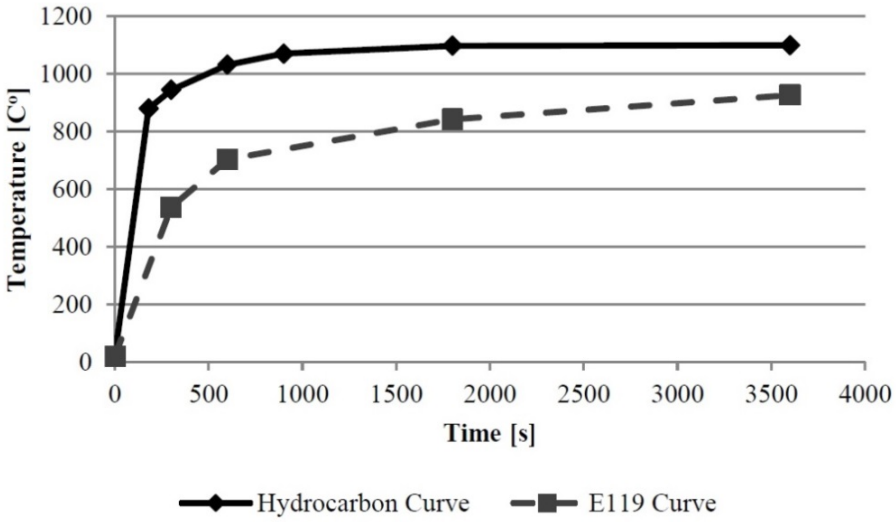

Figure 1.1. Standard fire curve.

The proper heat transfer conditions when modeling the bridge fire have been intensively investigated by bridge engineering community. The complex nature of fires adds more challenges and complexities. Accordingly, in order to find a solution and an understanding from which engineers may work in addressing the complexities of a problem, fundamental closed-form solutions are essential. Unfortunately, in range of the bridge engineering world aforesaid closed-form solutions for modeling the temperature distributions and the heat transfer in particular structural components are also missing.

The most critical of such components in the most critical bridge system that may exist in a particular region is the main cable of a suspension bridge. However, *when it comes to fire exposure risk on suspension bridges, the most critical members are arguably suspender cables and the anchorages of these cables.* Inasmuch as, these aforementioned suspender system connects the bridge deck to the main cable and a vehicle fire on the bridge deck poses a significant threat to the integrity of the suspender cables and its anchorages. Briefly, the vehicles (potential risks) passing close to suspender system including the socket material are more vulnerable structural elements of a suspension bridge when compared with main cables, as shown in Figure 1.2 (Photograph by the author from 3^{rd} Bosphorus Bridge, 2015).

Figure 1.2. Passing through a vehicle nearby the suspender cable.

The long spans are only made possible by the presence and function of the main cable and suspenders. These cables are (typically) non-redundant structural elements that serve to carry the dead and live loads from the bridge deck and live loads on it, respectively. More detailed information about suspension bridge concept provided in Chapter 2.1. According to literature review in Chapter 2.2 - Fire Hazards in Bridges,

the failure of these cables would undeniably mean the failure of the bridge structure leading to significant economic effects and even potential loss of life. Unfortunately, in similar fashion to other areas of bridge engineering, a generally accepted practice for modeling fires and their energy transfer to these cables does not exist.

The suspender cables and main cables of suspension bridges represent the structures load-bearing element. In recent years, they are typically composed of tens of thousands of parallel high-strength galvanized steel wires. Most generally, a wire with a diameter 5-5.5 mm is used in the main cables whereas wires with a diameter 7 mm are used for parallel wire strands in suspender cables. These cables are terminated with steel sockets, as said cable anchorages and connections, which transfer the tensile force from end-to-end structural components, as shown in Figure 1.3 (Photographs by the author from 3^{rd} Bosphorus Bridge, 2015). The socket contains an inner cone, which receives the end of the strand. The cavity between wires and cone is filled either with a hot casting material such as zinc alloy or more newly with a cold casting material which is resin socketing system. When applying the axial load, the wires and casting material drawn into the interior conical recess in the socket. Subsequently, axial load is transmitted between strand and socket by a wedging action, Figure 1.3 illustrates the socket and nut from inside the deck. More detailed information about cable anchorage and connection concept provided in Chapter 2.1.3.

Figure 1.3. Typical suspender system components; main cable, cable band, suspender cable (left-hand side), End Anchor of cable; socket and nut (right-hand side).

Aforementioned components of the suspension bridge are under constant attack by environmental factors-such as rain, wind, intense heat, UV radiation, etc.-that, over time, lead to the initiation and progression of corrosion. As is known, corrosion can lead to any number of issues affecting the wires strength and ductility including cracking, corrosion pitting, section loss, embrittlement, and in-service wire breaks (Betti *et al.*, 1998, West *et al.*, 2005). As such, the life expectancy and structural integrity of the suspension bridge is highly dependent on the condition of these components (Shi *et al.*, 2007). Unfortunately, due to aging and the aforementioned corrosion issues, (Main and Luecke, 2010) and Haight *et al.*, 1997) found that three of four major suspension bridges analyzed had lost approximately 30% of their original cable strength. They found that factors of safety for the cables which once ranged between 2.7 and 4.5 are now in the range of 2.0 to 3.0 (Main and Luecke, 2010).

Besides of the cold-drawn wires above-mentioned unpleasant condition, the socketing materials (including both hot and cold casting medium) critical temperatures for socket material is also considerably low. Isabel and Roger (2012) reported that the estimated failure manner at high temperatures is "socket draw" where the socketing media in the socket creeps in an intolerable way, allowing relative movement between strand and socket. At the limit, the strand pulls entirely through the socket.

It is quite obvious from the aforementioned fire events, the reduction of the safety factors of cables and the poor performance of the strand sockets at elevated temperature that if positioned properly fire poses a significant risk to the integrity of the suspender cables and the socket material therefore the entire structure itself. Despite the severity of the threat of and the shocking numbers associated with fires on bridge infrastructure, fire safety and design for bridges remains an under-studied and under-codified area of bridge engineering. As cited in Garlock *et al.* (2012), the NFPA 502: Standard for Road Tunnels, Bridges, and Other Limited Access Highways acknowledges the threat of fire, but states rather generally that bridges or elevated highways "shall be protected" from "high-temperature" exposure (NFPA, 2008) - with no guidance on how such protection should be provided. Furthermore, the European standard for traffic loads on bridges (CEN, 2003) fails to address the handling of fire loads in any of its provisions Garlock

et al. (2012). As such, recent years have seen an increase in the amount of attention paid to the issue of bridge fires with researchers studying their effects on a variety of bridges and specific structural components. For instance, Mendes *et al.*, (2000) studied the effects of a ship fire on the girders of a cable-stayed bridge (Vasco da Gama bridge) while Bennetts and Moinuddin (2009) considered the effects of fire on the actual tendons of a cable-stayed bridge, and, in line with the structural component of interest in this work, Main and Luecke (2010) analyzed both low- and high-temperature effects on the main cables of suspension bridges. Gross and Cauffman (2011) suggest treating fire as a design load to ensure that bridges are able to survive these kind of fire events and conclude that experiments must be conducted to verify bridge fire response in order to implement performance based design.

Although the motivation of analyzing the fire resistance of bridge components exists in all, each of these studies has taken drastically different approaches to modeling and defining the fire hazard on their respective bridges of interest. As such, it is important to provide reliable data from experimental finding in order to check compatibility and to improve fire modeling techniques and to provide valuable data for future researchers.

In brief, the properties of cold-drawn steel and socketing materials are more susceptible to elevated temperature and degrade at an earlier rate when compared to hot-rolled mild steel. More detailed information about micro-structure and chemical composition of high-strength wire and socketing materials provided in Chapter 2.1.1. Therefore, the mechanical properties of PWS system including high-strength parallel wire strand and socketing material at high temperatures and after cooling performance must be experimentally examined in order to guide the fire resistance design and post-fire evaluation of residual load carrying capacity of PWS cables and the socket material for suspension bridges.

1.2. Contribution to State-of-the-Art

The bridge design and analysis world lacks the guidance of standardized codes for considering fire scenarios. Although such standardization is absent, a number of researchers have applied state-of-the-art fire modeling techniques in an attempt to accurately depict the scenarios of interest in their particular problems. Motivated by actual bridge fire incidents, these researchers which mentioned in Chapter 2.2.2 brought modeling standards from the fire engineering community into their bridge analyses, thereby providing a roadmap for the efforts of future researchers. Furthermore, such a lack of standardization has forced these researchers to base their studies of temperature distributions and mechanical responses within structural components on finite element models with backing from neither experimental findings nor fundamental analytical solutions.

From another view, the author claims that even if no collapse in case of a suspension bridge fire, engineers are often uncertain in how to evaluate fire-induced damage due to a lack of experimental findings on bridge structural members such as suspender cables. Previous experimental fire research has focused on buildings but bridges are very different to buildings as their structural members usually sustain bigger loads, larger span lengths, and have different boundary conditions and cross sections. These specific features make advisable the development in parallel of both experimental and theoretical studies (Garlock *et al.*, 2012).

One of main focus of the thesis is the high-strength galvanized PWS system, which is commonly used for main cables and recently used in suspender cables of modern suspension bridge applications and the anchoring component of the suspender cables which is called socket material. This thesis presents a detailed review of the state-of-the-art on fire hazard in bridges, based on literature review. Thus, bringing a database to the bridge community with reliable data for the mechanical and tensile properties of parallel wire strands (PWS) and socket material at high temperatures and after cooling.

The objective of this research to experimentally evaluate the effects of a nineteen PWS and socket systems under elevated temperatures caused by a truck/vehicle related fire. The experimental setup will evaluate the overall behavior of PWS system and measure the extension-temperature history of the collection of strands. The steel material properties at elevated temperatures will be evaluated for an individual strand for the future supplemental numerical analyses. The numerical analyses will be validated by these experiments. The testing objectives are as follows:

(i) Determine the mechanical properties of the high-strength for a nineteen parallel wire strand including:
- Tensile properties at ambient and elevated temperature,
- The reduction in ultimate strength at elevated temperature,
- The rupture temperature of steel strand or socket draw when held at a constant load level,

(ii) Identify the critical temperatures below which socket draw does not affect the integrity of the connection in the case of hydrocarbon pool fire.

(iii) Investigate the relationship between extension, temperature, and time at the given temperature load from hydrocarbon standard fire (UL-1709) and realistic pool fire scenario.

1.3. Scope of the Research

The remainder of the thesis is divided into six chapters. Chapter 2 is focused on the background of the structural components of suspension bridge along with the mechanical properties of cold-drawn wires which forms PWS system at and after elevated temperature. Chapter 3 outlines the testing program and the experimental setup and test procedures. Chapter 4 presents the observations of the testing program. Chapter 5 provides an evaluation of the test results. Chapter 6 summarizes the results of the thesis, and also provides conclusions and recommendations for future research on this topic.

2. BACKGROUND

In this chapter, the background of this research topic is presented. Firstly, an extensive literature review for major structural elements of suspender system in suspension bridge included, then a detailed literature review of the state-of-the-art on fire hazard in bridges investigated, lastly the studies previously completed on the mechanical properties of high-strength steel wires and socket material at elevated temperatures based on the literature review included.

2.1. Major Structural Elements of Suspender System in Suspension Bridges

The suspension system includes a parabolic main cable and a vertical suspender cable connecting the deck to the main cable. The suspension system is in tension and requires considerable anchorage at both ends. The cables are fracture critical and load path non-redundant. Figure 2.1 shows plan view of a typical suspension bridge. The most common suspension bridge system has three spans: a large main span surrounded by shorter side spans.

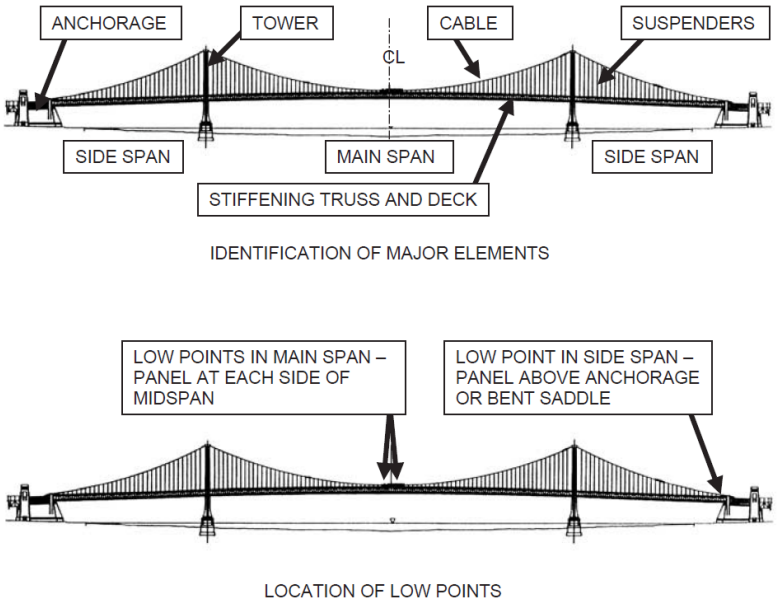

Figure 2.1. Typical suspension bridge.

The parts of the cable system other than the cable itself, such as the anchorages of the suspenders to the cable, affect the performance of the wires. They are discussed below in relation to the bridge component they are part of. Therefore, the major structural elements are identified along with the low points of the cable, which are significant for understanding suspension bridge concept and the evaluation of the test results which are referred to in Chapter 5.

In this chapter, only major structural elements of suspender system are examined. Thus, the main focus of this study is that PWS hanger cables, on which research reports have rarely been written up to now and its socketing system for both main cables and suspenders for long-span suspension bridges.

2.1.1. High-strength Galvanized Steel Wires for Bridge Cables

Figure 2.2 shows the timeline of the maximum tensile strength of zinc-coated (galvanized) cable wire and the maximum center span of suspension bridges in the world. A significant increase in wire strength made it possible for the Akashi Kaikyo Bridge to become the world's longest suspension bridge in 1998. Compared with the Humber Bridge, the longest bridge before that time, an increase of about 200 N/mm2 wire strength enabled a roughly 600 m span increase in the Akashi Kaikyo Bridge.

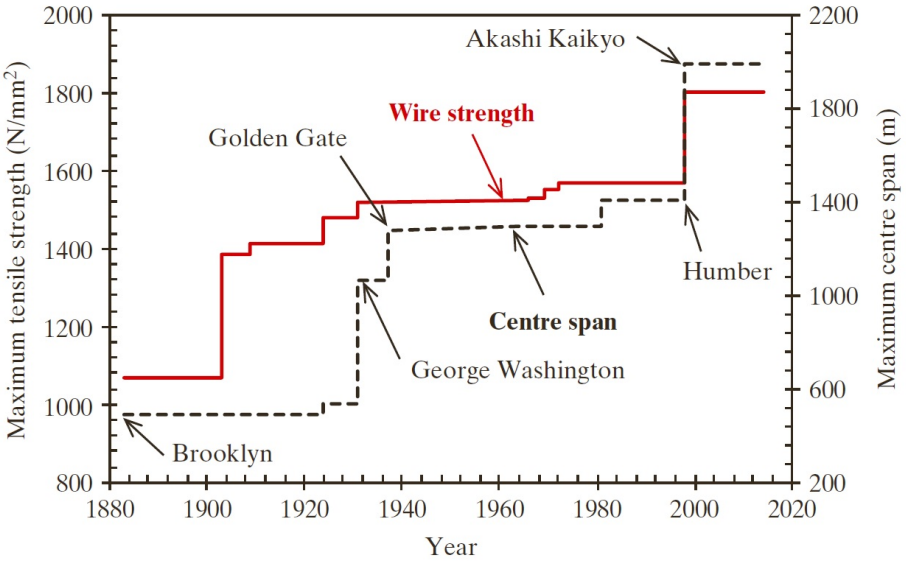

Figure 2.2. Timeline of wire strength and center span (Hirakida *et al.*, 2008).

The necessity of expanding for the center span length obviously increases the needed main cable diameter. The diameter upper limit of the main cable is considered to be around 1.1 to 1.2 m from the perspective of ease of construction and quality. The strengthening of a bridge wire and an enhancing in allowable bearing force are well-known to be effective for fixing up this cable diameter constraint.

2.1.1.1. An Overview of Strengthening Steel Wires. Steel is an alloy which consists of iron and carbon (carbon being between 0.002% and 2.1% of the total weight) and high strength can be achieved for wires by transforming the microstructure to a pearlite lamellar structure with an approximately 0.8% carbon content as shown in Figure 2.3. Exceeding 0.8% carbon content results in a structure that is hard but brittle and tends to fracture under cold-drawing. In pearlite state, the steel has a laminar microstructure with alternative soft and hard layered phases. The interval between the layers is called lamellar spacing.

The key to allowing high strength and ductility for pearlitic steel is to form a clear lamellar structure (as shown in Figure 2.4) and reduce the layer spacing through the use of both heat treatment (patenting) and cold working (cold-drawing). The patenting process involves heating or austenitizing (as shown in Figure 2.3) a wire rod and subsequently rapidly quenching into a lead or salt bath held at 500-600^{o}C (Tarui, *et al.*, 2002). Cold-drawn process is characteristically drawing the high carbon wire rod through a die or a continuous series of dies at temperatures beneath the recrystallization temperature. Therefore, the cold-drawn process is reducing the steel rods diameter, in other words, it's a metal-reducing process. The process of cold-working is clarified by Callister and Rethwisch (2008) as an escalation in the dislocation density which in turn increases the stress required deforming the metal.

Thus, the phenomenon of lamella collapse occurred due to the heat effect during the zinc-coating (galvanizing) process at around 450°C. This had been a serious obstacle to increasing wire strength for a long period of time. Adding Si and Cr to the steel helps maintain the lamella structure, which was discovered through extensive research

activities and eventually led to an approximate 200 Mpa increase in its tensile strength, which had been unachievable until then (Takahashi *et al.*, 1994). Also, through the observations of the microstructure at an atomic level, it is now well understood that Si and Cr have an inhibitory effect on carbon diffusion from the cementite layered phase (hard carbide phase shown in black in Figure 2.4). This wire with a clearly layered microstructure may be regarded as a naturally formed composite material.

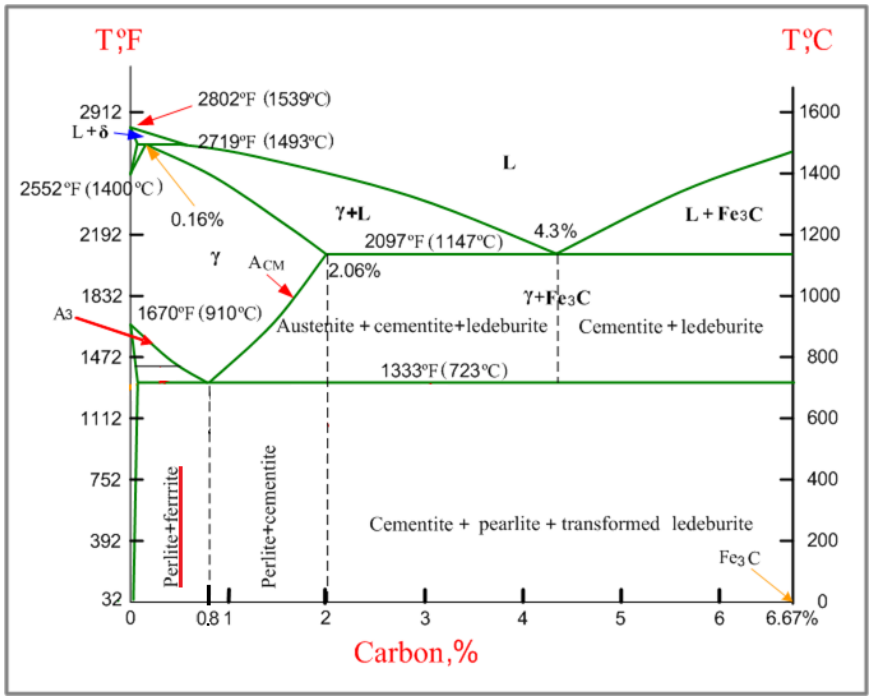

Figure 2.3. Iron-carbon phase diagram.

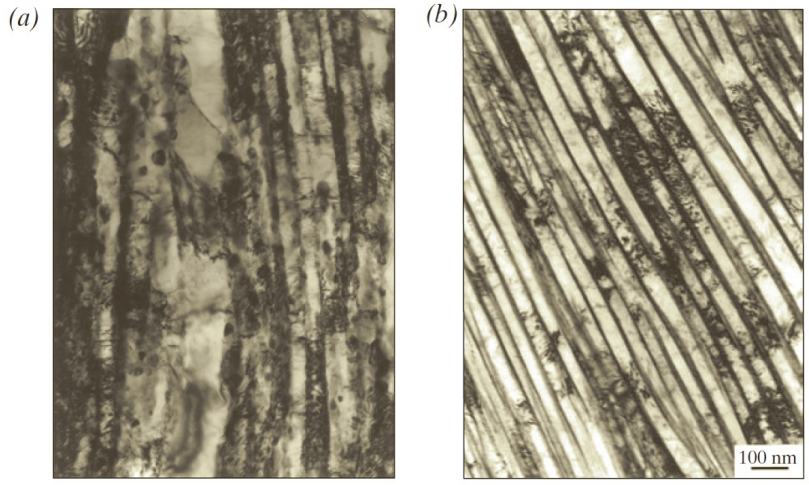

Figure 2.4. Differences in layer configuration (Tarui *et al.*, 1994); (a) Traditional wire (b) Si and Cr added wire.

2.1.1.2. Chemical Composition of High-strength Wires. The following table lists including the elements in cable wire and their approximate weight by percent. Note that accordingly AISI Classifications, approximately 0.8-2.0% and 0.3-0.8% carbon content considered as high-carbon steel and medium-carbon steel, respectively.

Table 2.1. Elements in wire and approximate weight by percent.

Element	**Weight by Percent**	
	Minimum	**Maximum**
Carbon	0.65	0.84
Sulfur		0.04
Phosphorus		0.04
Manganese		0.8
Silicon		0.15
Nickel		0.12
Chromium		0.1

2.1.2. Parallel Wire Strand (PWS) Cables

The PWS cables has a great tensile strength and maintenance convenience compared with the other cable types. Nevertheless, the advantages of using strands with parallel wires had been known for a long time, the problems related to the reeling process excluded the introduction of these strands in actual construction for many years. The reeling obstacle is related with the detail that the curving of a PWS with undistorted cross sections would cause an elongation of the wires at the outside and a contraction of the wires at the inside of the curve. With reels of realistic dimensions, the required strains in the wires would result in intolerable stresses.

In the 1960s, real tests on the reeling options were uncovered in the USA, and it was concluded that the PWS, through a local distortion of the wires inside the bundles, could actually be reeled and unreeled without generating intolerable permanent distortions. From a description of the trial test with a 37-wire strand, the author claimed that the strand was found to continue considerably its original shape while being unreeled and reeled. After static tests showed that repeated reeling did not affect the

mechanical or physical properties of the strand (Durkee, 1966). Thereafter, the tests with 61-, 91- and 127-wire strands were conducted.

2.1.2.1. PPWS Cables for Main Cables. Main cables of suspension bridges are the most vital components in these superstructures. Such cables consist of many thousands of pre-fabricated parallel high-strength steel wires, and the typical diameter of a bridge wire is about 5 mm. The main cable size is adapted over the towers to follow the angle changes and the difference in stresses between the side span and the main span. The main cables are supported by saddles at tower top and anchored in anchorage blocks located in both ends of bridge.

Parallel wire cables are categorized by the construction methods, such as the air-spinning (AS) method and pre-fabricated parallel wire strand (PPWS) method. The core of the cable consists of closely-packed galvanized steel wire strands as shown in Figure 2.5. Inner strands usually have hexagonal cross-sections to optimize the compaction operation. The cross-sections of the strands adjoining the periphery are adjusted so as to give the entire cable core a circular cross-section after compaction.

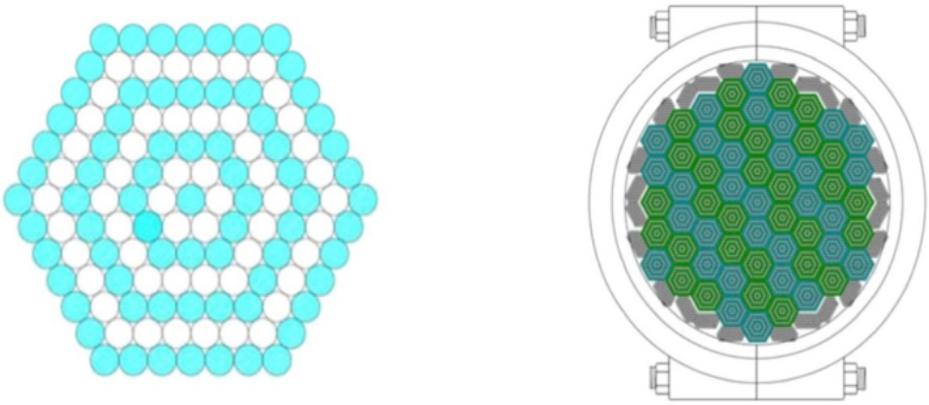

Figure 2.5. Detail view of a single 127-wire strand (left-hand side), the outline of a Cable Band (right-hand side).

For PPWS, each hexagonal strand is composed of 127 wires as presented in below Figure 2.6 and Figure 2.7. Suspension bridge cables are loaded in tension; they transfer the entire weight of the bridge deck and any traffic that might be on it, more than

several hundred thousand tons, to the suspension towers, and to anchor points at each end of the bridge.

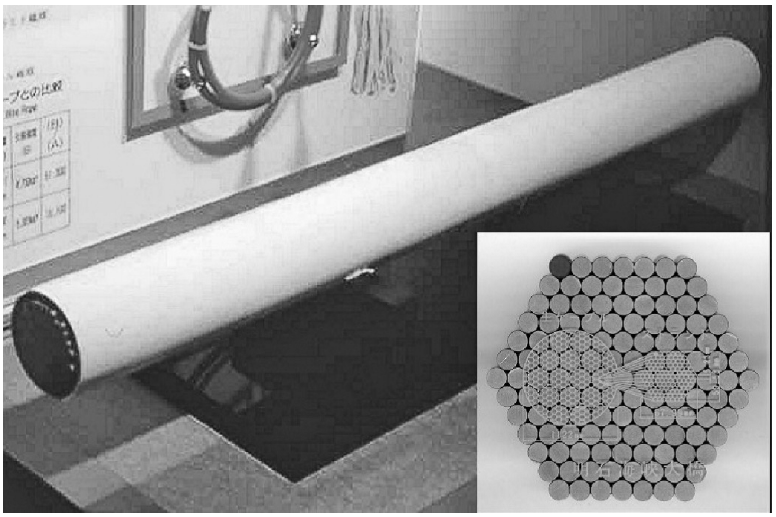

Figure 2.6. PPWS cable of 127 wires, used in the Akashi Kaikyo cables.

The core is wrapped by a continuous, pre-tensioned wire layer, and it is radially clamped at regular intervals along its entire length to ensure geometrical integrity and tightness, and to enhance strain transfer to any broken wires.

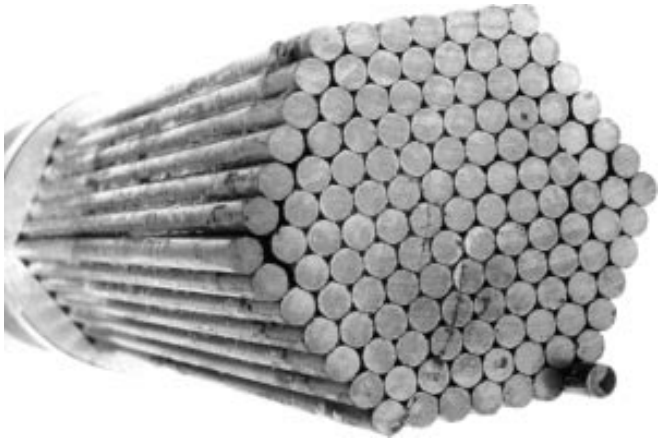

Figure 2.7. PPWS with #127 of 5 mm wires (Bisan Seto Bridges).

The parallel wire cables were used for the Brooklyn Bridge for the first time (completed in 1883) and are used for most modern suspension bridges. A mid-sized bridge cable, such as the one used in the Manhattan Bridge in New York, can be about 50 cm in diameter, with about 8.500-9.000 wires while larger cables, approximately

0.75 m to 1 m in diameter (e.g. the 3^{rd} Bosphorus Bridge, Verrazano Narrows Bridge and the George Washington Bridge), contain about 14.000-28.000 wires. For instance, 3^{rd} Bosphorus Bridge cable properties as shown in below Table 2.2.

Table 2.2. Cable Properties of 3^{rd} Bosphorus Bridge.

Division		**Unit**	**Main Cable (PPWS)**	**Stiffening Cables (PSS)**	**Hanger Cable (PWS)**
Material Properties	Young's modulus (E)	MPa	205.000	195.000	195.000
	Specific weight (ρ)	kg/m^3	7.998	9.100	9.500
	Tensile Strength (Minimum) ($f_{u,k}$)	MPa	1.860	1.960	1.770
	Diameter of one wire (Φ_{wire})	mm	5.4	15.7	-
Section Properties	Area of one strand (A_{strand})	mm^2	2.905	150	-

2.1.2.2. PWS for Suspender Cables (Hanger cables). The main cables of a suspension bridge system support the total bridge deck load through suspender cables. The suspenders are attached to the main cable at clamshell clamps, which are also termed cable bands as shown in Figure 2.8.

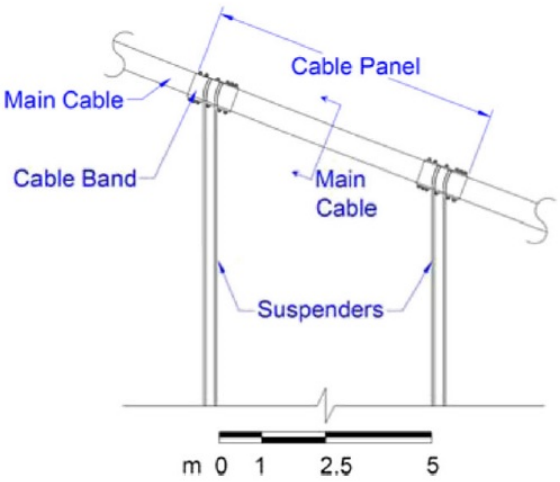

Figure 2.8. Schematic elevation view of a suspension bridge with major structural elements highlighted.

An alternative suspender cable of the parallel-wire strand cable with straight wires was proposed in the 1990s under the name “New PWS Cable” as presented in Figure 2.9. In PWS suspender cable, the wire bundle is a little twisted with a long way to ease reeling and unreeling and force the strand self-compacting when exposed to an axial tension. The PWS cables are also characterized by having the protecting polyethylene cover which is usually used in long span cable stayed bridges extruded directly onto the wire bundle and therefore no void will occur between the wires and the surrounding pipe. With the elimination of the spiral rope and the voids for cement grouting the PWS Cable is more compact than traditional PWS cables or the center fit rope core (CFRC).

It is also known that the HDPE sheath (as shown in Figure 2.9) used to prevent from external factors such as humidity, rain, intense heat and UV radiation ignites at 330°C. When the sheath starts to burn, there is an impulsive rise in cable temperature (PTI, 2012).

Suspenders are expected to last between 35 and 65 years. PWS cable suspenders cannot be bent over the cable like rope suspenders, they require a socket. They are stronger and thus lighter than rope suspenders. PWS are socketed and pin connected, under the cable bands.

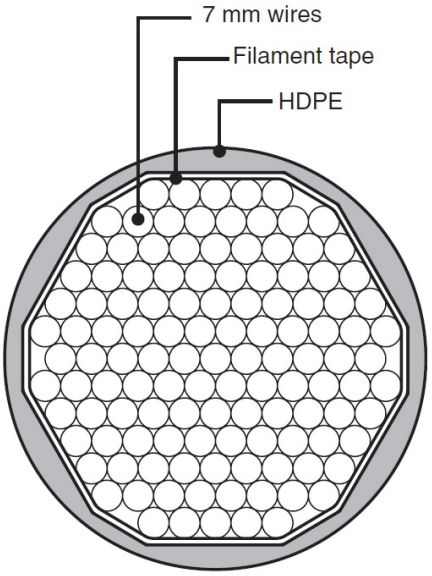

Figure 2.9. Modern PWS cable.

2.1.3. Cable Anchorage and Connection (Socket Material)

In suspension bridges, the components of the cable system are attached to the deck and when connecting the superstructure and the substructure superior details have to be worked out. Concurrently, these details are particularly vital, as the cables constitute the main load-carrying components of the suspension system.

When it comes to the anchoring of pre-fabricated strands, the conventional way is by socketing the ends of the strands. A socket for a PWS is simply made of a steel cylinder with a conical cavity as illustrated in Figure 2.10 and then the broomed end of the strand is inserted. Afterwards the conical cavity is filled with a metallic alloy having a comparatively low melting point. Once the PWS cable is exposed to tension, a wedge action will arise. Thereafter, a tri-axial state of stress in the cone that within the socket will successfully support the force transmission from the wires.

This socket is generally used as a dead-end anchor where jacking equipment cannot be easily connected; it is called as the simple bearing socket. In addition to the simple bearing socket, other more sophisticated socket systems are also found. Nevertheless, the simple bearing socket is selected for the experimental study and therefore only the simple bearing socket is described in this chapter of the thesis.

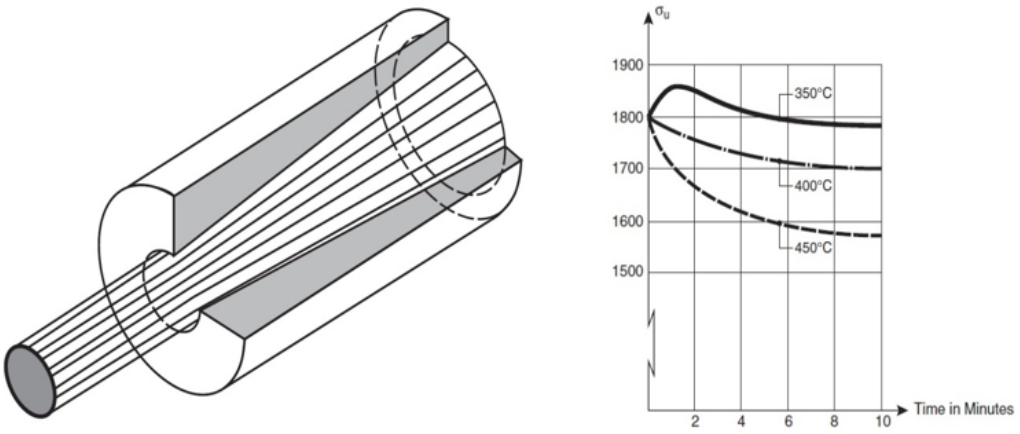

Figure 2.10. A typical simple socket for a strand (left-hand side), influence of pouring temperature on the ultimate strength of wires (right-hand side).

In point of fact that the high strength mechanical properties of the wire is reached throughout the cold-drawing method as it mentioned in Chapter 2.3 below. In this regard, a strength decrease might occur on condition that the metallic alloy needs an elevated pouring temperature. This situation is shown in Figure 2.10 which indicates the outcome of breaking tests with cold-drawn wires exposed to pouring temperatures of 350^{o}C, 400^{o}C, and 450^{o}C at varying time intervals.

It look as if the decrease in strength will be upwards of 10% if a pouring temperature of 450°C is continued for farther than four minutes. The pouring metal is made of alloys containing zinc, lead, copper or aluminum. It is likely to preserve below the pouring temperature of 350^{o}C with lead alloys. Nevertheless, in the cause of disadvantageous creep properties and severe health consequences, these alloys have been disallowed recently. As an alternative, non-ferrous metals (alloys based) mainly on zinc are preferred, needing a pouring temperature of 400-450^{o}C. A great resistance against creep appears to be succeeded by a Zn-Cu alloy with 2% Cu on weight percentages (BS EN 1774:1998).

When it comes to cold-drawn wires the strength drop explained above is not as much of importance as the wires have previously been exposed to high temperatures throughout the galvanizing process.

The inside of the socket material might be filled with a hot casting material (for instance the metallic alloys categorized above). However, in order to increase the fatigue resistance of the anchorage it was chosen to use a cold casting material consist of epoxy resin, zinc dust, and small hardened steel balls (diameter 1-2 mm) (Andra, and Zellner, 1969). In order to anchor PWS more advanced socket, as presented in Figure 2.11 (left-hand side) was successful developed by F. Leonhartin 1968-1970, when Mannheim Bridge was built. In this system, the wires are put through holes in a locking plate at the termination of the socket. The wires arranged with button heads in order to upgrade the resistance in opposition to the slipping of individual wires.

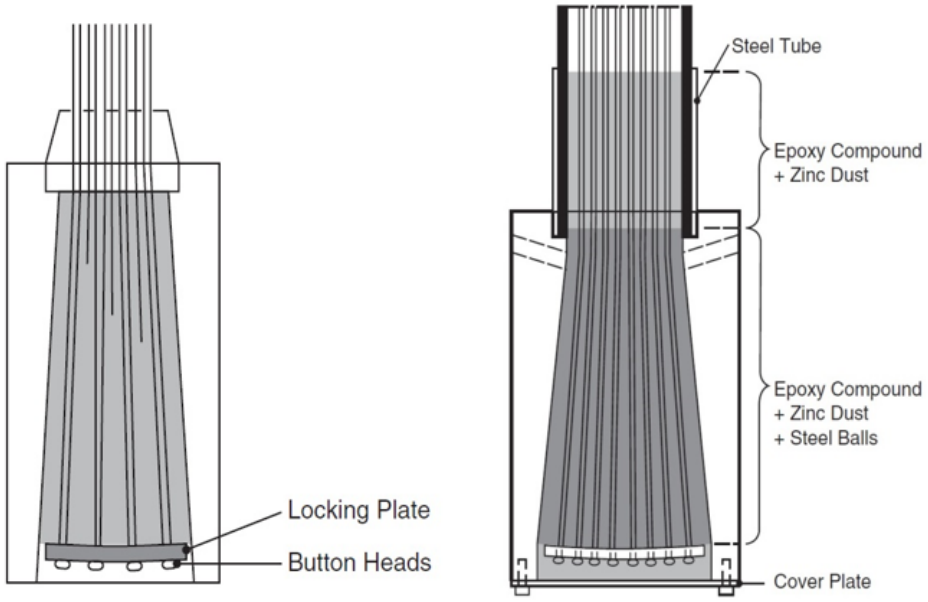

Figure 2.11. A socket for parallel wire strand (left-hand side), HiAm socket for PWS (right-hand side).

Figure 2.11 illustrates a classic socket based on the usage of a cold casting material. To specify the developed fatigue resistance of this socket it was known as a "HiAm" socket, where HiAm imply high amplitude. It began to widely use the cold casting anchorage for hanger or suspender cables. Until now all wire hangers of cold casting anchorage adopt the epoxy-base resin and steel shot as cold casting padding. There are typically two kind of cold casting preferred for Resign Socketing System as following:

(i) Polyester base binder: Polyester has styles of saturation and unsaturation polyester. The shortage of polyester base binderies greater shrinkage rate, lower glue tenacity, worse chemical resistance and waterproof.

(ii) Epoxy-base adhesive: Epoxy-base adhesive is composed of epoxy resin, curing agent, increased toughness agent, epoxy resin solidified has good physical and chemical property.

Table 2.3. Comparison of performance between Epoxy Resin and Unsaturation Polyester Resin.

Item/performance	**Epoxy Resin**	**Unsaturation Polyester Resign**
Tensile Strength (Mpa)	65∼80	50∼70
Elasticity Modulus (Mpa)	100∼150	90∼100
Elongation (%)	2∼5	1.5
Shear Strength (Mpa)	30∼50	10∼20
Distortion Temperature (^{o}C)	180	60∼80
Max. Permissible Temp. (^{o}C)	110∼121	60∼80
Hot Shortness (%)	1∼2	7
Chemical Resistance	Good	Fine

Note: The contrast (including performance comparison) can be regarded as the materials of a general comparison due to their values depend on the formula and requirements of specific occasions.

For the simple bearing socket the measurements will usually be within the intervals specified in Figure 2.12, as long as the socket is consist of steel with a yield stress of 250-300 MPa. Commonly, the slope β of the conical cavity will be slightest for sockets with cold casting material and largest for sockets with metallic alloys.

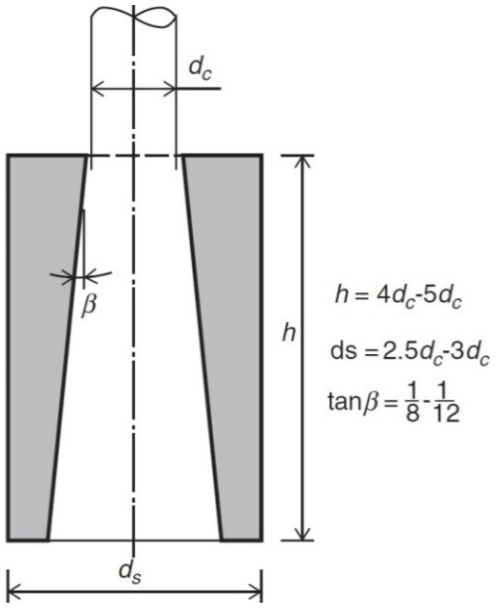

Figure 2.12. Typical dimensions for bearing socket.

While analyzing the compressive stress, the bearing area does not always cover the whole area of the socket end. Hence, when it comes to use shim plates shaped as displayed in Figure 2.13, the effective bearing area is assumed to contain only the shaded areas. Only if an enlarged bearing area is necessary, a socket with a collar, as shown in same Figure 2.13, might be used.

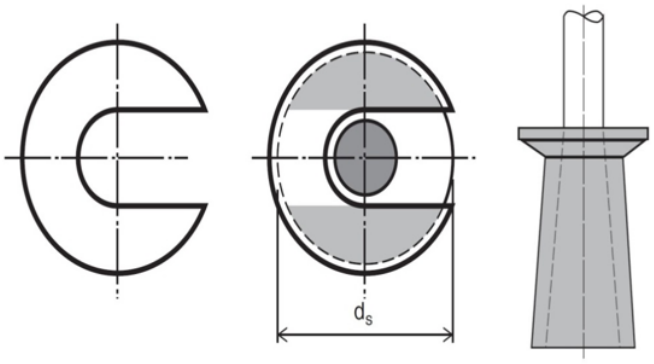

Figure 2.13. Bearing area (left-hand side), socket with collar to increase bearing area (right-hand side).

As well as the sizing of the socket end in order to confirm the transmission of the strand force as compression, analyzing of the wall thickness is also needed as the side pressure from the casting material causes a ring tension within the socket walls. The designation of the wall thickness is regularly depending on the following estimated technique. The method lie behind to safe dimensions in general terms that the ultimate strength of the strand anchor will not be controlled by the socket itself (Schleicher, 1949).

The effective length of the cable socket is supposed to be 2/3 of the total length, as demonstrated in Figure 2.14. Additionally, it is assumed that the pressure from the casting material performs under an angle ϕ with the internal surface of the strand socket wall, equivalent to a coefficient of friction $\mu = tan\phi$. Although, the hot casting materials $tan\phi$ will regularly be preferred to a value of 0.2, the cold casting materials filled in HiAm sockets will provide a value of $tan\phi$ equal to 0.45.

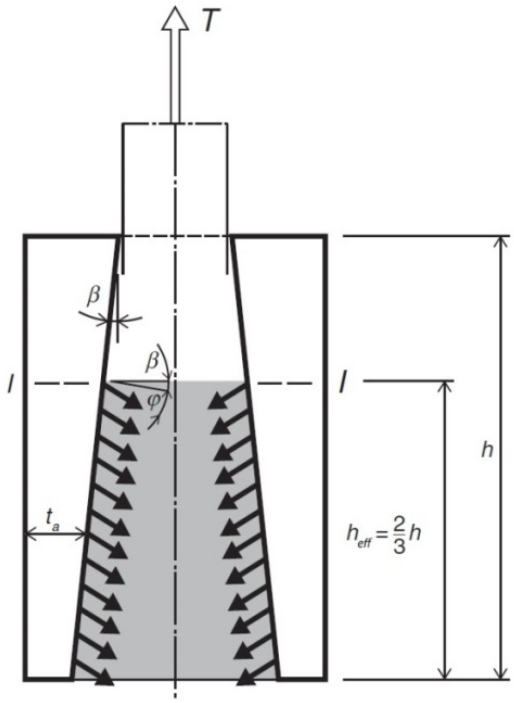

Figure 2.14. Idealized force transmission from the socket to the casting material inside the cone.

The entire ring tension P_r is obtained by:

$$P_r = \frac{T}{2\pi tan(\phi + \beta)} \tag{2.1}$$

where T is the strand force and β is the conical cavity.

Assuming that the ring tension is taken by the effective part of the strand socket with a height of h_{eff}= 2/3h causes to the following equation:

$$\sigma = \frac{3P_t}{2ht_a} = \frac{3}{4\pi}\frac{T}{tan(\phi + \beta)} \tag{2.2}$$

where t_a is the average thickness of the strand socket wall in the effective part.

It is essential that the axial stress in Section I-I, as shown in Figure 2.14, shall be confirmed, as the entire strand force T must be transferred through this section.

2.1.4. Cable Bands

These cable bands (or clamps) also impose significant compressive radial loading on the main cable surface and facilitate load sharing of the strands underneath the band through enhanced surface friction as shown in Figure 2.15. Some of the clamping action is also provided by the cable bands that serve as attachment points for the PWS cable or vertical suspenders that connect the bridge deck to the main cable.

Cable bands consist of two cylinder halves bolted together over the circumference of the cable. The number of bolts per cable band is dependent on the slope of the cable at the suspender attachment point. The friction from squeezing against the cable prevents it from sliding down the cable.

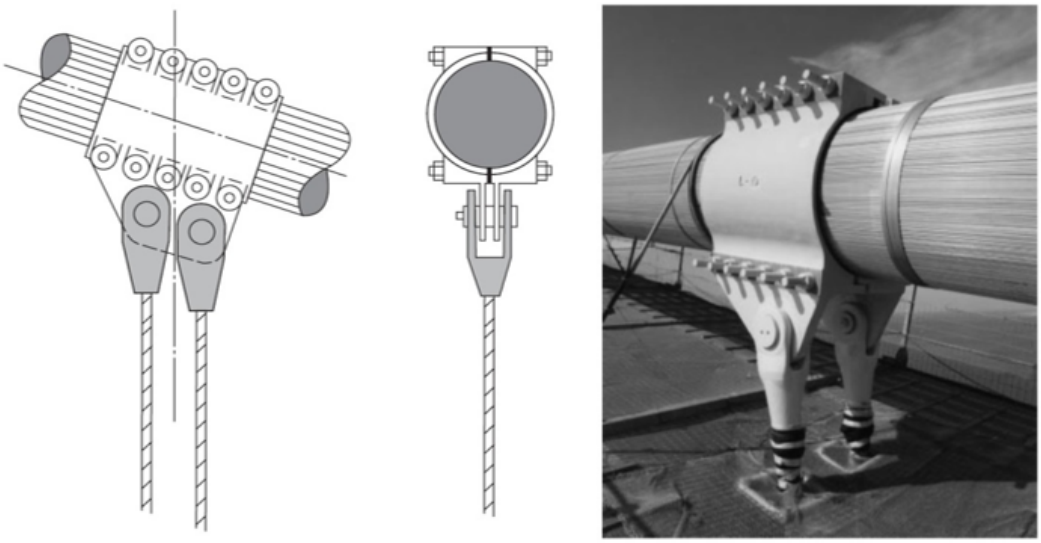

Figure 2.15. Hangers connected with fork sockets to cable bands (left-hand side), Cable Band in the Akashi Kaikyo Bridge (right-hand side).

2.2. Fire Hazard in Bridges

2.2.1. Structural Fire Engineering

It is well known that fire is a severe hazard and poses a significant threat to structures including buildings and bridges. When fire subjects to the structural member,

thermal elongation and weaken material properties of the material are expected. Since fire is such a severe threat, codes and specifications have been put in place to minimize its potential destructive effects. The basic concepts of structural fire engineering are to prevent structural collapse and to prevent the spread of fire, and to limit the damage. Life safety and economic impact are the primary factors that govern the required fire resistance. Fire resistance is provided through passive and active systems. Passive systems, such as intumescent paints and sprayed on fire resistant materials, are always in place. Active systems, such as sprinkler systems, fire extinguishers, or oxygen suppression systems, require a triggering mechanism before they provide fire suppression. Fire resistant design of structures can be simply expressed as followed:

$$\textit{Required Fire Resistance} \leq \textit{Provided Fire Resistance}$$

For buildings, the required fire resistance is a function of the type of construction, type of structural element, the importance factor, and the height or area. The provided fire resistance is a function of the structural member's ability to maintain its function at elevated temperature. Structural fire resistance for buildings is required by the IBC (2012). Specifications often provide guidance in terms of what is required and how to achieve that resistance (AISC 2011; ACI 216.1-14).

A correct estimation of the temperatures in structural member cross sections is the first and most vital step in order to analyze fire-induced forces and finally to estimate the fire performance of a structural system (Selamet, 2017). Thus, structure fire resistance is typically achieved via a prescriptive approach (Gross and Cauffman 2011; PTI 2006). In the prescriptive approach to fire resistance, engineers determine the required fire resistance based on building and construction classifications and then select building materials and/or fire suppression systems that provide the required fire resistance rating. Historically, both the required fire resistance and provided fire resistance are derived in units of hours. The provided fire resistances are based on the ASTM E-119 Standard Fire Test (ASTM 2014). To date, a wide range of E-119 tests have been performed for a variety of building assemblies, and the results are published to help engineers choose structural components (reference UL standards).

There are three categories for which specimens are assessed: load bearing capacity, integrity, and temperature on the unexposed side (ASTM E-119-14). Specimens do not necessarily need to pass all three categories for the test to be a success. For example, beams and columns are only required to maintain the load bearing capacity while a non-load bearing wall may be required to maintain integrity and meet a maximum temperature requirement for the unexposed side. Fire protection for bridges is specified by the NFPA 502: Standard for road tunnels, bridges, and other limited access highways (NFPA, 2001). The three categories required by NFPA 502 are as follows:

(i) Maintain life safety,
(ii) Mitigate structural damage and prevent progressive structural collapse,
(iii) Minimize economic impact.

The standard does not provide guidance on how to meet the requirements, and the engineer must decide what level of protection to provide.

In the literature, the standard fire rating requirements for PWS suspender cables does not exist, however, the PTI published a document called the Recommendations for Stay-Cable Design (PTI, 2012) and this recommendations might be useful and applicable for a nineteen PWS system for the experimental program. In this reference book, minimum fire resistance for stay cables is specified in Section 4.5 as follows:

"Fire rating requirements will be established by the Owner if these are to be a project criterion". In lieu of Owner requirements, a 30-minute minimum time rating based on the E-119 fire curve is required. The stay strand and stay system are subject an external heat source of 1100^oC (The furnace must be capable of reaching 1100^oC within the first five minutes of testing and maintain this temperature throughout the test) and must demonstrate "fire endurance" a temperature below 300^oC for at least 30 minutes. If the stay-cable and stay-system meet the temperature requirements, the test shall be repeated in a tension frame where the tension element is placed at 45% minimum ultimate tensile strength (MUTS). The stay cable must maintain the load

without slip for at least 30 minutes. The 300^{o}C temperature is chosen because it is known that the cold-drawn steel used in cable stay design enters the plastic domain at 400°C and the HDPE material used to prevent cable corrosion ignites at 330^{o}C. When the HDPE ignites, there is a sudden increase in cable temperature (PTI, 2012).

The PTI required resistance is based on the E-119 fire curve and is a prescriptive design approach. Performance based fire design is an alternative to the prescriptive approach. Performance design still needs to meet the same basic objects as prescriptive design, but it is not limited to the published E-119 test results. In this type of structural fire design, the engineer selects the design fire that the structure is exposed to, performs a heat transfer analysis, and then calculates the structural response.

2.2.2. Identifying the Bridge Fire

A literature review of the state-of-the-art is carried out on defining the bridge fire. Aforementioned, bridge fires are referred to as hydrocarbon fires or liquid pool fires. They can reach very extreme temperature within the initially few minutes of fire exposure and distinguished by fast heating rates. A liquid pool fire forms when a combustible liquid spills on the ground, its liquid begins to vaporize, and the vapor is ignited. (Garlock *et al.*, 2012).

These fires can be divided into two categories:

(i) Confined (the spread of the burning liquid is limited by the presence of a physical barrier),
(ii) Unconfined (no physical restraint) (Iqbal *et al.*, 2004).

A confined pool fire has a large surface area and produces high heat loads for a short duration. On the other hand, an unconfined pool fire will burn longer than a confined pool fire, which has a minor surface area and generates low heat loads for a long duration.

One of the most important steps required in determining the heat loading from a liquid pool fire is to calculate the heat release rate (Modak, 1977; Mudan, 1984; Iqbal *et al.*, 2004) which shows how powerful the fire is. This is an experimentally derived value which is based on the material properties of the fuel as well as the geometry of the pool (which in turn depends on the flow of leaking fuel).

Specific standard hydrocarbon fire curves for design exist; nevertheless, they have limitations for application to bridges. Hydrocarbon pool fires (CEN, 2002; ASTM, 2004), exceeds 100^oC within initially few minutes and endures to rise during the fire period. This is inaccurate ever since fires will sooner or later burn-out their energy source.

There are further time-temperature curves for relating the fire hazard associated with RWS curve (from the Netherlands), RABT-ZTV curve (from Germany) and petrochemical fuels, for instance the hydrocarbon improved curve (from France). However, tunnels have altered oxygen and air circulation surroundings than bridges and these curves have been developed for tunnels.

Valuable information about several vehicle fire scenarios is provided in Barber *et al.* (1994). Even though, this research was performed for the Oresund tunnel, the comprehensive information on gasoline characteristics can be used to improve a model for bridge fire scenarios (Lykke *et al.*, 1998; Falbe-Hansen *et al.*, 2000).

As an illustration, Mendes *et al.* (2000) have improved a fire model to investigate the effect of a ship fire on the girders of a cable-stayed bridge under Vasco da Gama Bridge (Portugal). Stoddard (2004) improved a fire curve modified to the scenario of a railway tanker fire that damaged a prestressed concrete bridge. Dotreppe *et al.* (2006) examined the collapse of a tied arch caused by the explosion of a gas pipe by taking into account six several fire zones corresponding to the hydrocarbon curve of the Eurocode (CEN, 2003). Bennets and Moinuddin (2009) have suggested numerous fire scenarios to define the impact of a heavy-duty truck fire, of a freighter fire, and of a LPG tanker fire on the tendons of a cable-stayed bridge and in line with the structural component

of interest in this work. Main and Luecke (2010) developed both low-temperature and high-temperature effects on the main cables of suspension bridges. Gross and Cauffman (2011) propose handling fire as a design load to ensure that bridges are able to survive these kind of fire hazards and recommended that experiments must be performed to verify bridge fire response in order to implement performance based design. Woodworth *et al.* (2015) proposed to use a CFD model in order to estimate the effects of a pool fire on a stay cable bridge. For Woodworth *et al.* (2015) study, noteworthy simplifications were applied in regard to the cross-sectional calculation for the temperature increase in the stay cable.

The most noteworthy study having been undertaken by Quiel *et al.* (2015). In their work, a streamlined framework was proposed in order to measure the degree of loss caused by an identified fire hazard. This methodology can be used to estimate the effects of a variety of fire kinds, sizes, and locations in order to create an envelope of performance for which the risk of damage and the effectiveness of potential fire protection measures can be evaluated. In accordance with Quiel *et al.* (2015) study, the estimation of a bridge's response due to a fire hazard simply contains of four stages:

(i) Defining the fire's characteristics and geometry such as footprint, flame height, duration, fuel properties and intensity.

(ii) Calculating the heat transfer from the fire to the structural elements;

- Heat transfer to the structure is calculated using a modified discretized solid flame (MDSF) approach, and the resulting thermal response of the bridge's cables is then calculated using multiple lumped thermal masses.

(iii) Calculating the temperature increase of the structural elements;

- These temperature time histories are then used to calculate the corresponding structural response.

(iv) Calculating the resulting material and mechanical response of the structural elements;

Hence, the fire models to be performed in the design of a bridge have not been provided by the bridge design codes. Consequently, all researchers have improved an

approach modified to their specific case study. There is a need to develop realistic fire scenarios specific for bridges that include the definition of critical parameters such as the location of the fire, the type of fuel load, the environment conditions, the features of the decay phase and the live loads to be considered in case of a fire event (Garlock *et al.*, 2012).

2.2.3. Bridge Fire Incidents

There has been a raise of fire related hazards in bridges in the last two decades. As stated previously, with the potential for significant strength loss and even collapse of the structures, bridge fires are a threat to economies, commerce, and human life alike. Increased ground transport of hazardous and highly flammable materials has led to an increase in the likelihood of fire damage to the ground infrastructure network (Battelle, 2004). Moreover, literatures review by Garlock *et al.* (2012) outlined that "the average number of annual vehicular fire incidents in the United States is 376,000 causing 570 civilian deaths and $1.28 billion in property loss".

This directly translates to possible weakening of bridge infrastructure due to the exposure to said fires. In the same paper, NYSDoT survey of bridge failure from 2008 listed of 18 states (including seismic states such as California) revealed that, of 1746 bridge failures, 52 collapses were a result of fire incidents while just 19 collapses resulted from earthquakes. In both 2007 and 2009, a 160-meter deck section collapse (MacArthur Maze or I-580 collapse in Oakland, CA, USA as shown in Figure 2.16) and a complete bridge collapse (overpass of I-75 near Hazel Park, MI, USA), respectively, involving composite steel girder and reinforced concrete slab decking were directly attributable to fires caused by gasoline tanker crashes. The first event mentioned, also referred to as the MacArthur Maze or I-580 collapse, and came at the hands of a fire induced by a tanker carrying a volume 32.6 m3 of gasoline (Garlock *et al.*, 2012). The deck collapse occurred just 22 minutes after the start of the fire and ended up costing the federal government $9 million in repairs and the San Francisco Bay area an estimated $6 million per day in economic impact (Bulwa *et al.*, 2007; Chung *et al.*, 2008; Noble *et al.*, 2009).

Another major bridge fire occurred on 2006 when a fuel tanker carrying 28.700 lt of diesel overturned near the bridge in AZ at the Bill Williams River Bridge (Stoddard, 2004). A car crashed into a fuel tanker transporting 50.000 lt of heating oil on the I-95 Howard Avenue Overpass in Bridgeport, CT in 2003. The bridge was supported by 30-inch deep steel girders spanning 22m. The heating oil spilled over a length of 100 meter and ignited. The fire lasted for two hours and the temperatures reached about 1100^{o}C. The high intensity of fire initiated significant buckling in steel girders carrying the overpass. This resulted in partial collapse of steel girders causing both northbound and southbound lanes to collapse. Following the fire, traffic in both directions had to be detoured. The refurbishment of this fire damaged bridge cost about $11.2 million (Garlock *et al.*, 2012; Van Horn *et al.*, 2012, Kodur *et al.*, 2012).

This is but one example of the dangers and associated economic effects (fortunately, no loss of life in this instance) that bridge fires pose to a nation and a region. The author presents further examples of major bridge fires and highlights that these events typically come at the hands of tanker crashes where any collapses associated with said accidents occurred in less than thirty minutes (Garlock *et al.*, 2012). It is important to note that fire is not just a threat to overpasses and interchanges.

Figure 2.16. Oakland Highway Bridge collapse, 2007 (left-hand side), Queensboro Bridge Fire hazard, 2013 (right-hand side).

Examples of vehicular fire events on complex bridge systems such as suspension bridges and stay-cable bridges are plentiful and range in size such as a 40-foot-long tractor-trailer fire on the Queensboro Cantilevered Truss Bridge in New York caused

some damage to structural steel and therefore partial temporary bridge closure as shown in Figure 2.16. Furthermore, a school bus and truck ignited the fire on The Mezcala stay-cable Bridge in Mexico. The Mezcala Bridge was closed after a fire resulted in rupture of one stay cable and reopened after the cable was replaced (Zoli and Steinhouse, 2007). Another event occurred 2005 in Greece (Zoli and Steinhouse, 2007) The Rion Antirion Bridge was struck by lightning six months after opening. The lightning strike ignited a fire and caused socket failure, resulting in the loss of a single stay cable. Again tractor-trailer crashed on the Zakim Cable-stayed Bridge in Boston (USA) and the outcome was that casing of 1 stay cable partially charred in 2014.

Moreover, a tractor-trailer fire on the Manhattan Suspension Bridge in New York (USA) caused partial temporary bridge closure in 2009. Another minor bridge fire occurred on 2012 when a passenger car passing across the bridge in New York at the Brooklyn Bridge. The fire again caused partial temporary bridge closure. A car fire occurred on the Great Belt Fixed Link Suspension Bridge in 2013 and caused temporary bridge closure. Table 2.4 summarizes some of the major bridge fire incidents in the past 25 years.

For an illustration, the threat to suspension bridges is of particular importance as they typically serve as the major arteries for traffic in a city or a region -in Istanbul (Turkey) alone, three suspension bridges service nearly 1 million commuters daily. Therefore, shutting down a suspension bridge for maintenance would require traffic detouring to nearby routes which can impose significant traffic delays in the affected region. Eventually, this would stress the flow of traffic and affect the commuters' pattern in the surrounding highway networks (CALTRANS, 2012).

In brief, it is rational approach that vehicle fires like to the abovementioned bridge incidents that have resulted in the failure of overpass bridges are at least a statistically possible hazard for suspension bridges that should be considered during design of the suspension bridges.

Table 2.4. Some major bridge fires in the last 25 years (Garlock *et al.*, 2012).

Bridge/location	**Date**	**Cause of fire**	**Bridge material**	**Damage description**
Bridge over 1-75 near Hazel Park,MI, USA	July 15,2009	A gasoline tanker struck an overpass on 1-75	Composite deck (steel girders + reinforced concrete slab)	Complete collapse of the bridge, which fell on the freeway below
Big Four Bridge Louisville KYİ,USA	7-May-08	Electrical problem of the lighting system, took two and a half hours to control the fire	Steel truss bridge	Minor structural damage, resulting in large amount of debris on the bridge
Stop Thirty Road, State Route 386 Nashville, TN, USA	20-Jun-07	A fuel tanker truck rear -ended a loaded dump truck. The tanker erupted into flames beneath the bridge	Concrete hollow box-beam bridge	The bridge sustained very little damage and traffic was reopened after minor repairs
I-80/880 interchange in Oakland, CA, USA	April 29,2007	A gasoline tanker crashed	Composite deck (steel girders + reinforced concrete slab) supported by reinforced concrete columns	A 160 m section of the interchange collapsed
Bill Williams River Bridge, AZ, USA	20-Jun-07	A gasoline tanker over-turned	Concrete deck (precast prestressed I girders + cast in place reinforced concrete slab)	Concrete girders were damaged by the fire and subsequently repaired, but it was not necessary to replace any of the girders
Belle Isle Bridge in NW Expressway, Oklahoma City OK, USA	28-Jan-06	A truck crashed into the bridge	Concrete deck (precast prestressed I girders + cast in place reinforced concrete slab)	Concrete girders Were slightly damaged by the fire. The safety of the bridge was assessed and the bridge was reopened to traffic
Wiehltalbridge in motorway A4İ Cologne-Olpe , Germany	August 26,2004	Following an accident, a gasoline tanker fell down and started a fire under the first bridge span	Orthotropic steel deck supported in concrete piers and abutments	Web buckiling in one of the Main girders of the bridge that experienced maximum displacements of x 120 mm and local plastic deformations in the cantilevering part of the steel deck
Bridge over the Norwalk River near Ridgefield, CT, USA	July 12,2005	A tanker truck carrying 30.3 m3 of gasoline overturned, caught fire, and burned out on the bridge	Concrete deck (precast prestressed box girders + cast in place reinforced concrete slab)	The deck was replaced by a new one but its beams were tested by the FHWA
1-95 Howard Avenue Overpass in Bridgeport, CT, USA	March 26,2003	A car stuck a truck carrying 30.3 m3 of heating oil	Composite deck (steel girders + reinforced concrete slab)	Collapse of the southbound lanes and partial collapse pf the Northbound lanes
1-20/1-59/1-65 interchange in Birmingham, AL, USA	January 5,2002	A loaded gasoline tanker crashed	Steel girders	Main span sagged about 3 m (10 feet)
1/80W/1-580E ramp in Emeryville, CA, USA	February 5,1995	A gasoline tanker crashed	Composite deck (steel girders + reinforced concrete slab)	Deck, guardrail and some ancillary facilities were damaged

2.3. Mechanical Properties of Cold-drawn High-Strength Galvanized Steel Wires at Elevated Temperature

Callister and Rethwisch (2008) clarified the process of cold-working as an escalation in the displacement density which in turn raises the stress required to deform the metal. The strength required to deform the alloy increases with the amount of cold-working performed. The cold-working properties which above-mentioned in Chapter 2.1.1 can be removed by exposing the steel to elevated temperature over and done with a process known as recovery.

Some of the thermal and mechanical properties such as the elastic modulus, variation of specific heat with temperature, and the thermal conductivity are fairly unaffected by the above mentioned process. Yet, the other mechanical properties at ambient and at higher temperature of mild steel and cold-drawn steel are considerably dissimilar.

Figure 2.17 illustrates the stress-strain curve of mild steel (left-hand side) and cold-drawn steel (right hand-side). The mild steel has a typical yield point followed by a yield plateau. Thereafter, the yield plateau changes to a non-linear strain hardening zone before the ultimate strain is reached. In contrast, the cold-drawn steel has identical yield peak and shifts directly from the linear elastic zone to a non-linear strain hardening zone.

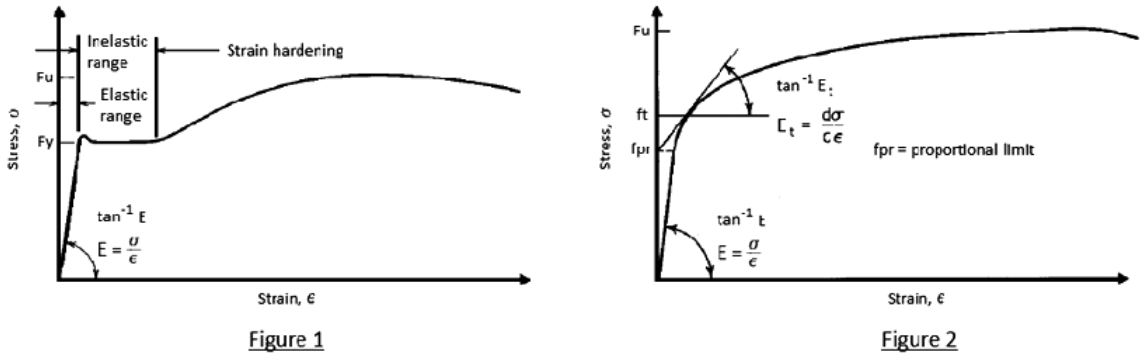

Figure 2.17. Mild steel (left-hand side) vs. Cold-drawn steel (right-hand side).

As mentioned before, cold-drawn steels characteristically have greater strength and lesser ductility compared to mild steels. The mechanical properties that are converted during the cold-drawing process can be recovered at higher temperature. Therefore, at elevated temperatures, these steels undergo superior reductions in the terms of mechanical properties. The Eurocode (2004) reduction factors for the design yield stress are illustrated in the below Figure 2.18. The reduction factors for cold-drawn steel (prestressed steel strand) forms an S-shaped curve which begins to decrease at 200^{o}C. The rate of decrease is constant until approximately 600^{o}C where the curve begins to flatten out. The reduction for cold-drawn steel is always greater than the reduction for mild steel, and it is essential that the appropriate reduction factor is used in practice.

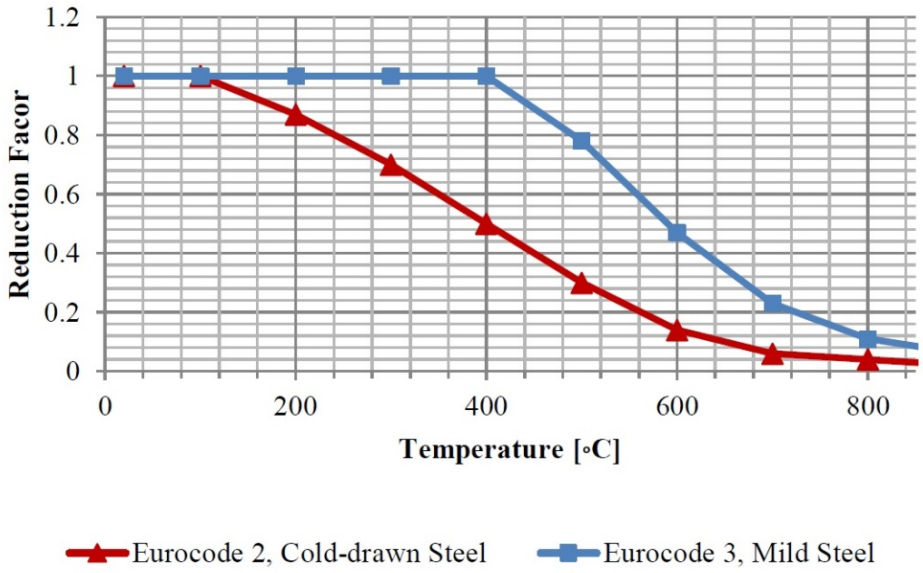

Figure 2.18. Eurocode (2004) Model Yield Reduction Factors.

The demonstrated reduction values from Eurocode (2004) are applied to stress-strain model for mild and cold-drawn steel at elevated temperature. At room temperature, the assumed elastic-perfectly plastic model is typically used for steels according to aforementioned material model (Franssen and Zaharia, 2005).

The high temperature model consists of firstly a linear elastic region, secondly a parabolic region, then a perfectly plastic region, and lastly a linearly declining region.

The last region models the decline in strength at particularly high strains. The stress-strain model that can be modified to represent both mild and cold-drawn steels at temperatures between 20^{o}C and 1200^{o}C as illustrated in Figure 2.19.

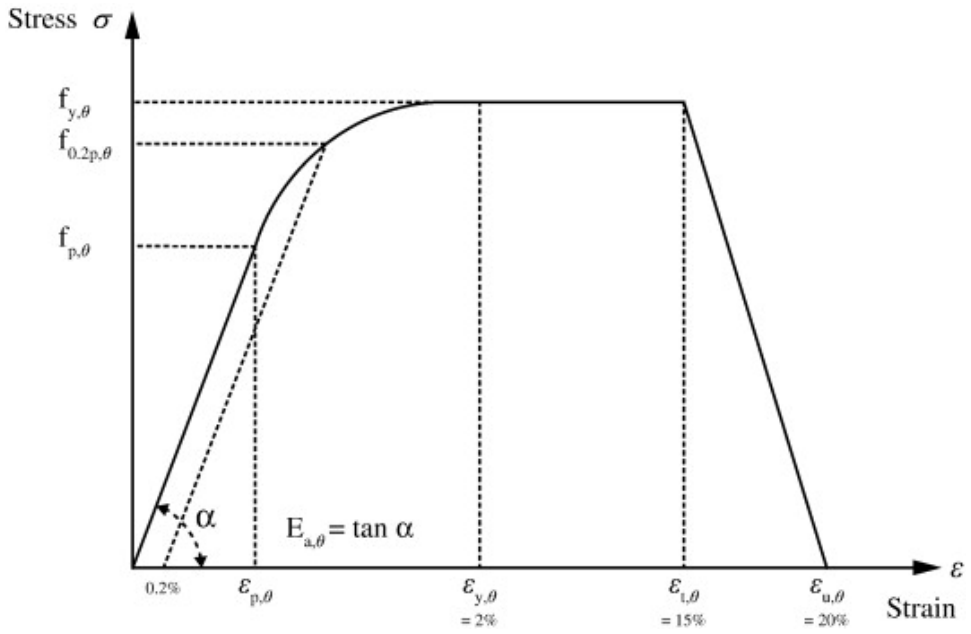

Figure 2.19. Eurocode (2004) Stress-Strain Model for Mild Steel.

This material model uses the similar equation for both cold-drawn and mild steel; nevertheless, the reduction values are dissimilar. As presented above model in Figure 2.18, the yield reduction factors are more brutal for cold-drawn steel.

The material model accepts that when the yield stress is reached, the cold-drawn steel will perform perfectly plastic up until it reaches the ultimate strain limit. At that point, the material stress linearly drops until rupture. One of the aims of this study is to verify this stress-strain model with including the strain-hardening zone. For a performance-based design for fire-resistant bridge wires, it is important to use a model that predicts the actual behavior of the high-strength wires.

2.4. The Behavior of Cold-drawn Steel and Cast Sockets at Elevated Temperature

2.4.1. Former Experimental Studies of Cold-drawn Steel at Elevated Temperature

In the past, numerous experimental studies have been tested the tensile properties of mild steel at high temperature. On the other hand, cold-drawn steel wire has received limited attention. Thus, most of the test programs were performed prior to 1970. The outcomes from former experiments have not been confirmed during the recent years. Indeed, as it is well known fact that the chemical composition and therefore mechanical properties of cold-drawn steel may vary depending on the year of manufacturing date and the country of origin.

Abrams and Cruz (1961) uncovered the tensile strength reduction curves of prestressed steel strand. Nowadays, the findings from this former experimental study are still used in ACI, PCI, and PTI. Other scientists have shown interest in the mechanical properties of single tendons from the 7-wire strand, residual strength testing, and the mechanical properties of similar steels (A421).

Due to the difficult nature of gripping a strand (bundle of wires) for a tensile test, many researchers chose to experiment using the single wire approach. One of the main goals of this thesis is that uncovering the tensile properties of a nineteen parallel cold-drawn wire strand with 4 meter long at rapid rise temperatures such as pool fires and this kind of comprehensive experiment has not been studied yet. This section of the thesis outlines the past work done on cold-drawn steel wires which is parallel to this thesis goal in chronological order:

Abrams and Cruz (1961) a number of tests that were carried out by Abrams and Cruz (1961). The sets of tests were conducted by using the 7-wire strands (Grade 1725 Mpa) with 10 millimeter diameter, a universal testing machine, and an electric furnace.

The first stage of testing procedure including that the strand was initially loaded to a set stress level and afterwards the specimens were heated until failure. The initial prestress was selected at 55% and 70% of MUTS and the heating rates were chosen at 2.8, 5.5, and 8.3^{o}C / min. and the prestressed strands inserted in concrete. The prestressing level was retained throughout the test and the temperature at rupture was recorded.

The rupture temperature for the 55% and 70% of MUTS prestressing was approximately 426^{o}C and 315^{o}C respectively. The author also figured out that the heating rate has a minor effect on the rupture temperature. At temperature of 205^{o}C, less than 10% ultimate strength was gone, while 50% ultimate strength is lost at 427^{o}C. The test was also carried out on strands of 6.35mm and 11.11mm diameter and it was found that the cold-drawn wire strand size does not affect the percent loss of ultimate strength.

Holmes *et al.* (1982) once, the specimen was prestressed to 70% of MUTS then it was heated up till the rupture or reaching the target temperature (maximum). The test was concluded that all of the prestressing steel specimens were ruptured at the temperature of 300^{o}C. Holmes *et al.*, recommended that the prestressing value shall be between 50% and 60% of MUTS instead of 70%. In order to provide a well demonstration for in-service conditions for prestressed steel which prestressed value loss over time in practice.

Neves *et al.* (1996) the test results show residual strength loss occurs at maximum temperature between 300 and 400°C. The strand advances due to cold-drawing process back completely of the initial strength up to 300 and 400^{o}C, in other words the residual strength stay nearly stable. However, when the temperatures exceeding 700^{o}C, the strength loss occurred up to 60%. Moreover, in the case of fire events that was between 800 and 900^{o}C, it was concluded that cooling by water jet trigger the tendon to become brittle which increasing the tensile strength while decreasing the strain at rupture. Hertz (2004) the crystalline structure of cold-drawn rods loosens beyond 300^{o}C. If the subjected temperature is more than 400°C, the residual properties of cold-drawn

steel undergo irreversible losses. At the temperature of 600^{o}C the influences of cold-drawn working are disappear and the steel performs similar to mild steel. If the cold-drawn steel is subjected to temperatures exceeding 800^{o}C, the cold-working mechanical properties are completely disappears and the residual material performs as mild steel.

Atienza and Elices (2009) carried out two sets of tests which were tensile and relaxation tests at elevated temperature and relaxation tests subsequently a simulated fire. For every single test, 5 mm commercial 0.77% carbon cold-drawn steel wires were used. Instron tensile testing machine with an attached furnace was preferred for the test.

At first test, the specimen was placed in the testing machine and heated to the set temperature for the tensile testing at elevated temperature. Specified temperatures vary from 100 to 600^{o}C at intervals of 100^{o}C. The test outcomes indicated a strong correspondence to British Standard and Eurocode 2 recommended standards. There is a gradual reduction in the ultimate strength of the wire beyond the temperature of 100^{o}C.

In the second phase of the program including the relaxation tests at high temperature. The tests indicated that there is noteworthy prestress loss as the temperature increases. The outcomes also demonstrates that the percentage of prestress loss is dependent upon the initial prestress level. The study included initial prestress loads from 10 to 90% of the wire strength.

The “behavior after fire” testing demonstrates that after 250^{o}C the mechanical properties reduced. At 400^{o}C this decrease “is very important”. Above 400^{o}C recrystallization of the steel microstructure occurs and the advanced properties produced throughout the cold-working process are lost. The recrystallization processes is dependent upon both time and temperature.

2.4.2. Former Experimental Studies of Cast Sockets at Elevated Temperature

At ambient temperature, the socket has a competence of 100%, which means that it is able to transmission static loads up to the certain minimum breaking strength of the strand. In case of axial fatigue, a hot casting media filled socket is as capable as a cold casting media filled one (Ridge *et al.*, 2001), even if former strand failures have been stated (Hobbs *et al.*, 1983) close to sockets filled with pure zinc.

In case of elevated temperature, limited number of studies has previously been conducted to explore the performance of socketing systems, the most significant study having been carried out by Oplatka and Feyrer (1986). In their work, hot casting (metal based) and cold (polymer based) casting materials were used in order to assembly wires and socket material and these materials were tested in both static and fatigue modes. Nevertheless, tests were conducted using a different elevated temperature, which makes comparison of the performance difficult. Moreover, according to Isabel and Roger (2012) test results critical temperatures for long time duration such as around between 210 and 223^{o}C were likely to reach rapidly in an unprotected condition for socket materials and 160^{o}C if a proprietary resin compound, Wirelock^{TM}, is used.

3. TEST PREPARATION AND TEST PROGRAM

Chapter 3 provides information about the experimental test program that was accomplished for this research project. Specifically, this chapter outlines the test specimens, test equipment's, test setup, and test procedures.

The test program includes static tests and transient elevated temperature tests which held at constant load for gasoline pool fire hazard in suspension bridge. The proposed gasoline pool fire hazard and standard hydrocarbon pool fire scenario that were exposed to the test specimens.

The individual wire has a diameter of 5.1 mm and guaranteed ultimate tensile strength of 1860 Mpa. Each of the specimens consists of a total of 19 wires and a socket material for each termination. The transient tests were performed by firstly loading the cable system to a target level of stress (typical stress levels for cable-stay bridges were chosen). Secondly, when the strand and the socket were at the desired stress level, the furnace was switch on and the system was subjected to the fire scenarios. Lastly, the strand system was maintained at the chosen stress level until the wire specimens rupture or socket draw (wire pull out) due to temperature increase. The same abovementioned procedure was followed for all fire tests. Furthermore, in one the fire test the specimen was protected from fire in order to examine the particular behavior of the wire strand under fire and after cooling static test. Moreover, socket material and wire strand were assembled by using either hot casting material or cold casting material as it mentioned in Chapter 2.2.5 Cable Anchorage and Connection (Socket Material).

The constant temperature test is not performed because the purpose of this kind of tests is to evaluate the cable performance at a specified target temperature. Thus, constant temperature tests are universally used to establish the material performance at a variety of temperatures; nevertheless, they are not realistically demonstrative of real fire exposure, throughout which an element is exposed to variable temperatures.

The main aim of this testing is to evaluate the behavior of PWS system under pool fire scenario.

3.1. Test Specimens

The zinc-coated cold-drawn wire strand and socket material that are used of our experimental study are presented in this chapter. The wire was conformed to the requirements of ISO 19427 and this procedure. Test specimen with 1860 Mpa grade with a nineteen parallel wire strand is chosen for test program. The strand socket material was conformed to the requirements of DIN 17100 and this below mentioned procedure.

- Brief Introduction of Wire Manufacturer

(i) Wire manufacturer : GÜNEY ÇELİK A.Ş.,

(ii) Location : Hacı Sabancı Org. San. Böl. Süleyman Demirel Bulv. No: 2 Sarıçam / Adana / Türkiye,

(iii) Telephone : +90 322 394 50 30 / Fax: +90 322 394 50 70,

(iv) Web-site : http://www.guneycelik.com.tr

Figure 3.1. Aerial view of the Güney Çelik production facility.

- Brief Introduction of Socket Material Manufacturer

(i) Socket manufacturer : ASİL ÇELİK A.Ş.,

(ii) Location : Gemiç Köyü Mevkii 16800 Orhangazi/ Bursa/ Türkiye,

(iii) Telephone : +90 224 280 61 00 / Fax: +90 224 280 62 00,

(iv) Web-site:http://www.asilcelik.com.tr.

Figure 3.2. Aerial view of the Asil Çelik production facility.

Construction of Asil Çelik premises has started in 1974 and the company has started operating in 1979. Technical assistance and know-how contract has been signed with German company THYSSEN EDELSTAHLWERKE AG for acquiring primal engineering services and advanced production technologies.

- Summary of the Materials used for Test Program:

(i) Φ5.1 Steel wire (1860 Mpa),

(ii) Strand socket (ST52.3),

(iii) Zn-Cu alloy for socket casting,

(iv) Reinforced filament tape for seizing.

3.1.1. Specimen of PWS (Parallel Wire Strand)

3.1.1.1. Wire Manufacturing and Quality Control. Inspection certificate for wire rod is presented in Figure A.1

Table 3.1. General process of manufacturing high-strength galvanized bridge wires.

No	**Manufacturing process**	**Quality control**
1	Receiving Wire Rod	- In order to identify, the wire rod shall be stocked based on the specification. The inspection certificate of raw material is presented in Appendix A.
2	Heat Treatment of wire rod	- To ensure the homogeneous grain, wire rod shall be treated with heat - Heat treatment flow (Isothermal heat treatment). Heating (900^{o}C)→Isothermal heat treatment pot (580± 10^{o}C)→Cooling
3	Cleaning of wire rod	- Remove the oxidized scale - Surface treatment with BORAX for lubrication of wire drawing - Cleaning flow HCI pot (7∼25%, 40∼60^{o}C)→Cleaning pot (Frequency, 2)→BORAKS ($Na_2B4O_7.10H_2O$), (10∼20%, 80∼100^{o}C)→ Drying (100∼200^{o}C, 20∼60 min.)
4	Wire drawing	- Go through the 9 dies continuously - Diameter : 5.1 +0.08, -0.05 - Speed : 180±20m/min.
5	Zinc coating	- Zinc coating flow (300g/m^2) 1) Isothermal heat treatment pot (remove the internal stress) 2) Hydrochloric acid pot (remove the oxidized scale) 3) Cleaning pot (surface cleaning). 4) Drying 5) Zinc coating pot 6) Purity of molten zinc ≥ 99.95 % Heat treatment (400∼500^{o}C)→HCI pot (7∼25%, 30∼60^{o}C)→ Drying (150∼200^{o}C)→Zinc coating (420∼480^{o}C)

3.1.1.2. Quantity of PWS. Net length and weight of the specimen as shown in below.

Table 3.2. The quantities and weight of the net length of PWS specimens.

Item	**No. of wires Φ x n**	**Nominal Length (m)**	**No. of Strands (ea.)**	**Unit weight of a Strand (kg/m)**	**Total Weight (kg)**
Specimen Cable	5.1 x 19	4,36 (0,18+4,00+0,18)	5	3,07	66,93

3.1.1.3. Mechanical and Dimensional Properties of Zinc-Coated Wire. Test results for specimen wires are preseneted in Figure A.2, Figure A.3 and Figure A.4.

Table 3.3. Mechanical and dimensional properties of the wire specimens.

Item	Value	Remark
Nominal diameter	5.1 mm	
Nominal wire area	20.43 mm^2	
Wire nominal strength	1860 N/mm^2	Vendor confirmed
Tensile strength	1910 N/mm^2	Average value of tested wires
Proof stress (0.2% yield stress)	1560 N/mm^2	Average value of tested wires
Characteristic Breaking Load	39.07 kN	Average value of tested wires
Modulus of elasticity	190 - 210 kN/mm^2	
Minimum elongation	4.5% in 500mm gauge length	

3.1.1.4. Length of Manufacturing. The dimensions of the specimens are shown in Figure 3.3 below. Total length is 4360 mm and nominal length between socket heads is 4000 mm. After cutting by the designed length, the strand is finalized after fixing sockets at both ends.

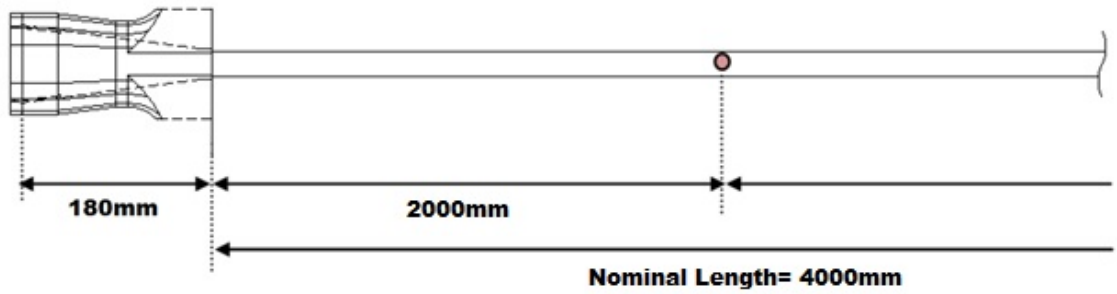

Figure 3.3. Dimensions of the test specimens.

3.1.1.5. Specification of PWS. The cable specimen (parallel-wire bundle) has the hexagonal configuration shown in below Figure 3.4, representing the most compact possible configuration of a nineteen parallel wire strand.

5-19 PWS Strand Section (Hexagonal Shape)

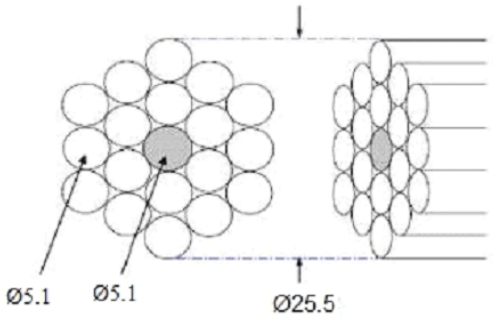

No. of wires Ø x n	Size (mm)	Nominal area (mm^2)	Unit weight (kg/m)	Breaking load - AUTS (kN – tonf)	
				39.07 kN (Average value of tested wires)	
5.1 x 19	25.5	388,14	3,07	742.33 kN	74,50 tonf

Figure 3.4. Strength and dimensional properties of the 5-19 PWS strand (Hexagonal shape) specimens.

3.1.1.6. Tape Seizing. In an axial direction, the filament tapes are wrapped 5 times on the bundle of wires in 50 mm interval in order to maintain hexagonal shape of a strand. The wrapping layer shall be uniform and compact without any surface damage of the tape such as broken parts or scratches. The quality requirement of filament tape is below. Technical data sheet is presented in Figure 3.5 and Appendix H.

Type	Bi-Directional Filament Tape
Width	50 mm
Total Thickness	0.14 mm
Tensile Strength	2600 N/100 mm width
Elongation at Break	6%
Adhesion to Steel	109N/100mm width

Figure 3.5. General tape technical data table and picture.

Figure 3.6. PWS specimens preparations for socketing.

3.1.2. Specimen of Socket Material

The simple bearing socket is selected for the experimental study and it is described in Chapter 2.1.3 above. The socket (anchoring apparatus) shown in the 3D drawing (in Figure 3.7) serves to anchor PWS strand which was used in the test program. A socket is attached to the cable at both ends and has a cylindrical outer circumference and a conically extending inside circumference. The conical inner circumference narrows from the back toward the front end and cavity angle of 4°C inside the basket. On the back end, that is, the end of the anchoring socket having the largest diameter.

As shown below Figure 3.8, the array plate has nineteen through bores corresponding in number to the number of wires. The spacing of the through bores is selected in accordance with the intended uniform spacing of the wires of the spread-apart end of the wire bundle and the envelope of which has the shape of a hexagon. For this experimental program, in total 10 pieces of sockets were manufactured according to related specifications.

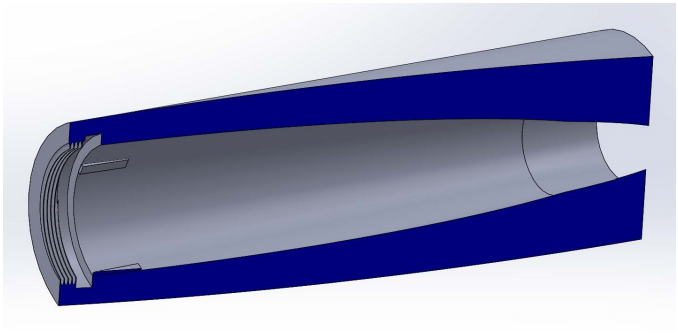

Figure 3.7. Side cross-sectional view of the socket material.

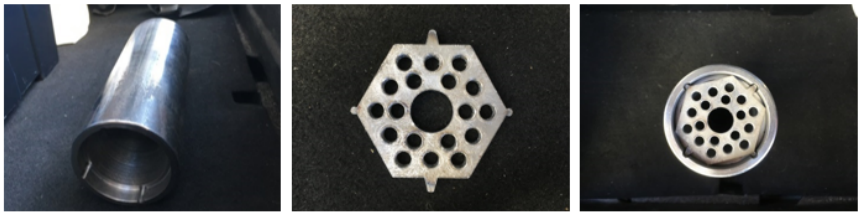

Figure 3.8. Front view of the socket material, the array plate, the combination of the socket material and the array plate.

3.1.2.1. Mechanical Properties of the Socket Material. The strand socket material confirmed with the DIN 17100 (ST52.3) international standards. The socket was free from any surface damage. No welding on socket is allowed.

Table 3.4. Mechanical properties of the socket material.

Division	**Y.P N/mm2**	**T.S N/mm^2**	**E.L %**	**Charpy absorbed energy (J)**	
				Impact test temperature	V-Notch Specimen 3 piece Avg.
ST52-3	355 Min	550 Min	18 Min	20	27 Min

3.1.2.2. Dimensions of the Socket and the Array Plate. The length of the socket was determined by considering the required bonding length and the stability of the casting medium using the procedure specified in Chapter 2.2.4. The dimensions for the cone-shaped socket head and array plate are illustrated in Figure 3.9 and Figure 3.10. Steel was machined according to this shop drawing. After machining, surplus material shall be gouging and grinding.

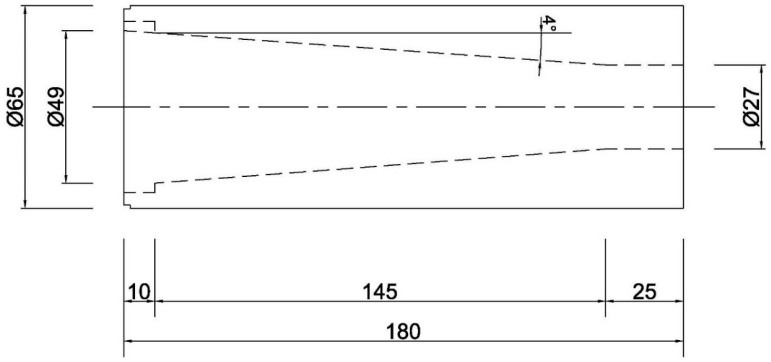

Figure 3.9. Socket dimensions of the strand specimens.

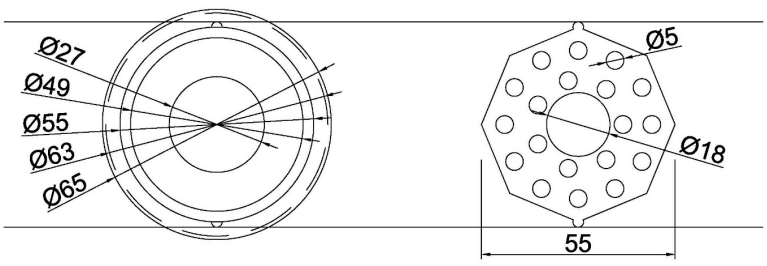

Figure 3.10. Socket and array plate dimensions of the strand specimens.

3.1.2.3. Socket Manufacturing Process. Before machining process, the mild steel bar was cut according to desired length of the socket material. Semi-automatic horizontal band saw machine as shown below Figure 3.11 was used to cut solid steel bar.

Figure 3.11. Band saw machine (left-hand side), Mild steel bar and cut bar (right-hand side).

During the manufacturing of a socket material, machining processes is needed to remove excess material. Turning is a machining process performed by a device called lathe is used as means of removal. After cutting process, turning process was implemented as shown below Figure 3.12.

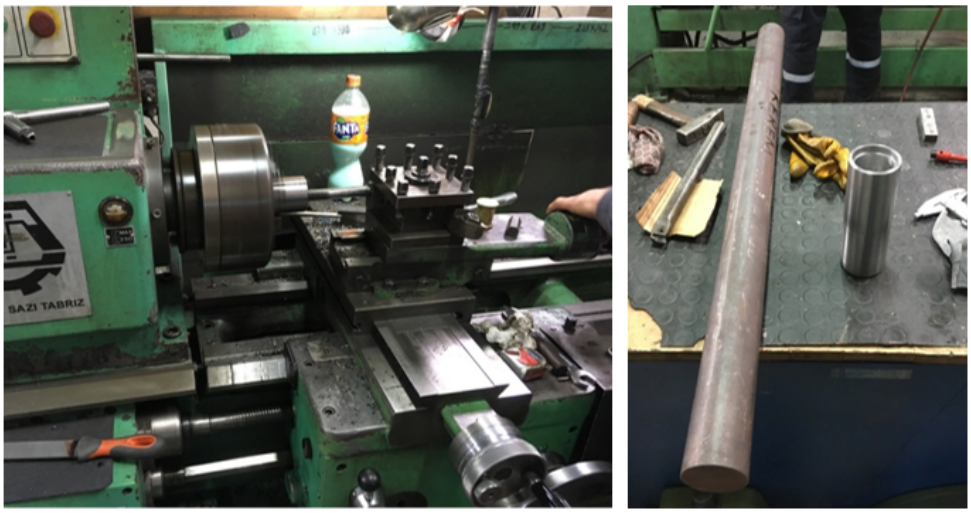

Figure 3.12. Lathe machine mild steel bar (left-hand side9 and machined socket material(right-hand side).

3.1.3. Assembly of PWS and Socket Material

A method is described for a nineteen of parallel high-tensile steel wire as below. The end of the strand is introduced into a fixed anchoring socket and sealed with a pourable material. In order for the anchoring socket to have improved properties under static stress, without requiring additional structural safety features, and yet can be manufactured at less expense, it is provided that the strand opened for some distance from the associated end in such a manner that the wires extend uniformly all the way through the conical inner region of the anchoring socket.

3.1.3.1. Hot Casting Method. The hot casting socketing procedure is conformed to the requirements of ISO 17558, EN 13411 this procedure:

(i) Before the socketing, until the opened length of nineteen of parallel wire, the socket material and the array plate were removed dirt, impurities and grease from the surface by degreasing process as shown in below Figure 3.13 (Caustic soda → Flux cleaner → Water).

Figure 3.13. Caustic soda (#1), Flux cleaner (#2), Water (#3) and degreasing process for parallel wires.

(ii) After the cleaning process, the sockets and wires were visually examined carefully for signs of physical damage.

(iii) The geometric center of strand shall be in accordance with that of socket on its both ends. The length needed for socketing is 180 mm. All wire shall be

in position of special made array plate as shown in Figure 3.14. Once wire is positioned at array plate, it doesn't need to measure the tolerance of socket location because the array plate is made optimum size including considered area during the pouring. Hereby, the individual wires are spaced apart uniformly, with the slight twisting of the strand causing the individual wires to open up in a straight line and in a conical pattern, without bending as shown in below Figure 3.14, in a uniform manner over the entire area that will later receive the casting material. As a result, the cast cone inside the socket can be manufactured more accurately in terms of its length and its grip on the individual wires. In this manner, it is also assured that the wires are anchored in the same section, or uniformly, so that relative movement between them is avoided.

Figure 3.14. Wire position at array plateau.

(iv) Advantageously, the socket holding plate (as shown in Figure 3.15) used in the base area of the anchoring socket simultaneously acts as a sealing element for the anchoring socket while the viscous casting material is being introduced.

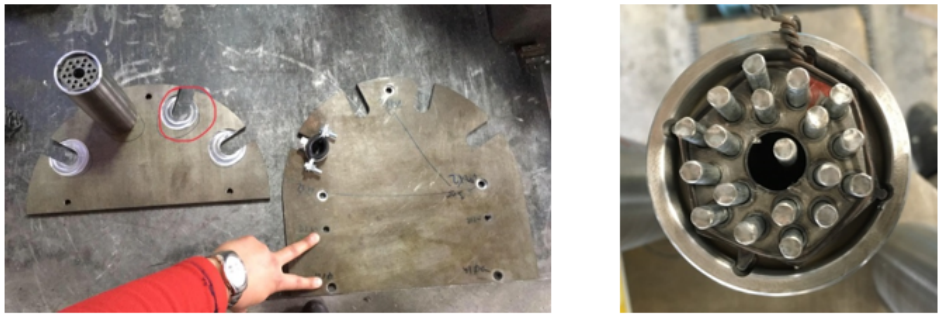

Figure 3.15. The socket holding plates (left-hand side) and the array plate and socket (right hand-side).

(v) Additionally, the base of the socket was sealed with clay to prevent casting material escaping from the base of the socket as shown below Figure 3.16. Sealing is vital to prevent voids at the bottom of the socket. It is worthy of note that two-thirds of available wedging forces are concentrated in the bottom third of the socket. Therefore, voids must be eliminated as they could cause premature failure of the socket.

Figure 3.16. Top view of the specimen and socket holding system just before the socketing (left-hand side), sealing the base of the socket with clay for both socketing methods (right-hand side).

(vi) Socket inserted arranged strand shall be fixed to the socketing table by socket holding plate as shown in Figure 3.17. The strand shall be fixed to keep the straightness and perpendicular by clamping of middle height of socketing table as shown below. The height from floor to socket is 4.5m.

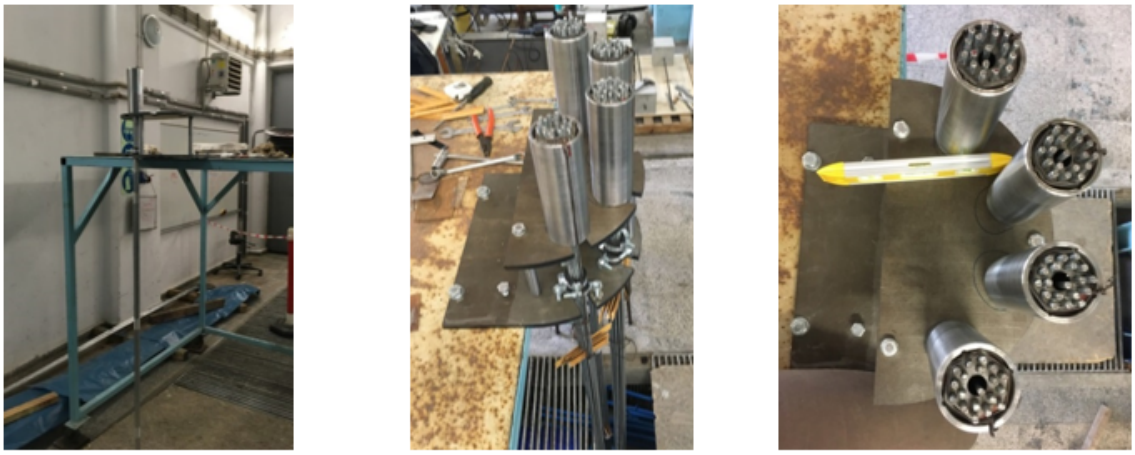

Figure 3.17. The socket holding system.

(vii) Axis of the strand and base surface of the socket shall be in a right angle in any direction, the tolerance is less than 0.5 deg. Therefore, the axes of the strand and socket were carefully aligned.

Figure 3.18. Adjusting and leveling the socket holding system.

(viii) Zinc-Copper Alloy (Zn 98±0.2%, Cu 2±0.2% on weight percentage) was used to cast to fix the sockets with a strand as shown below.

Figure 3.19. The Zinc-Copper Alloy weights.

(ix) The socket was uniformly preheated to 175^{o}C±25^{o}C in order to prevent the casting material from premature solidification and to ensure the permeability inside the sockets. The pre-heater was used as shown below Figure 3.20. Thermometer has to be checked regularly against other calibrated thermometer. The checks to be performed at start of work and at interval during the work.

Figure 3.20. The Zinc-Copper Alloy weights.

(x) The casting was carried out in the range of 460^{o}C±10^{o}C considering the temperature reduction of alloy material. The heat checks were performed at start of

work and at interval during the work.

Figure 3.21. The heat check for alloy material.

(xi) Molten Zn-Cu alloy was then poured into the sockets. The casting was one continuous operation as shown below. Hot casting is a skilled operation that must be performed by competent personnel after casting process was completed; a direct metal-to-metal joint is established between the metallic casting material and the wires or strands of the cable or bundle.

Figure 3.22. Hot casting operation by competent founders.

(xii) Cooling was applied air cooling method when casting alloy become up to fully cooling. The cooling time after socketing was approximately 3∼4 hours.

Figure 3.23. Pictures of test specimens assembled by hot casting method.

3.1.3.2. Cold Casting Method. A cold socketing compound which was commercially available Wirelock^{TM} was used to fix the sockets with a strand. Certificates and TDS for Wirelock^{TM} are presented in Appendix B. It was decided not to test the cold socketing compound in this fire test programme as it is flammable, although it is used for suspender cable applications.

The cold casting socketing procedure is conformed to the requirements of ISO 17558, EN 13411 and this procedure:

(i) First five steps of hot casting procedure that is outlined above were also implemented for cold socketing method.

Figure 3.24. Preparation for socketing (left-hand side), prior to clamp the wires on socket holding system (right-hand side).

(ii) Compound consists of two containers one liquid and one with powder. All of the resin was poured into the powder after then it was mixed for 2 minutes. While mixing, the compound must turn a green/blue color.

Figure 3.25. Observation of green/blue color.

(iii) After mixing, the compound was slowly and continuously poured down one side of the socket to ensure good penetration and to allow air to escape.

Figure 3.26. Preparing strand & socket, mixing, pouring.

(iv) After pouring the specimen was ready in 1 hour.

Figure 3.27. The specimen was ready to static test.

3.2. Test Equipments

The detailed technical specifications for all equipments which were used in this test program contained in Appendix section.

3.2.1. Hollow Plunger Cylinder (Hydraulic Cylinder)

Plunger cylinder which allows for both pull and push forces, was used for tensile testing before and at the fire test. The hydraulic cylinder is shown in Figure 3.28.
Brand Name: ENERPAC
Model: RRH- Series

Figure 3.28. Front view of the hydraulic cylinder.

Table 3.5. Specifications of the hydraulic cylinder.

Cylinder Capacity	Stroke	Model Number	Max. Cylinder Capacity		Oil Capacity		Coll. Height	Ext. Height	Out. Dia.	Cen. hole Dia.	Weight
ton	mm	RRH-1001	kN		cm^3		mm	mm	mm	mm	kg
			Adv.*	Retr.*	Adv.	Retr.					
95	38		931	612	505	333	165	203	212	79,2	33
*Adv. = advance *Retr. = retract											

3.2.2. Pan Cake Load Cell (100tf)

Tension and compression load cell was used for the tests. The load cell is shown in Figure 3.29 and the insrument calibration report is presented in Figure F.1

Brand Name: CAS Co. Ltd.

Model: LSU - 100T

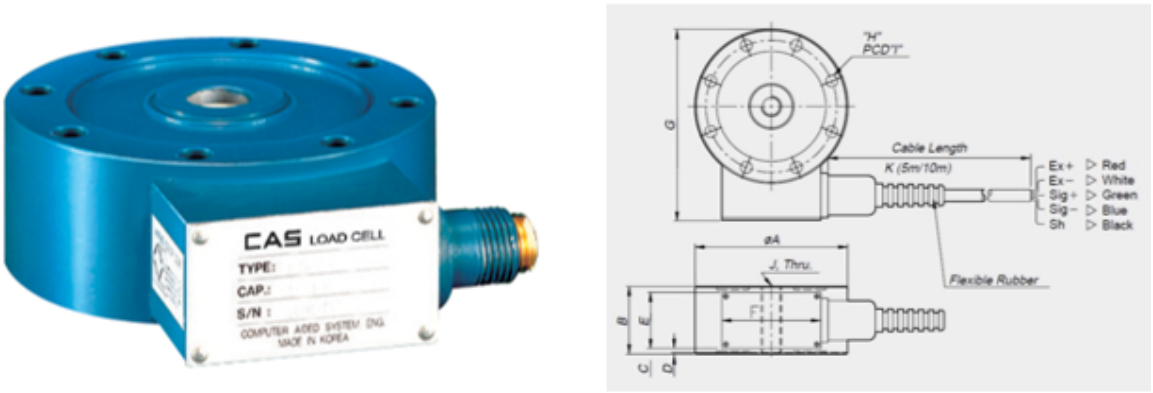

Figure 3.29. Front view of the load cell and load cell dimensional drawing.

Table 3.6. Specifications of the load cell.

Max. capacity	**tf**	**100(LSU)**	
Rated output	mV/V	2.0^o±0.005	
Zero balance		0 ±0.02	
Accuracy class		A	B
Combined error	%	0.02	0.05
Repeatability	%	0.01	0.02
Creep for 30min.	%	0.03	0.03
Zero Value	%/10 ^{o}C	0.03	0.03
Output value	%/10 ^{o}C	0.03	0.03
Excitation Recommended	V	10	
Maximum Resistance	V	15	
Input	Ω	350 ±3.5	
Output	Ω	350 ±3.5	
Insulation	MΩ	> 2,000	
Compensated temperature range	^{o}C	-10 to +40	
Operating temperature range		-20 to +80	

3.2.3. Distance Sensor

The total extension of the specimen was measured with piston ram displacement.
Brand Name: SICK
Model: Dx50-2

Measuring range	200 mm ... 30,000 mm, 90 % remission [1) 2)] 200 mm ... 17,000 mm, 18 % remission 200 mm ... 10,000 mm, 6 % remission
Resolution	0.1 mm
Repeatability	0.5 mm ... 5 mm [2) 3) 4)]
Accuracy	± 7 mm [4)]
Response time	0.83 ms ... 75 ms, 0.83 ms / 3.33 ms / 8.33 ms / 25 ms / 75 ms [5)]
Switching frequency	1,000 Hz/250 Hz/100 Hz/33 Hz/11 Hz [5) 6)]
Output time	0.33 ms/1.33 ms/3.33 ms/10 ms/30 ms [5) 7)]
Light source	Laser, red [8)]
Laser class	2 (IEC 60825-1:2014, EN 60825-1:2014)
Typ. light spot size (distance)	10 mm x 10 mm (at 10 m)

Figure 3.30. Laser distance sensor (left-hand side), technical data (right-hand side).

3.2.4. Linear Potentiometer (Electronic Circuit Series)

The potentiometer was used to detect and measure linear position and velocity using a flexible cable. As the transducer's cable extends along with the PWS, it causes the spool and sensor shafts to rotate. The rotating shaft creates an electrical signal proportional to the cable's linear extension or velocity.
Brand Name: OPKON
Model: ERTL

Figure 3.31. Linear Potentiometer.

3.2.5. Thermocouples for Steel Temperature

Thermocouples to measure steel specimen temperatures shall be insulated double glass fiber insulated wire as per EN 1363-1 Fire Resistance-Tests -Part 1: General Requirements. It shall have minimum 0.5 mm diameter. They shall be used once only. In this study 0.8 mm Type K wire is to be used. The thermocouples are double ceramic insulated and 1200^{o}C fire retardant. For fixing of thermocouples on the specimen, pipe clamps were used.

3.2.6. Fire Furnace

The test furnace as per EN 1363-1 shall be design to work with liquid or gaseous fuels, is shown in below Figure 3.32. In this study, Turkish Standards Institution (TSE) indicative furnace was used and is being worked with natural gas. Furnace lining and material density requirements comply with EN 1363-1. Fuel and air ratio shall be approximately 4% when the test sample is non-combustible as per EN 1363-1. In this furnace verifications were done by TSE as yearly basis.

The furnace has 1.55 meter depth and cube shaped. The furnace controller has a mechanism for implementing a specific rate of heating and furnace control center is presented in Figure 3.47. The furnace has three independently heated zones that are monitored and controlled by a temperature control system, as described in EN 1363-1 and also controlled by means of calculating mean temperature of the plate thermocouples.

Furnace thermocouples shall be plate thermometers which is approximately 150 mm long by 100 mm wide by 0.7 mm folded and shall be made by folded nickel alloy plate. Thermocouple wire (type K) shall be fixed to geometric center of it. Thermocouple wire properties shall be comply with EN 60584-1, which is contain mineral insulation in heat resistance steel alloy sheath of nominal diameter 1 mm to 3 mm. TSE Fire Laboratory uses 1 mm diameter Type K thermocouples. Plate thermocouples shall be insulated with a pad of inorganic insulation material nominally 97 mm

by 97 mm by 10 mm thick, density (280 ± 30) kg/m^3. Thermocouples calibration is being performed and periodically verified with TSE calibration department and with TSE Fire Resistance Laboratory calibrator. After 50-hour thermocouples shall not be used any more as per EN 1363-1 Fire Resistance-Tests -Part 1: General Requirements. Thermocouples temperature values is being controlled by software in order to follow the proposed time-temperature curve and recorded by software per second. The furnace zone has a type K thermocouple mounted to exterior of the heating panels. The furnace control temperature ranges from 300^{o}C to 1200^{o}C.

Figure 3.32. Fire Furnace from TSE Laboratories Complex.

The pressure in the fire furnace shall be measured by sensors described in EN 1363-1 Fire Resistance-Tests -Part 1: General Requirements. The sensors shall operate within the limits specified in EN 1363-1 Fire Resistance-Tests -Part 1: General Requirements.

3.2.7. Steel Test Frame

The cable specimen was installed and tested in horizontal steel test frame as shown below Figure 3.33 and Figure 3.34. The steel test frame was specifically designed by the author for this project by using structural analyzing program (SAP2000) which presented in Figure C.3. Test frame plan (Autocad) and part list are presented in Figure C.1 and Table C.1, respectively. Even though the steel members were insulated from fire, the steel profiles and plates were overdesigned on purpose due to the undesirable creep condition for steel members under both compression load and elevated temperature. If creep strains occur on the steel elements of test frame, than the measurement of elastic modulus and heat transfer rates on the wires will not be accurate.

Figure 3.33. Side view of the steel test frame.

Figure 3.34. General views of the steel test frame.

3.2.8. Socket Locker

The socket locker was specifically designed and manufactured in order to locked one end socket to the test frame and locked other end of the socket to the piston ram of the hydraulic cylinder. Therefore, there are two socket lockers which manufacturing pictures are presented below. Mill test certificate and quality cetificate for socket lockers are presented in Appendix D. After machining and cutting of the socket lockers, wire erosion (EDM) cutting was implemented for both socket lockers in order to cut thin sections without deformation as shown below figures. Lastly, threading process was conducted in order to lock and lock-out when changing of the specimens prior to completion of the current test.

Figure 3.35. View of the socket lockers after machining process and EDM control panel.

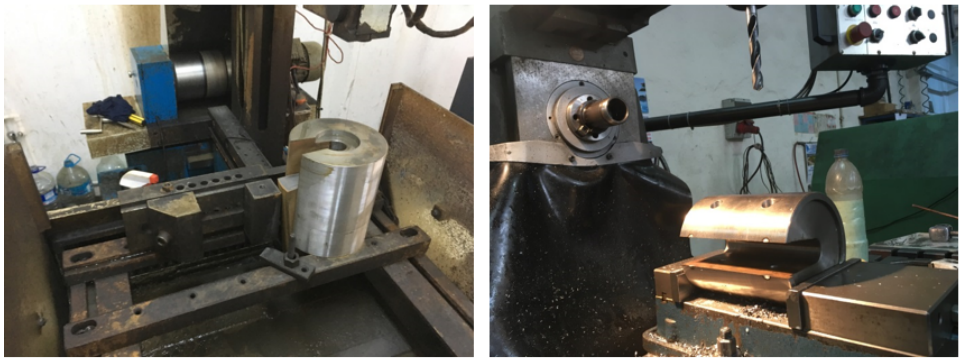

Figure 3.36. View of the socket locker after EDM cutting process (left-hand side) and the socket locker after threading (right-hand side).

3.3. Gasoline Pool Fire Scenario

Two time-temperature curves are used in the furnace for the cable testing. The first one is standard hydrocarbon fire (UL 1709) which was used for Test 3. The second fire curve is created by Fire dynamics simulator (FDS) program simulating a tanker fire. The second (natural) fire curve has limited fuel; hence unlike hydrocarbon fire, it has a cooling phase. Both fire curves are plotted in Figure 3.37.

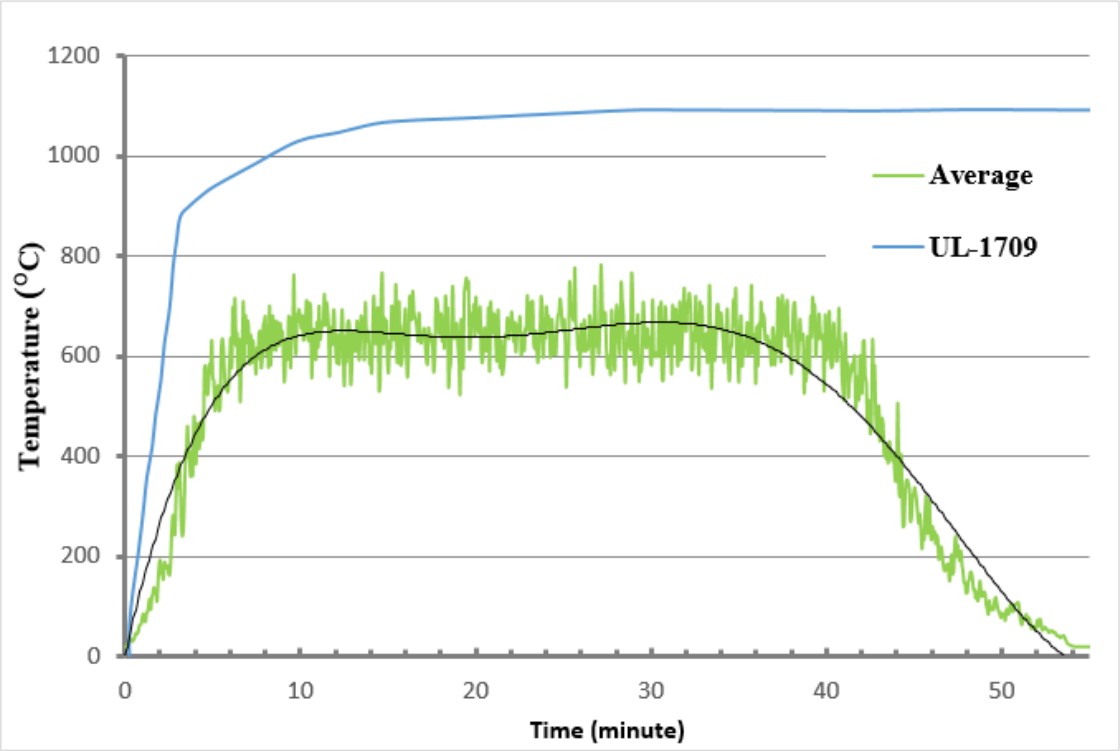

Figure 3.37. The average temp. for designed pool fire scenario (Average) and standard hydrocarbon pool fire (UL-1709) time-temp curve.

The fire load from a burning gasoline tanker estimated using MacArthur Maze Fire in 2007 as a case study. On April 29, 2007, a tanker truck carrying 32.6 m3 of gasoline crashed while traveling on a connector ramp from southbound I-80 to I-880 in the MacArthur Maze freeway corridor near Oakland, CA, USA (Quiel *et al.* 2015). The peak heat release rate HRR per area is estimated as 1.67MW and the calculated fuel burning rate from given HRR curve is shown in Figure 3.38. The gasoline will burn out in less than 60 minutes. Benzene (C6H6) molecule is assumed to be the reaction

material used in the combustion process. The details for the combustion are shown in Table 3.8.

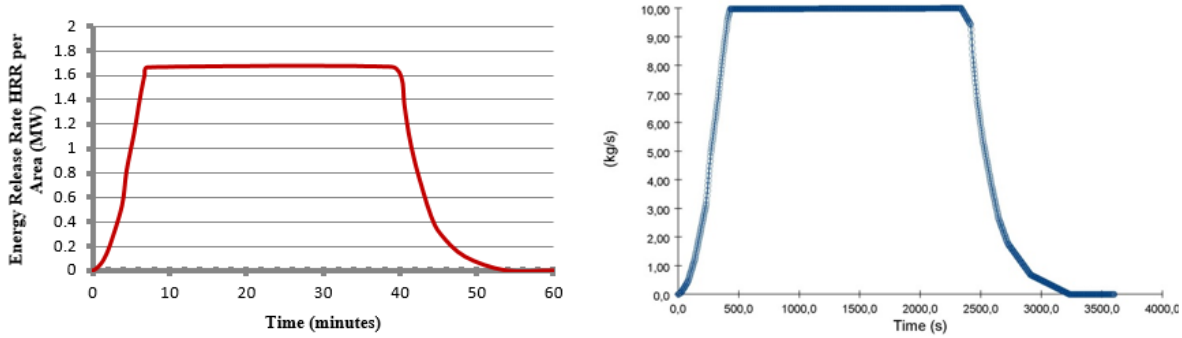

Figure 3.38. The estimated HRR curve per fire burning area for the gasoline tanker explosion and the simulated fuel burning rate.

Table 3.7. Combustion details.

Reaction Material used in Combustion	Benzene
Molecule	C_6H_6
Heat of combustion	40MJ/kg
CO yield	0.067
Soot Yield	0.181
Hydrogen Fraction	0.14

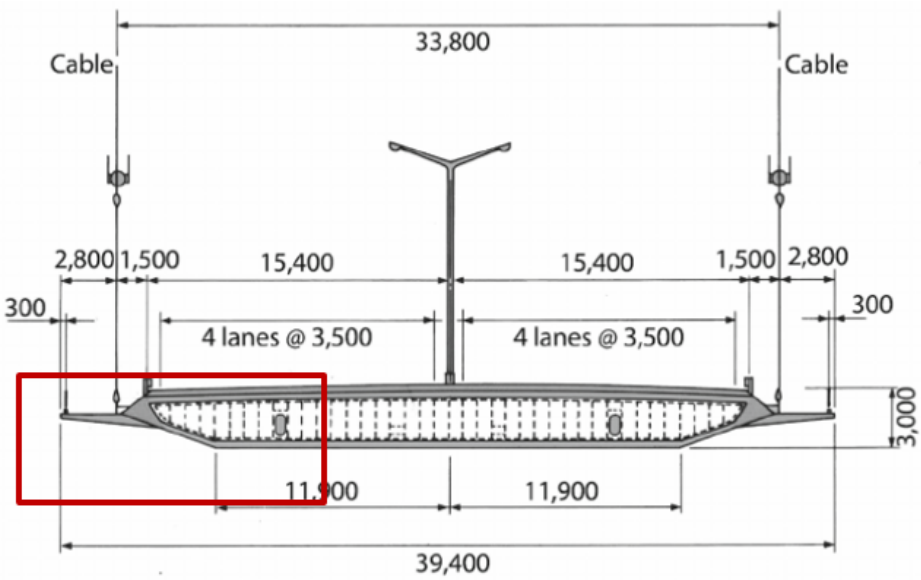

Figure 3.39. Fatih Sultan Mehmet Bridge main span and deck dimensions (Kilic *et al.*, 2017).

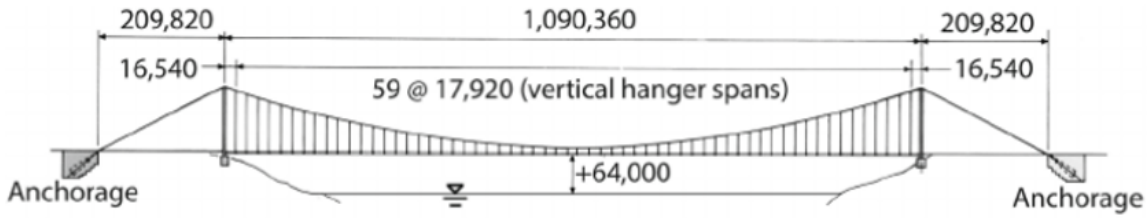

Figure 3.40. Side elevation and plan of the Fatih Sultan Mehmet Bridge (Kilic *et al.*, 2017).

The suspender cable location and fire burning area are chosen according to Fatih Sultan Mehmet Suspension Bridge dimensions as shown in Figure 3.40 and Figure 3.39. Here, the distance between each suspender is approximately 20m. The gasoline spill will steadily outflow from the tanker, and the gasoline will leak onto the deck, which is assumed to cover half of the deck (2 lanes) and 4.3m wide cable region (approximately 12m in total). The spill (burning) area or the footprint of the tanker is therefore 12m by 20m rectangle.

A snapshot from FDS analysis is shown in Figure 3.41. The soot particles (smoke) as well as fire flames are shown at the instance when peak HRR is released from the tanker. The temperatures near the cable location at 0.5m, 1.0m and 1.5m are plotted in Figure 3.42. The average temperature - time curvature of these locations is plotted in Figure 3.37 and this curvature was used for Test 4 and Test 5.

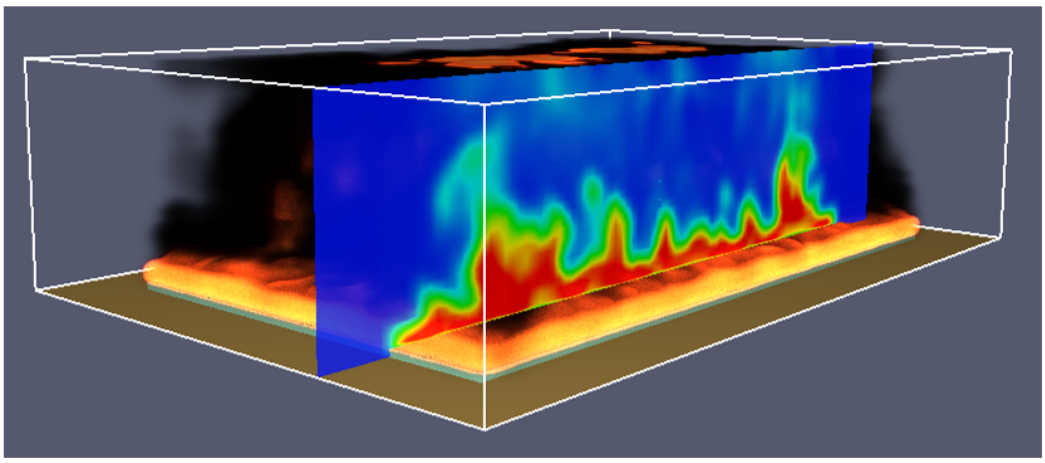

Figure 3.41. FDS analysis fire flame and smoke snapshot at peak HRR (7 minutes).

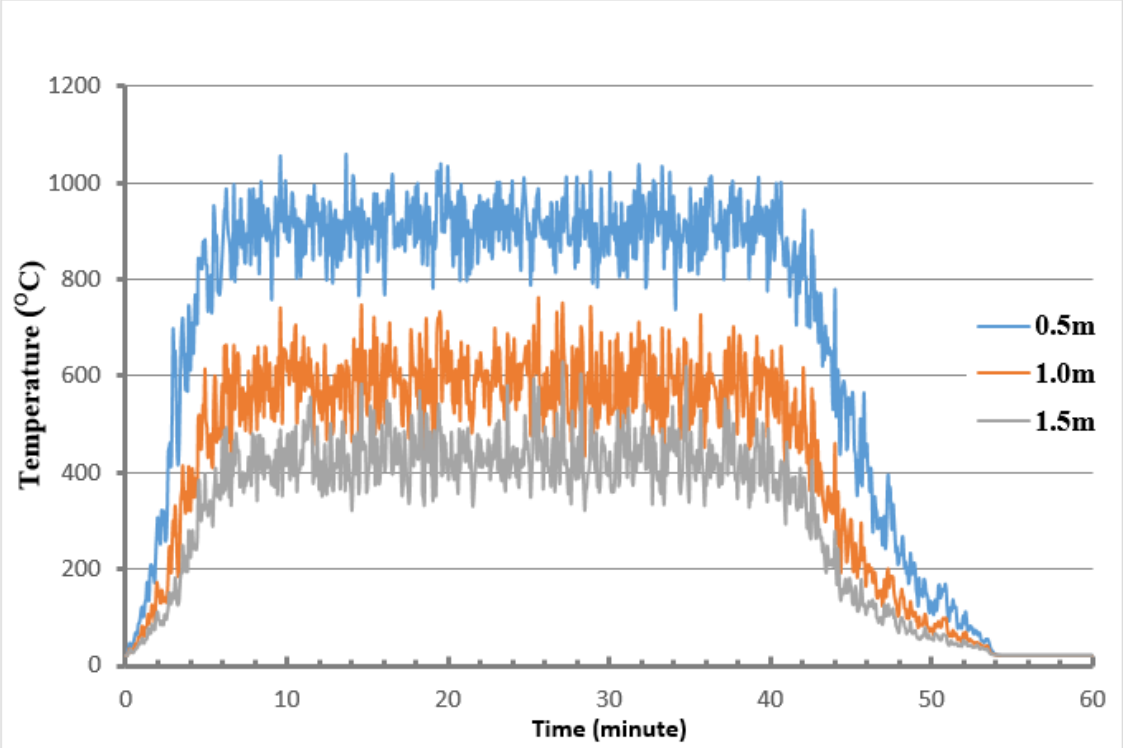

Figure 3.42. Temperatures near the cable location at 0.5m, 1.0m and 1.5m.

3.4. Test Setup

Testing was carried out using a specially designed steel frame and a hollow plunger cylinder which allow for pull and push forces. 3D views of test system are presented in Figure C.2. The cable specimen was assembled in the horizontal large test frame. One end socket of the specimen was gripped at the one end of the frame and was placed inside the furnace so that directly heating nominal length was 1.20 meter for PWS. Other end socket of the specimen was pulled by hydraulic cylinder. In other words, a dead end (Figure 3.44) that was the fixed socket on the steel plate and an active end (Figure 3.44) that was moving socket by hydraulic cylinder which was supported with ratchet strap during the test in order to protect the test equipment in such cases like rupture or socket draw. The 5x19 cable setup is presented in Figure 3.43.

Figure 3.43. Cable setup for Static Test.

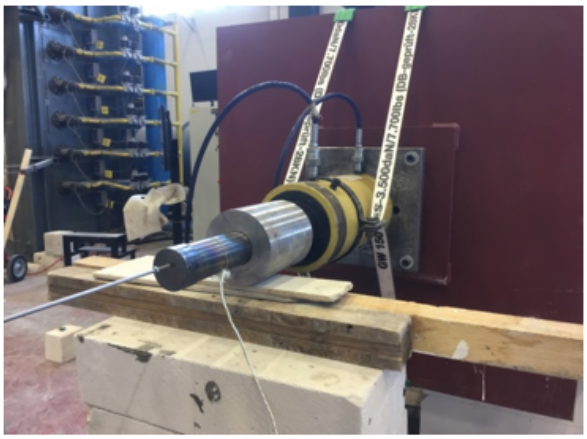

Figure 3.44. Dead (Passive) end (left-hand side) and active end of the socket head (right-hand side).

The socket and PWS specimens were instrumented with 4 type-K thermocouples. Six thermocouples were placed inside the furnace. One was attached on the socket material, referred to as TC1, and the others were placed at intersection point of the socket and strand with 30 mm intervals, referred to as TC2, TC3, ..., TC6, respectively. On the other hand, the out-of-furnace thermocouples were attached 1 meter next to TC6 with 1 meter intervals on the PWS, referred to as TC7, TC8. The last but one thermocouple was attached at the other intersection point of the socket and strand,

referred to as TC9. TC10 was placed at active end of the socket. The half of the testing system inside and nearby furnace was insulated by ceramic fiber blanket, as shown below figures. Each test followed the same sophisticated set-up procedure as presented below Figure 3.45.

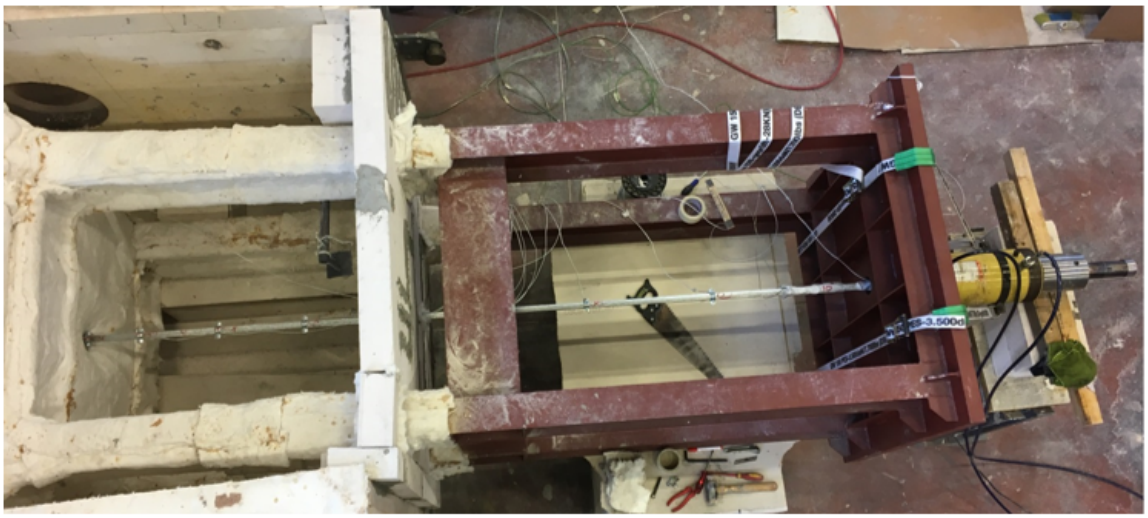

Figure 3.45. Top view of the cable setup for Fire Test.

In case of Test 5, the specimen was insulated with ceramic fiber blanket (128 kg/cm^3) with 25mm thickness as shown in below Figure 3.46. Its thermal conductivity is 0.11 W/Mk and specific heat is 1130 J/kg ^{o}C. The technical data sheet for ceramic fiber blanket and its adhesive are presented in Figure J.1.

Figure 3.46. Insulated socket head (left-hand side) and insulation of the specimen S5 with ceramic fiber blanket (right-hand side).

For the fire tests, the furnace is monitored and controlled by TSE engineers in the furnace control center as shown in Figure 3.47. For all tests, measurements, including the load cell signals were recorded by a testbox 1001 data logger and ram piston during test were recorded using a digital distance sensor or linear potentiometer. The data logger and laptop PC used to record the test data is shown in Figure 3.48. The system configured to read applied load, piston displacement continuously at a sampling rate of 1 Hz. Furthermore, strain gauges were used for some of the tests as shown in Figure 3.49.

Figure 3.47. The view of the furnace control center from TSE Laboratories Complex.

Figure 3.48. The view of the laptop PC and the data logger.

Figure 3.49. Strain gauge position on wire and TML strain gauge package.

All of related data should be gathered during and after both static and fire tests. These data including;

(i) Heat transfer rate or temperature-time history along the wire nominal length,
(ii) Load-displacement history,
(iii) Load level, temperature and location of the first and successive wire or socket failures,
(iv) Test pictures that give information on these tests.

3.5. Test Procedures

The test specimens have their own names which were S1, S2, S3, S4 and S5 in order to describe their characteristics. These names were used when discussing or reporting test results and the names could be found on the surface of sockets and tapes on the strand.

The following section outlines the procedures that were used for each kind of testing. All tests were completed at TSE Insulation Laboratories Complex between March 15^{th} and May 15^{th} 2018. The testing procedures were in accordance with the applicable ASTM's for multi-wire steel strand and are consistent with those used in previous studies.

For both static test and transient test, the specimen was proof loaded to 360 kN at ambient temperature and any socket draw was measured. Then the load was reduced to 5 kN, afterwards the following procedures were conducted.

The constant temperature test is not performed because the purpose of this kind of tests is to evaluate the cable performance at a specified target temperature. Thus, constant temperature tests are universally used to establish the material performance at a variety of temperatures; nevertheless, they are not realistically demonstrative of real fire exposure, throughout which an element is exposed to variable temperatures. The summary of the test program and test procedures is presented in below Table 3.8.

Table 3.8. Summary of the test program.

Test No.		**Specimen Name**	**Test Type**	**Casting Medium**	**Fire Type**	**Full Insulation (Y/N)**	**Initial Constant Load (kN)**
TEST 1		S1	Static Test	Zn-Cu alloy	-	-	-
TEST 2		S2	Static Test	Cold Socketing Compound	-	-	-
TEST 3		S3	Transient Fire Test	Zn-Cu alloy	Hydrocarbon fire (UL-1709)	N	325
TEST 4		S4	Transient Fire Test	Zn-Cu alloy	Pool fire	N	325
TEST 5	Part 1	S5	Transient Fire Test	Zn-Cu alloy	Pool fire	Y	325
	Part 2		Static Test After Cooling		-	-	-

3.5.1. Tensile Test Loading Sequence and Tensile Test Procedure

The specimens were submitted to static tests to determine the yield stress (%0.2 Offset), the ultimate tensile strength and the elongation at rupture. Furthermore, the PWS static loading tests were conducted to verify the results from the single wire tensile tests which were performed by the manufacturer is presented in Appendix A. Aforementioned two of the specimens were prepared for only static tests at ambient

temperature. One of the specimens was assembled by hot casting and the other one was assembled by cold socketing compound as shown below Figure 3.50. The assembly methods are explained in detail in above Chapter 3.1.3 above. Thus, the specimen S5 was subjected to static test after cooling which depending on same loading sequence and test procedure.

Table 3.9. Cable Static Test Criteria and Loading Sequence for 5.1 - 19 PWS.

Static Test for 5.1- 19 Cable Grade 1860 PWS				
Test Specification:	Particular Specification			
Criteria:	Strength >= larger value of 95% MUTS and %92 AUTS			
AUTS	742.33 kN			
MUTS	721.94 kN			
92% AUTS	682.94 kN			
95% MUTS	685.84 kN			
Larger Value (95% of MUTS)	**685.84 kN (Target force)**			
Load Steps:				
	%	Load (kN)	Keep time* (min.)	
	20	144.39	5	
	50	360.97	5	
	70	505.36	5	
	90	649.75	5	
	95	**685.84**	**5**	**Pass**
	100	721.94	5	

"Keep time" means the waiting time at the current load step during the test. During this time, the load level should be kept up in order to observe the pullout behavior at the head of the sockets.

The average of three (3) wire tensile breaking loads was 39.07 kN according to manufacturer test results, which was used as wire actual ultimate tensile breaking load. The cable specimen must reach the larger value of 95% of MUTS (Minimum ultimate tensile strength) and 92% AUTS (Actual Ultimate Tensile Strength) according to the test plan. If the breaking occurs at less than 95% of MUTS or 92% of AUTS the minimum breaking capacity, retest shall be carried out. The cable tensile load criteria

and the loading sequence for a specimen static test are given in above Table 3.9.

One of two possible outcomes was expected from each test:

(i) The entire strand would be pulled out from the socket material due to destruction of the bonding mechanism between the individual wires and the casting medium.
(ii) The wires in the specimen would be successively ruptured by the increasing load.

The first scenario was expected if the bonding resistance of the embedded wire in the casing medium could not withstand the ultimate tensile force of the wire. In such a case, the bonding strength of the embedded wire in the casting medium could be determined from the pullout force. The second scenario was expected if the bonding resistance of the embedded wire in the casting medium was sufficiently strong to withstand the ultimate tensile force of the wire. The pullout force of the specimen cannot be directly determined in such a case. However, it can be assumed that the pullout force is greater than the minimum ultimate force of the wire. (Yoo *et al.*, 2015).

Therefore, for the specimens, the first scenario was not acceptable. If any of the results fails to meet the requirements according to above load criteria, the failed strand shall be rejected and new wires shall be manufactured.

Two series of static loading test were performed:

- Test 1 - Specimen (S1) which was assembled by hot casting method.
- Test 2 - Specimen (S2) which was assembled by cold casting method.

Figure 3.50. Top view of S1 and S2 socket head.

Pull-out length can be determined as L_f - L_0 where L_0 (=1mm) was indicated by black line on the specimens as shown in Figure 3.51. L_f should be measured at least for three different wires after completion of the test. This initial procedure was followed for all tests in this project.

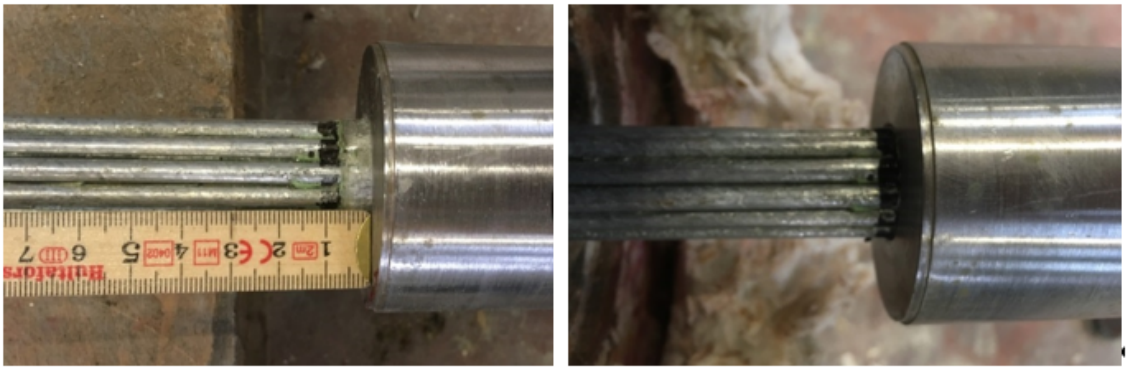

Figure 3.51. Measurement example of the L_f value (left-hand side) and black line on the specimens (right-hand side).

3.5.2. Transient Elevated Temperature Test Procedure (at Constant Load)

Three series of transient elevated temperature tests on the above mentioned specimens were performed. The test samples were socketed to determine the extension and

breaking strength of the strand under following conditions. Transient-state testing is clearly considered as the most realistic representation of an actual fire situation. However, transient tests are inherently more prohibitive in terms of time as well as interpretation of results. Loading and data acquisition procedures become significantly more demanding in comparison with steady-state tests. Therefore only a limited number of transient tests were carried out in order to provide a reliable representation of the actual behavior of PWS system. Three series of fire tests were performed:

- Test 3 - Hydrocarbon standard fire temperature-time curve (UL 1709) was exposed to unprotected specimen S3.
- Test 4 - Gasoline pool fire scenario time- temperature curve which is indicated in Chapter 3.3was exposed to unprotected specimen S4.
- Test 5 - Gasoline pool fire scenario time- temperature curve which is indicated in Chapter 3.3 was exposed to protected specimen S5. After fire test was completed if the specimen was not failed then after cooling static test was implemented when the specimen's temperature was drop to the ambient temperature.

The above mentioned fire scenarios exposed to the specimens. The 5-19 PWS system was firstly loaded to a desired stress level. When the strand system was tensioned to the predetermined stress level, the heating-up time was started. The strand system was held at the predetermined stress level during the test. The hydraulic cylinder held that the constant load by adjusting the piston head throughout any thermal elongation, creep, or relaxation. The test continued until the strand rupture or socket draw, and at that time temperature was recorded.

For this study, the estimated maximum time for failure of the unprotected specimens were 10 minutes and protected specimen was 50 minutes or it is assumed that firefighting efforts will be able to respond to the fire within 50 minutes of its ignition. Accordingly, it is estimated that result in failure in the range of 450 - 650^{o}C considering that previous fire tests on 7-wire strand as mentioned in above Chapter 2.4.1 - Former Experimental Studies of Cold-drawn Steel at Elevated Temperature.

Current design standards typically require that tensile stress in the suspenders should not exceed 67% of UTS, including material factors (Alampalli *et al.*, 2016). Furthermore, the test stress level was chosen as 45% of MUTS which is a load that is typical of cable-stay bridges (PTI, 2006) practice. Therefore, for the above mentioned fire tests the desired load was 325kN (45% of MUTS). Loading begins when temperature is stable enough.

Test 5 consists of two parts including transient elevated temperature test at constant load and static test after cooling. In such a way that specimen S5 was insulated with ceramic fiber blanket (128 kg/cm3) with 25 mm thickness as shown in above Figure 3.46. Its thermal conductivity is 0.11 W/Mk and specific heat is 1130 J/kg °C. If the specimen S5 is not fail until 60 minutes including a decay phase than the furnace was turned off and slightly opened, allowing the specimens to cool down naturally to ambient temperature. When the steel temperature drop at the room temperature, the hydraulic cylinder is started to pull one of the edge of the specimen S5 until it failed. In other words static test after cooling is implemented.

4. TEST OBSERVATIONS

4.1. General

A five series of testing procedures are outlined in Chapter 3 and this chapter summarizes the observations from the test program results. Both the static loading testing and fire testing are presented. After the tests, the specimen was removed from the test frame and the anchor heads were visually inspected.

For each fire test, the specimens were held under a constant load level typical to service level loads. According to PTI (2006), the tension elements are typically stressed to 45% of MUTS. The load level was chosen to determine the rupture temperature of in-service cable elements for suspender cables. Once the desired stress level was reached, the furnace was turned on while the cable maintained the stress level. The test was stopped once the PWS system failed and the ultimate rupture temperature was recorded. The rate of heating was obtained from the temperature history of the furnace prior to rupture.

Test 3 and Test 4 tests were conducted using the heating rates in accordance with hydrocarbon pool fire (UL-1709) and gasoline pool fire scenario. Test 5 was exposed to same heating rates with Test 4 but the S4 socket material and cable were insulated and later on S5 was exposed to static test after cooling which is outlined in Chapter 3. Both of the unprotected specimens S3 and S4 were failed in approximately 3 and 6 minutes. Failures occurred at or very close to the location of the thermocouple TC4 and TC3 respectively. On the other hand, protected specimen S5 was successfully passed the fire test and then static test after cooling was conducted.

Qualitative observations made during the test include the strand heating rate, physical changes to the specimens, cable expansion during temperature increase, failure surface examination, and the time elapsed between the first indication of failure and the moment of failure.

It is significant to take in to consideration that all specimens that were exposed to fire test experienced either a “cap and cone” tensile failure type or a necking down to a point tensile failure. These types of failure are an indication of a ductile failure and extremely ductile failure, respectively (Callister and Rethwisch, 2008). All heated specimens failed within the heated zone of the furnace, however, the specimens which were exposed to static tests at ambient temperature showed undesirable shear fracture failure type.

During the test, the furnace remained closed between temperature increases and decay phase. As per the TSE regulations the only possible way to observe the specimen was to wait until the furnace temperature cooled down to ambient temperature. All of data including plots of load vs. displacement, heat transfer vs. time along the wire nominal length, temperature vs. time and photographs of the specimens after testing have been included.

Due to the difficulties in establishing a clear contact on the wires, the strain gauge was not able to record any usable strain data. Therefore, the data which was obtained from strain gauges did not included in the test observations and test results chapter.

4.2. Test 1

The static test was performed on April 18^{th}, 2018. The force-extension relation along with the hydraulic cylinder piston opening pictures for the tensile Test 1 is shown in below Figure 4.1. S1 started to experience non-linear load-displacement behavior after exceeding a proportional limit of approximately 520 kN. The maximum load the cable reached is 704.46 kN which is 97.58% of MUTS. The displacement corresponding to the maximum load is 205.62 mm, which is 5.18% of the cable length between the bearing plates.

The test was terminated when there was a wire break after the cable reached the target load which is 686 kN (95% of MUTS). The cable passed the acceptance criteria.

During the failure a large amount of potential energy in the cable released - the strand recoiled with a load “bang”.

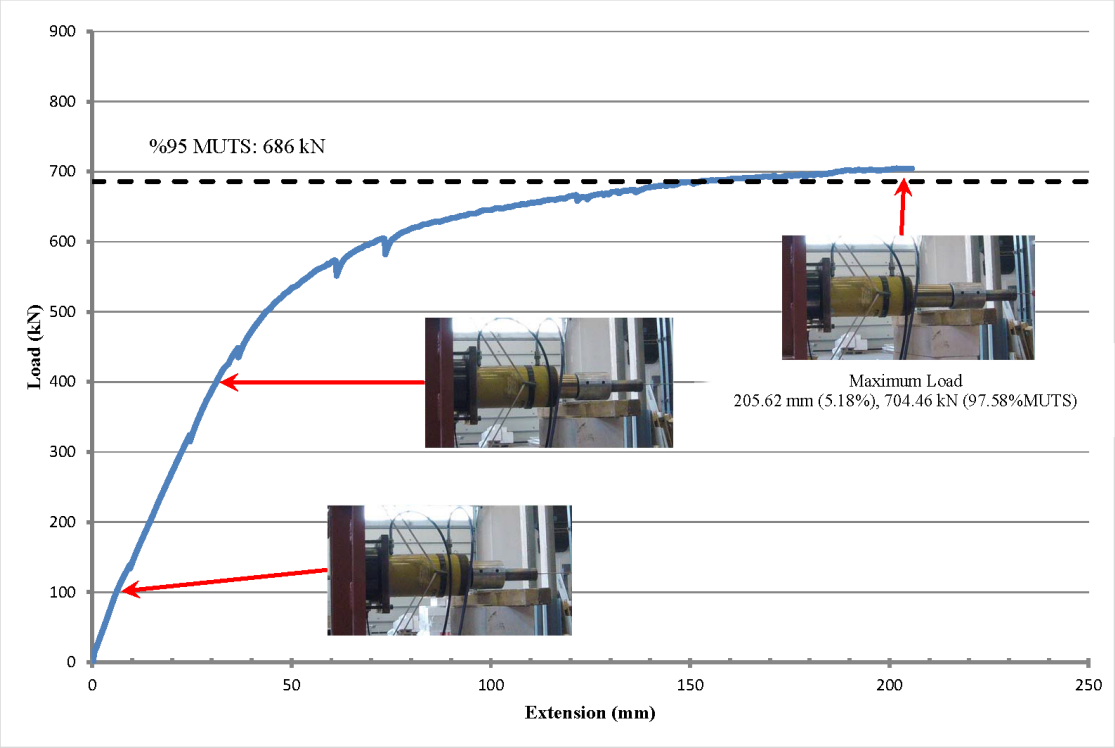

Figure 4.1. Force-extension relation for the static Test 1 including the view of the hydrolic cylinder piston ram opening at 100kN, 400kN and 700kN.

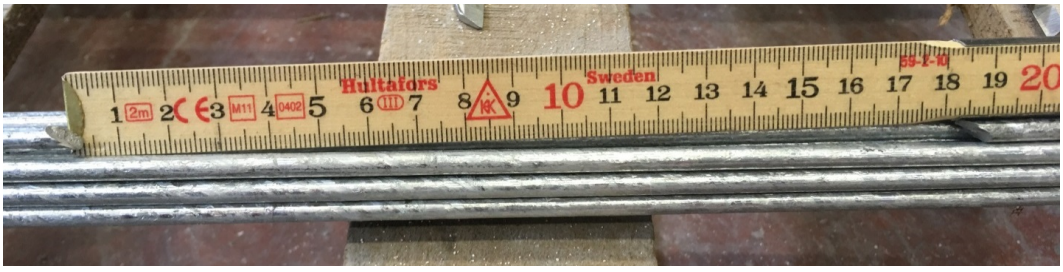

Figure 4.2. The wire fracture for S1.

After static test, the specimen S1 was removed from the steel test frame. The conditions of a dead end and an active end of the socket heads were visually inspected as shown in Figure 4.3 and Figure 4.5. The sockets were not dissected. There were no visible cracks or damage on the socket material. Figure 4.2 and Figure 4.3 show the typical wire breaks.

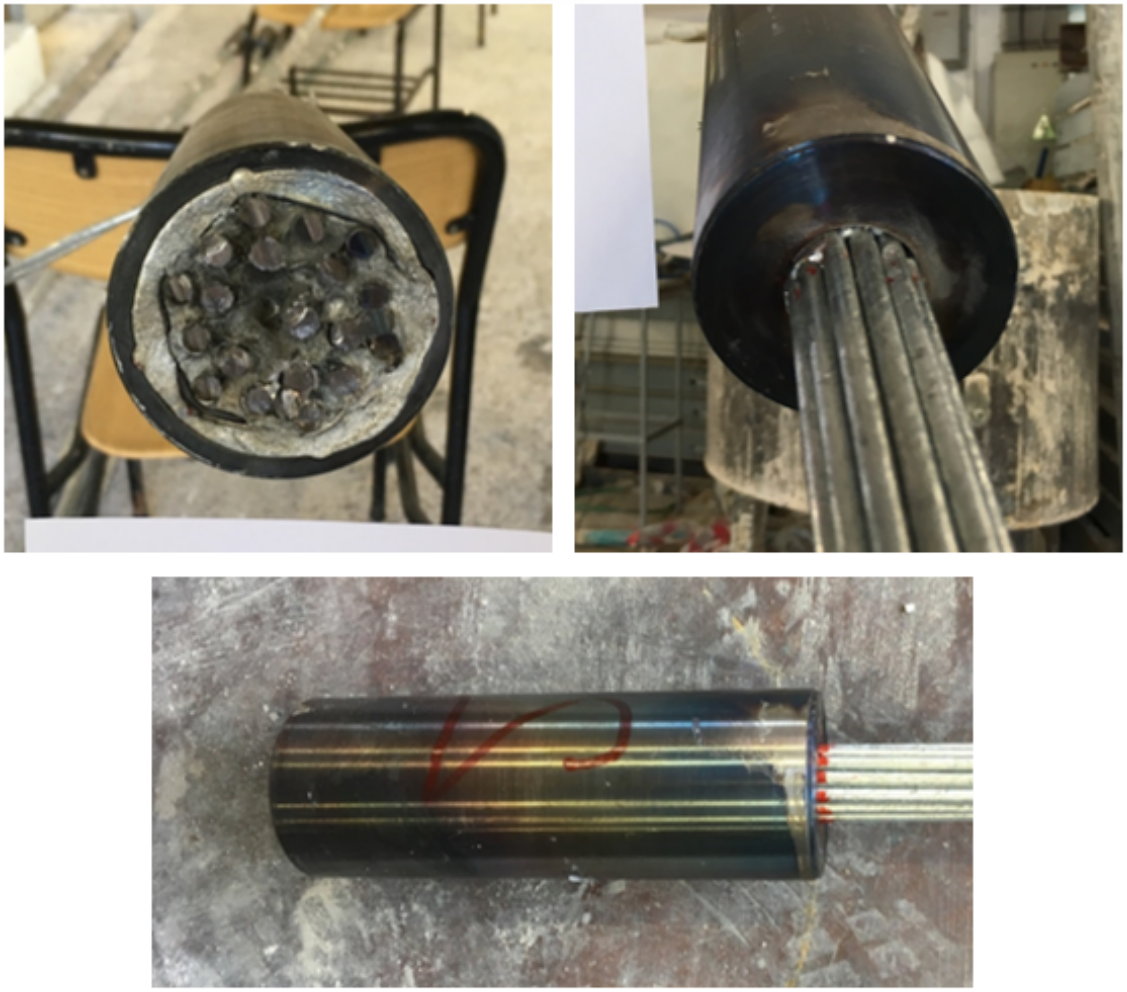

Figure 4.3. Condition of sockets after static Test 1.

Figure 4.4. Typical shear wire fracture for S1.

Figure 4.5. Condition both ends of the specimen S1.

4.3. Test 2

The tensile test was performed on April 19^{th}, 2018. The force-extension relation along with the hydraulic cylinder piston opening pictures for the tensile Test 2 is shown in below Figure 4.6.

The maximum load the cable reached is 695.59 kN (69.81) which is 96.35% of MUTS. The displacement corresponding to the maximum load is 190.66 mm, which is 4.80% of the cable length between the bearing plates. The test was terminated when there were two wire breaks after the cable reached the target load which is 686 kN (95% of MUTS). The cable passed the acceptance criteria.

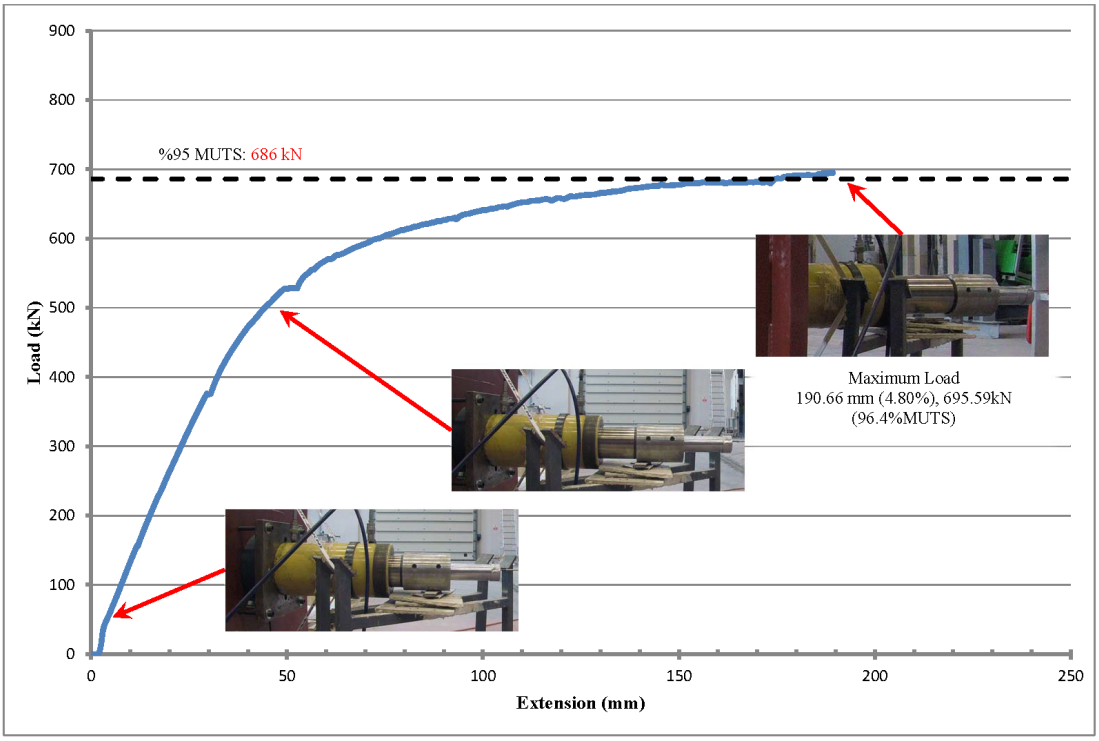

Figure 4.6. Force-extension relation for the tensile Test 2 including the view of the hydraulic cylinder piston ram opening at 50 kN, 500 kN and 695 kN.

The first ruptured wires observed around 20 cm next to the dead end socket and identified as external wire break. The second ruptured wire was located one of the internal wires which around 60 cm next to the dead end socket as shown in Figure 4.7 and Figure 4.9 shows the typical wire breaks.

Figure 4.7. The ruptured wire position for S2.

After static test, the specimen S2 was removed from the steel test frame. The conditions of a dead end and an active end of the socket heads were visually inspected

as shown in Figure 4.8 and Figure 4.10. The sockets were not dissected. There were no visible cracks or damage on the socket material.

Figure 4.8. Condition of sockets after static test.

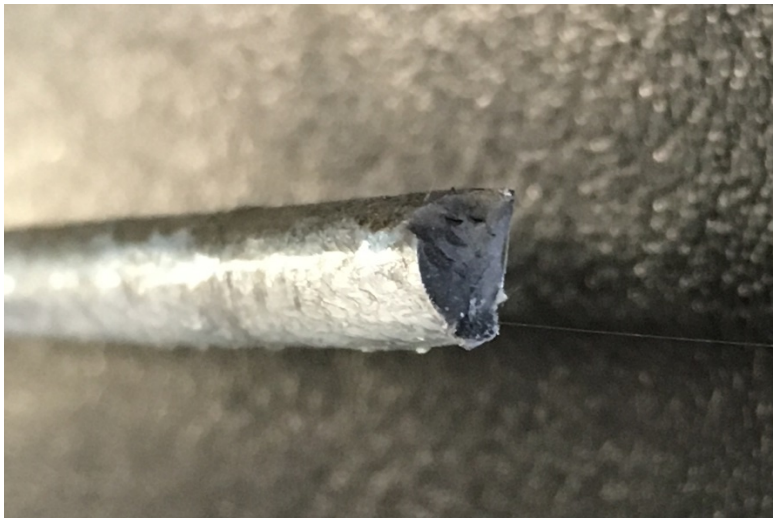

Figure 4.9. A wire fracture for S2.

Figure 4.10. Condition both ends of the specimen S2.

4.4. Test 3

Test 3 followed the procedure and setup outlined in Chapter 3.4 and Chapter 3.5. The fire test was performed on April 24th, 2018. The hydraulic cylinder applied a holding load of 325 kN. Afterwards the time- history for the hydrocarbon fire curve that is mentioned in Chapter 3.3 was exposed to the S3. Test 3 setup is presented in below Figure 4.11.

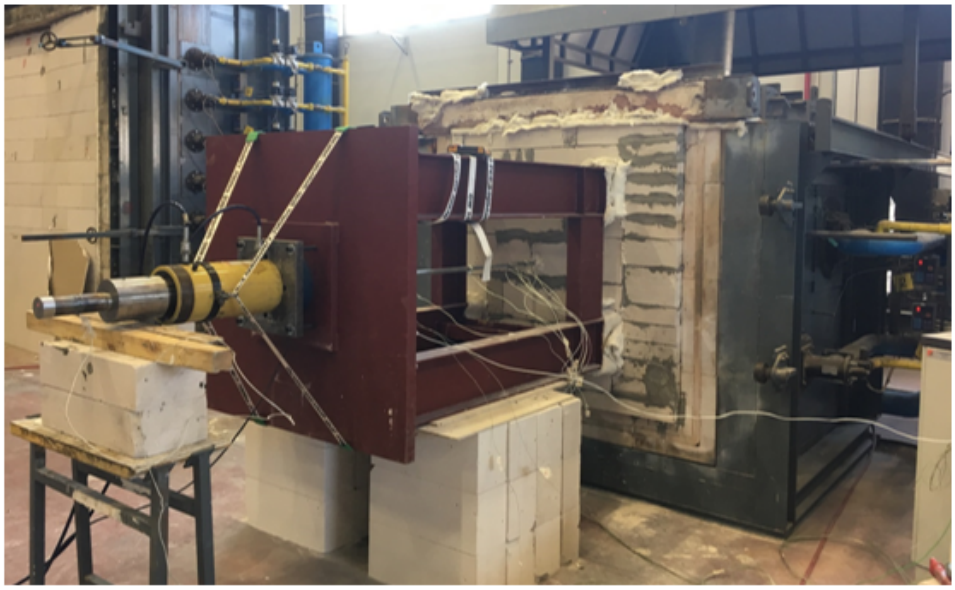

Figure 4.11. The view of the Test 3 setup.

The extension of the S3 was measured with piston ram displacement by laser distance sensor. During the initial loading the strand was deformed 19.35 mm and during the heating phase, the specimen deformed an additional 11.85 mm before rupture. Therefore, total extension was measured 31.2 mm. The failure occurred in 188 seconds (around 3 minutes) when the furnace started to heat up. Temperatures of inside and outside furnace thermocouples are plotted in Figure 4.12 and Figure 4.13. These figures show how the temperature increased at positions through the specimen as the furnace heated up.

The failure of the S3 was initiated by a single wire rupture that was then followed by subsequent rapid ruptures like a domino effect. Figure 4.16 shows the strand after failure. The break was considered violent and sudden. The failed wires splayed from each other and the ruptured wires displayed the cup and cone fracture type as presented in Figure 4.20. The strand ruptured section was very close to TC4 position as shown in Figure 4.16. The strand ruptured at a temperature of 592^{o}C (average temperature of the furnace) and at that specific time the temperature on TC4 was measured 608^{o}C. The cable showed signs of discoloration as presented Figure 4.18.

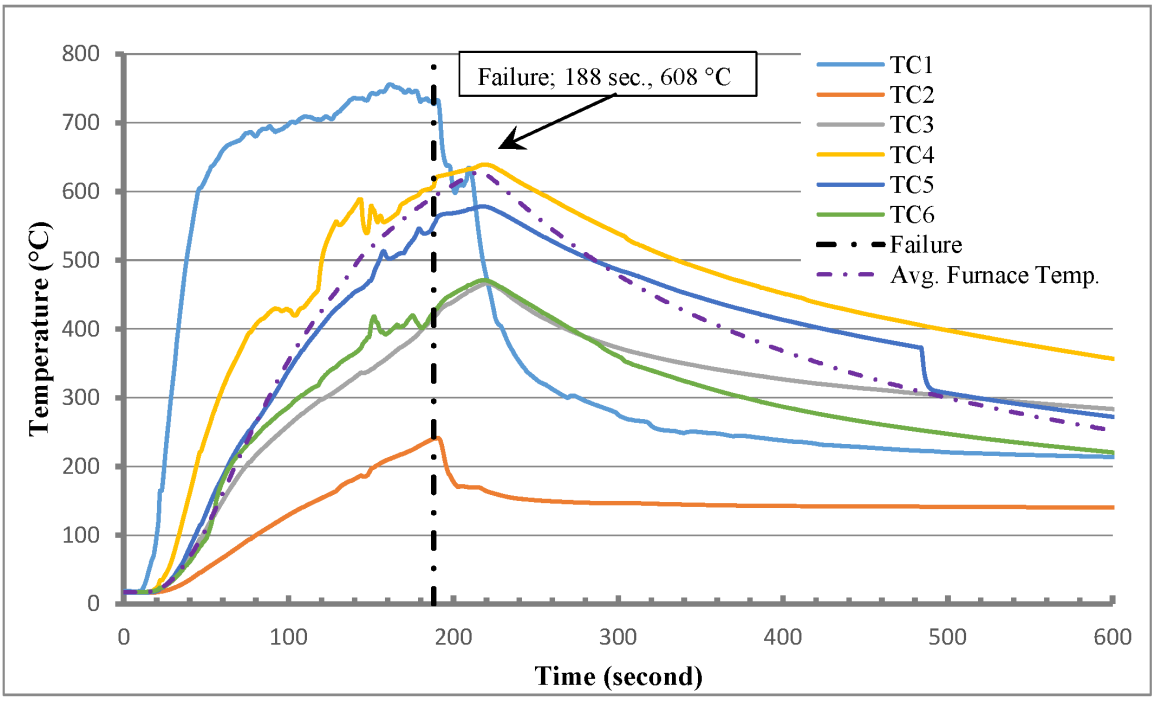

Figure 4.12. Inside furnace thermocouples for S3.

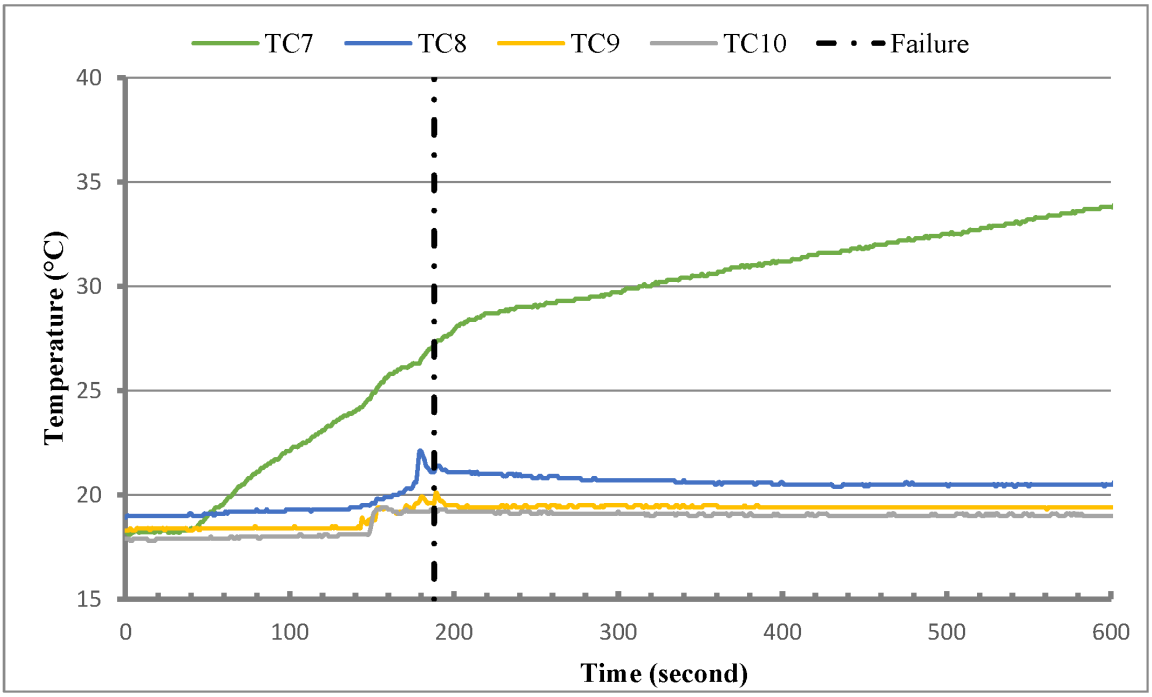

Figure 4.13. Outside furnace thermocouples for S3.

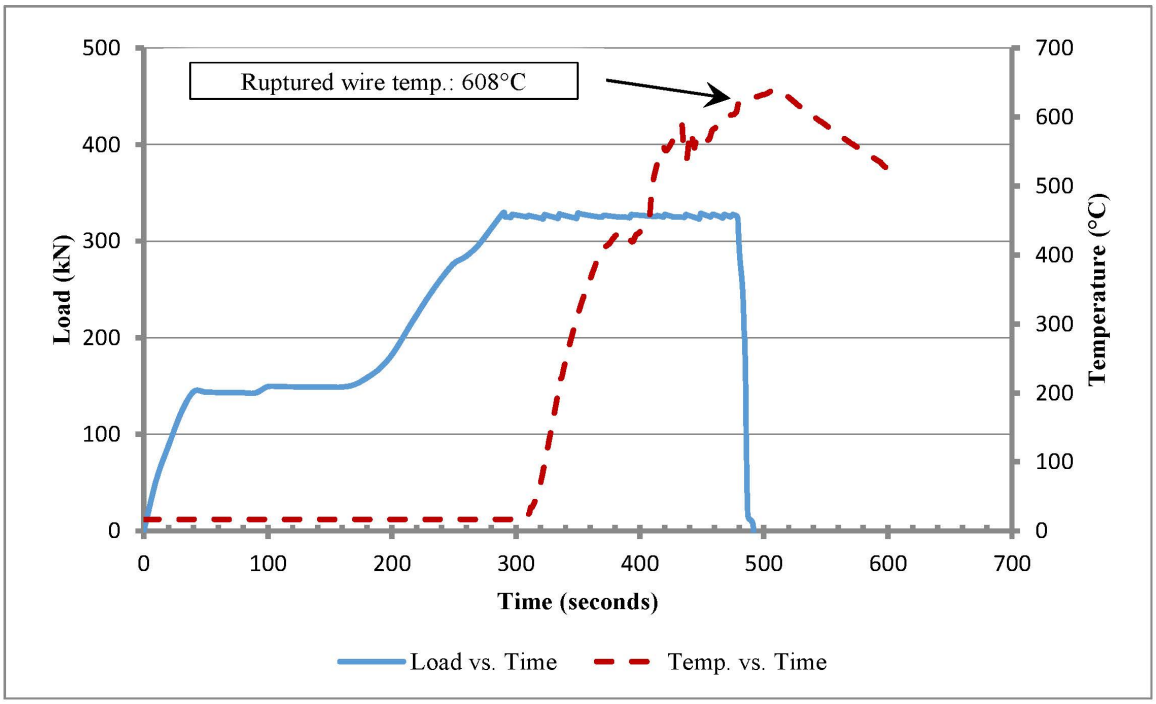

Figure 4.14. Time-history including Load vs. Time for S3.

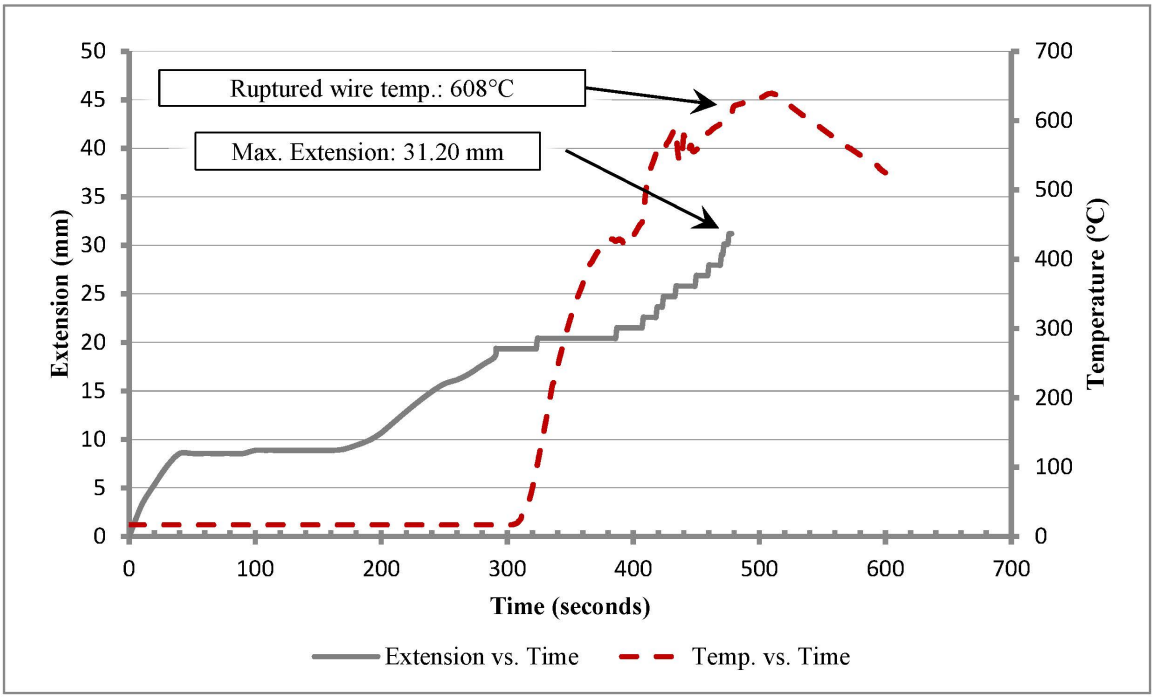

Figure 4.15. Time-history including Extension vs. Time for S3.

Figure 4.16. Ruptured section and TC4 position (left-hand side) and front view of rupture section (right-hand side).

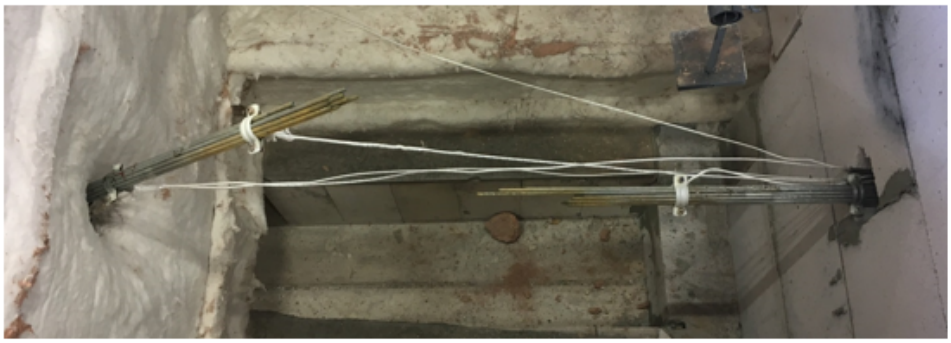

Figure 4.17. Failure view of S3 after fire Test 3.

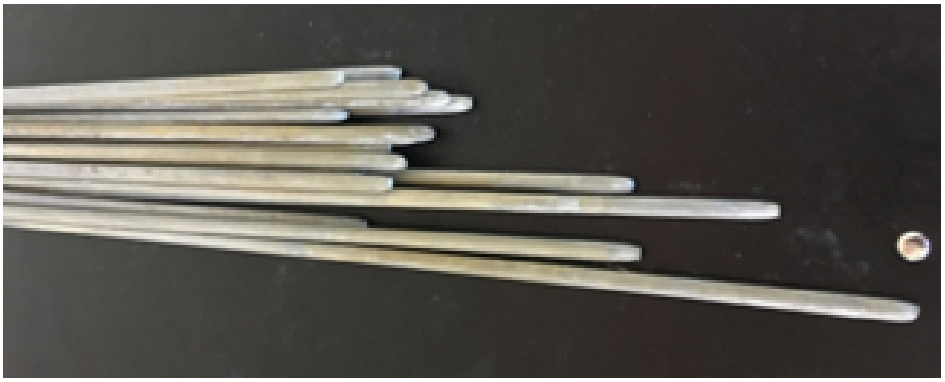

Figure 4.18. Discoloration of ruptured wires after fire Test 3.

Figure 4.19. Condition of dead end socket after fire Test 3.

Figure 4.20. A typical cup and cone wire rupture for S3.

4.5. Test 4

Test 4 followed the procedure and setup outlined in Chapter 3.4 and Chapter 3.5 The fire test was performed on April 30^{th}, 2018. The hydraulic cylinder applied a constant holding load of 325 kN. Afterwards the time- history for fire curve as mentioned in Chapter 3.3 was exposed to the S4.

The extension of the S4 was measured with piston ram displacement by linear potentiometer (Electronic circuit series) because the measuring performance of the distance meter is not found sufficient enough after the assessment of Test 3 data's outcome. During the initial loading the strand was deformed 19.05 mm and during the heating phase, the specimen deformed an additional 13.49 mm before rupture. Therefore, total extension was measured 25.34 mm as presented in Figure 4.28.

The load started to decline from the holding load after 3 minutes when the furnace started heat up. The failure (one wire ruptured) occurred in 364 seconds (around 6 minutes) when the furnace started to heat up. The failure of the S4 was initiated by a single wire rupture that was then followed by subsequent progressive ruptures. The same type of rupture as Test 3 was observed. Figure 4.21 shows the S4 condition before and after failure. After the first wire ruptured, the whole wires of the strand ruptured in around 2 minutes (exactly 447 seconds). The break was considered violent. The specimen exhibited a loud "bang" sound nineteen times one after the other. The strand ruptured at around 30 cm next to the socket and the S4 failed wires showed same signs of discoloration as S3 as presented Figure 4.22.

Temperatures of inside and outside furnace thermocouples are plotted in Figure 4.26 and Figure 4.27 and these figures show how the temperature increased at positions through the specimen as the furnace heated up. The ruptured section was very close to TC2 position as shown in Figure 4.21. The strand ruptured at a temperature of 527^oC (average temperature of the furnace) and at that specific time the temperature on TC2 was measured 485^oC.

Figure 4.21. TC2 position prior to Test 4 and front view of ruptured section.

Figure 4.22. Ruptured section.

The failed wires splayed from each other and the ruptured wires displayed the cup and cone fracture type as shown in Figure 4.25.

Figure 4.23. Condition of dead end socket after fire test.

Figure 4.24. Typical cup and cone two wire break fracture for S4.

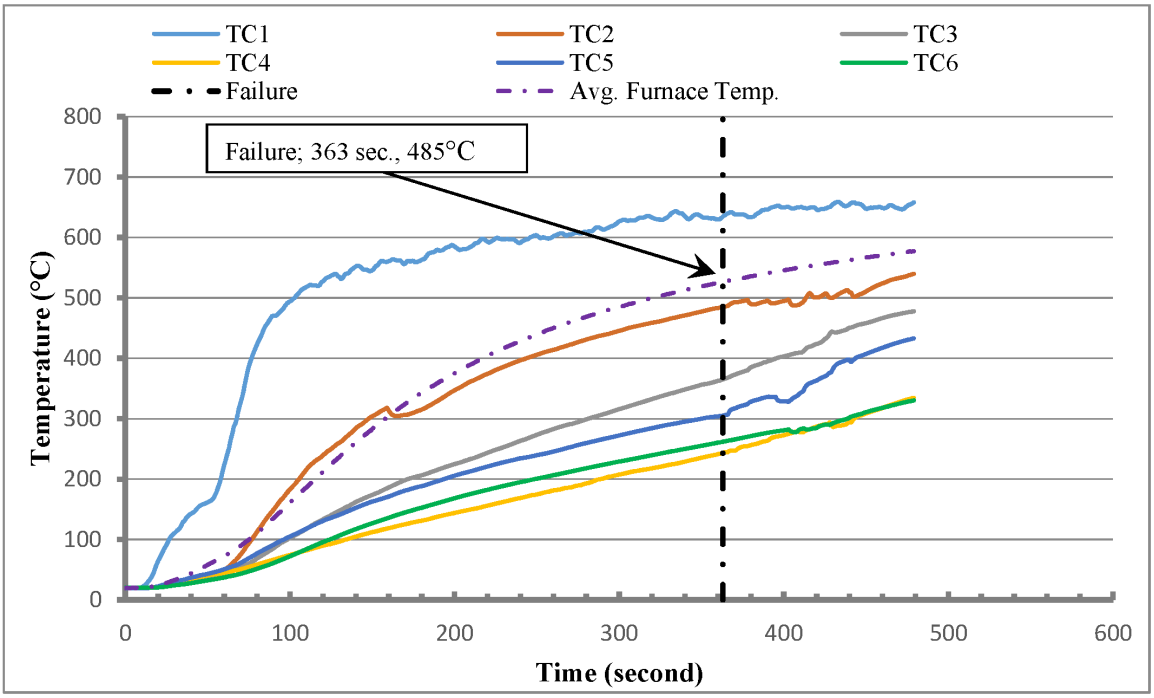

Figure 4.25. Inside furnace thermocouples for S4.

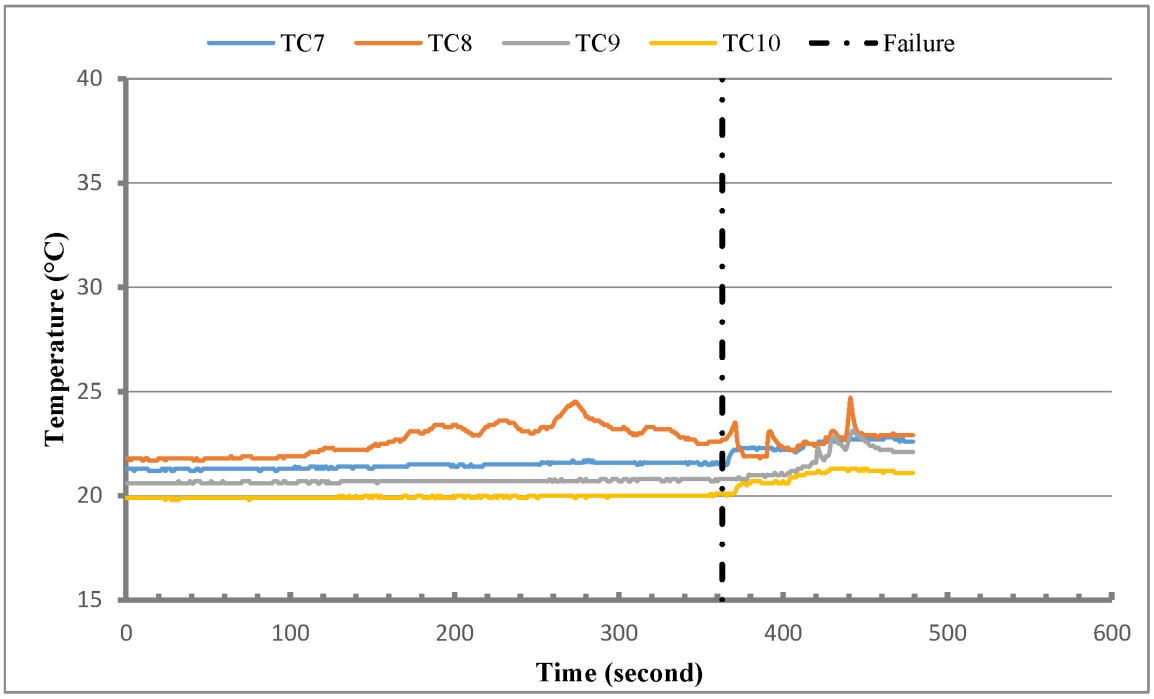

Figure 4.26. Outside furnace thermocouples for S4.

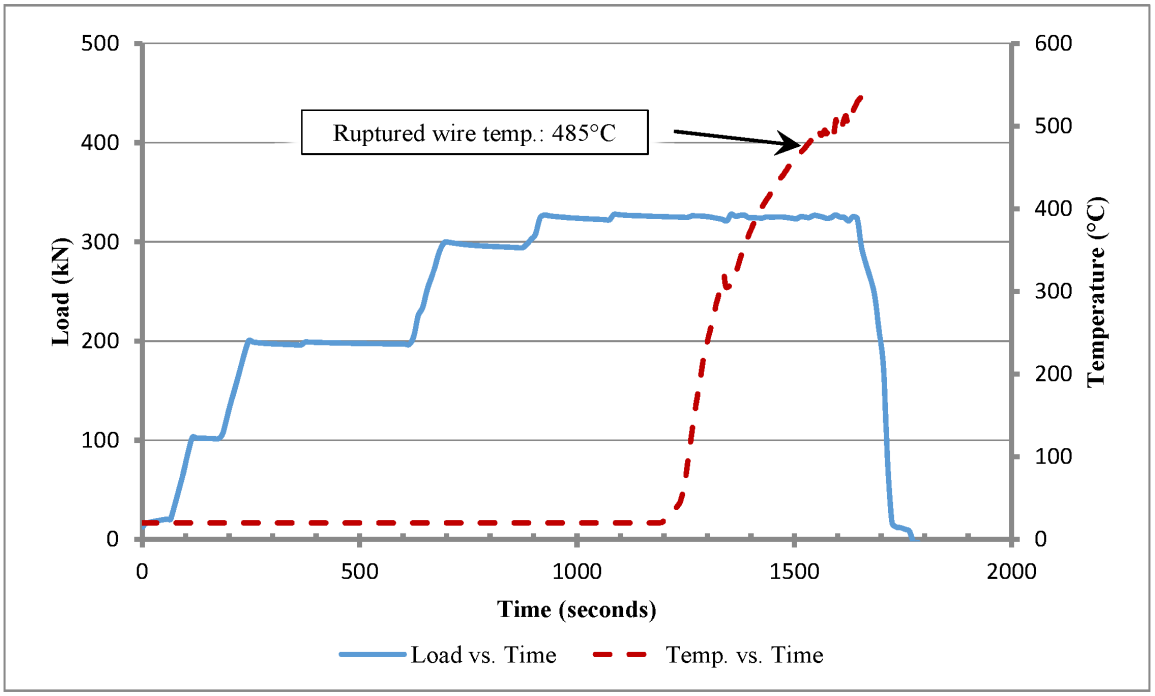

Figure 4.27. Time-history including Load vs. Time for S4.

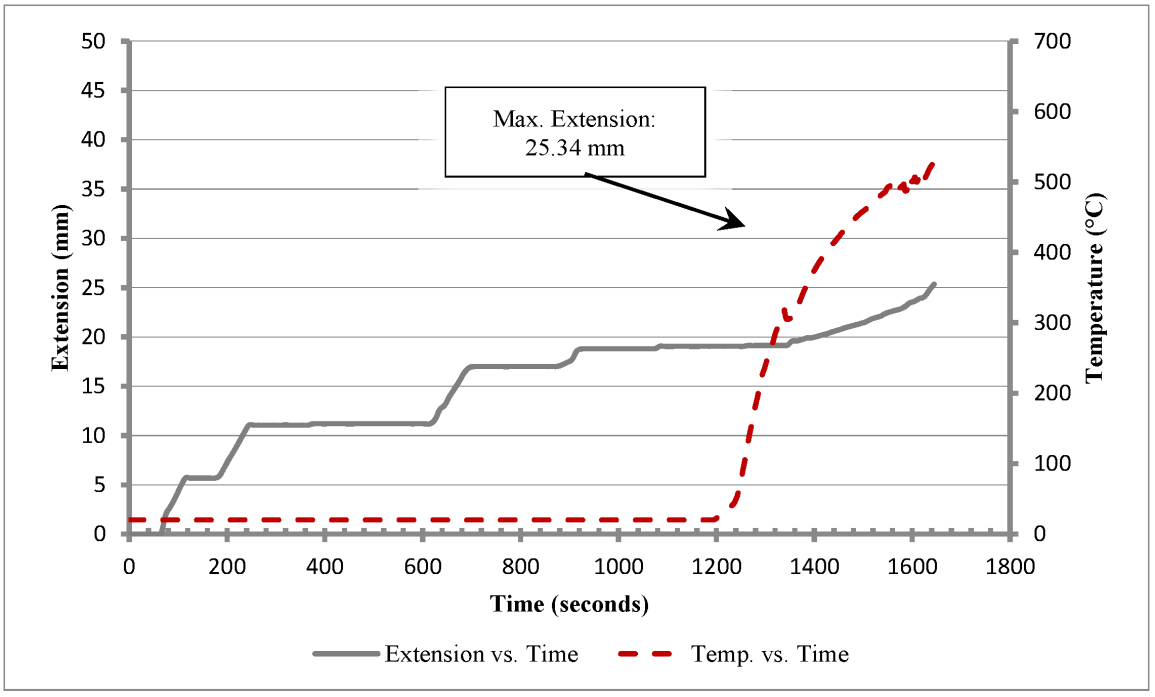

Figure 4.28. Time-history including Extension vs. Time for S4.

4.6. Test 5

Test 5 followed the procedure and setup outlined in Chapter 3.4 and Chapter 3.5. The fire test and after cooling static test was performed on May 2^{nd} and 3^{rd}, 2018. Afterwards the time-history for fire curve as mentioned in Chapter 3.3 was exposed to the S5. The hydraulic cylinder applied a constant holding load of 325 kN until the following day when static test after cooling was conducted. Therefore, Test 5 consists of two parts including fire test and after cooling static test. Test 5 general procedures as shown in below Table 4.1.

Table 4.1. Test 5 general procedure (Reminder).

Test No.		**Specimen Name**	**Test Type**	**Casting Medium**	**Fire**	**Full Insulation (Y/N)**	**Initial Constant Load (kN)**
TEST 5	Part 1	S5	Transient Fire Test	Zn-Cu alloy	Pool fire	Y	325
	Part 2		Static Test After Cooling		-	-	-

4.6.1. Part 1 - Transient Elevated Temperature Test (at Constant Load)

The extension of the S5 was measured with piston ram displacement by linear potentiometer (Electronic circuit series). During the initial loading the strand was deformed 21.09 mm. During the heating phase and after cooling, the specimen deformed an additional 6.07 mm. Therefore, total extension was observed 27.16 mm. In Figure 4.34 - Time- history including Extension vs. Time for S5 is presented.

Temperatures of inside and outside furnace thermocouples are plotted in Figure 4.32 and Figure 4.33 and therefore these figures show how the temperature increased at positions through the specimen as the furnace heated up. Note that the TC1 and TC2 malfunctioned during first 20 minutes of testing. Maximum temperature of the furnace was measured 683°C and heating phase was continued for around 40 minutes according to designed temperature-time graph as indicated in Chapter 3.3. For the fire Test 5, the failure did not occur.

Figure 4.29. S5 strand protection prior to fire test (left-hand side) and S5 condition after fire test 5 (right-hand side).

Figure 4.30. S5 socket protection prior to fire test and S5 socket condition after fire test 5.

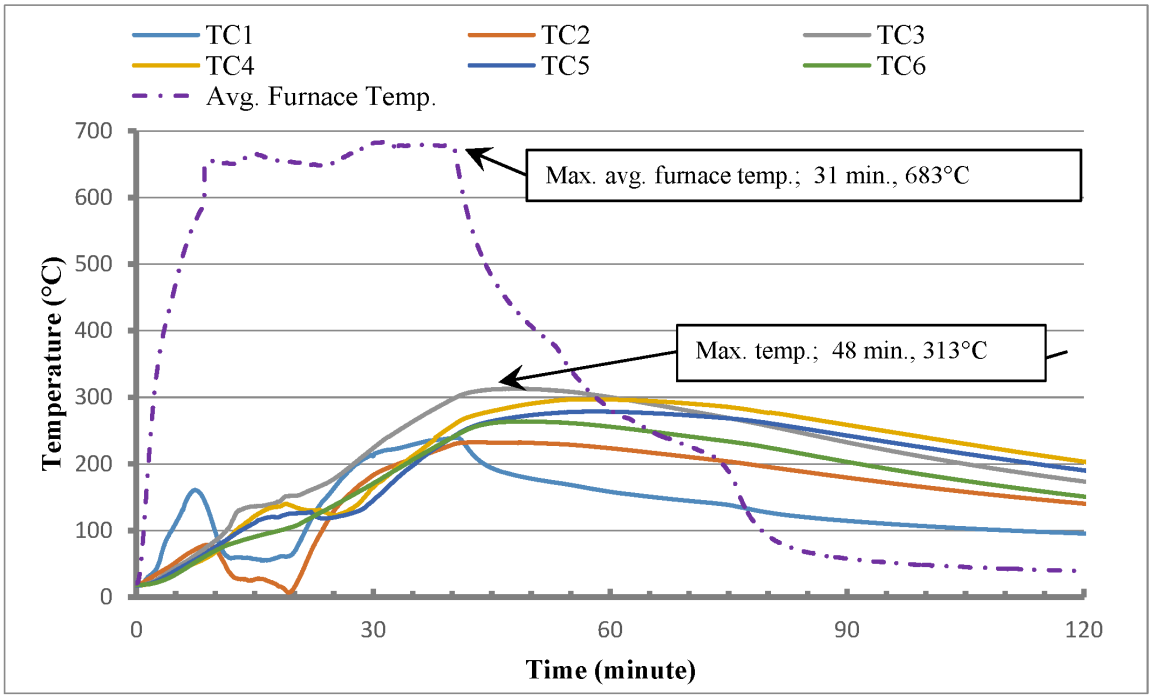

Figure 4.31. Inside furnace thermocouples for S5.

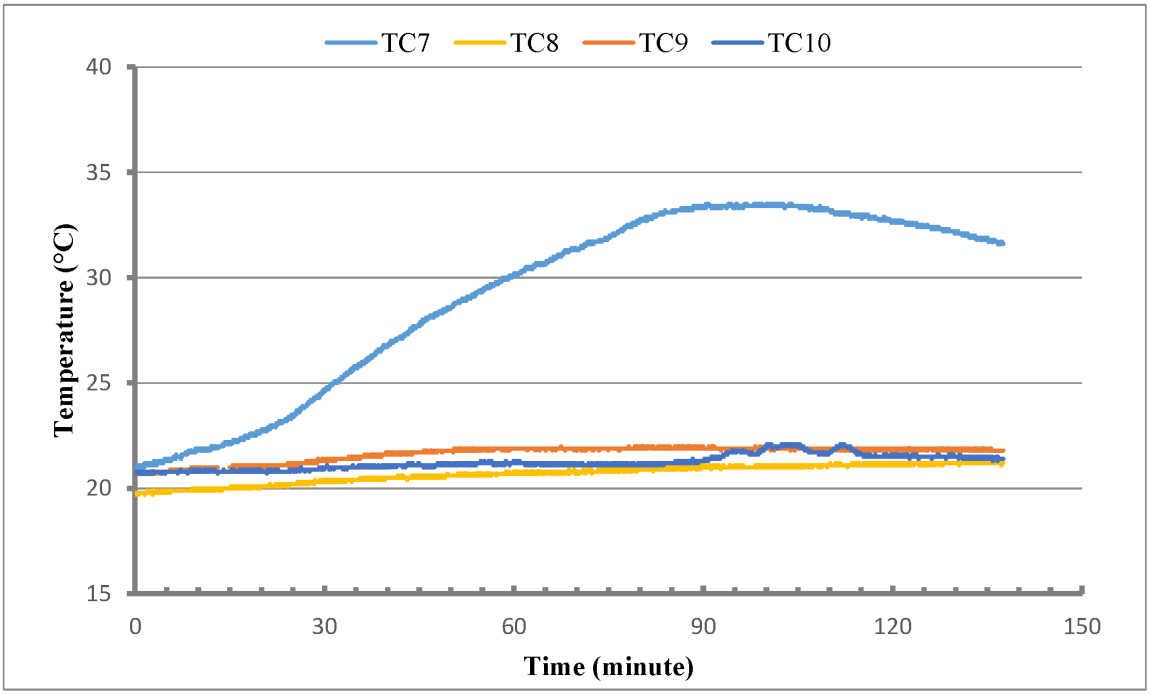

Figure 4.32. Outside furnace thermocouples for S5.

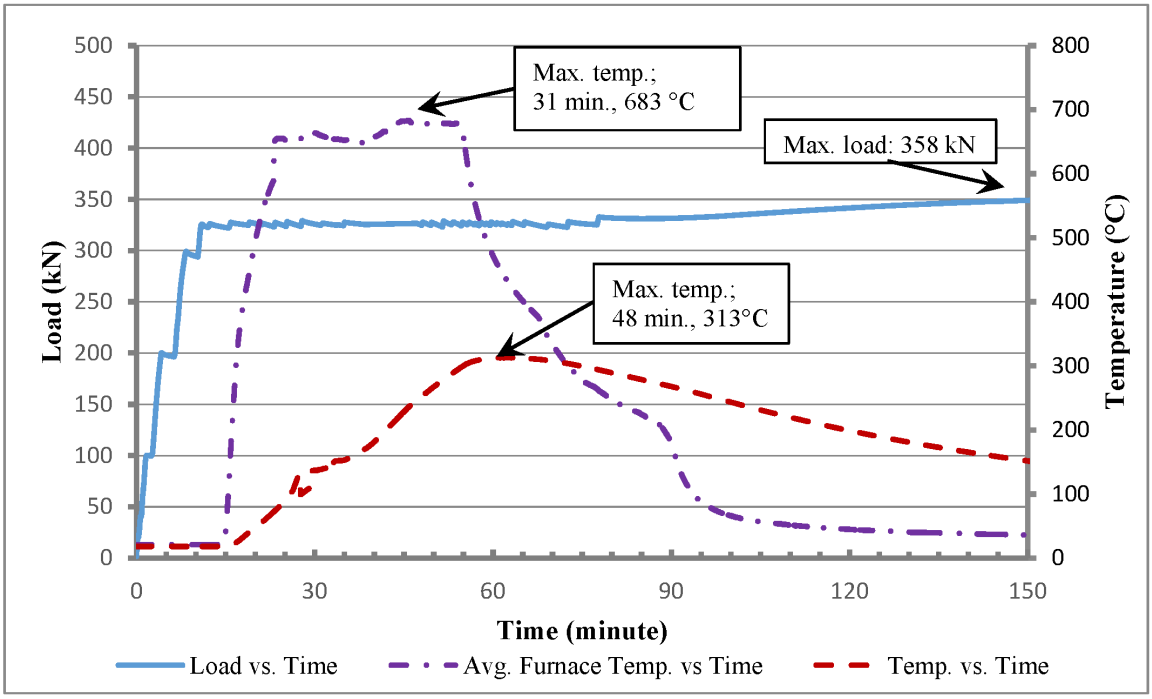

Figure 4.33. Time-history including Load vs. Time (S5).

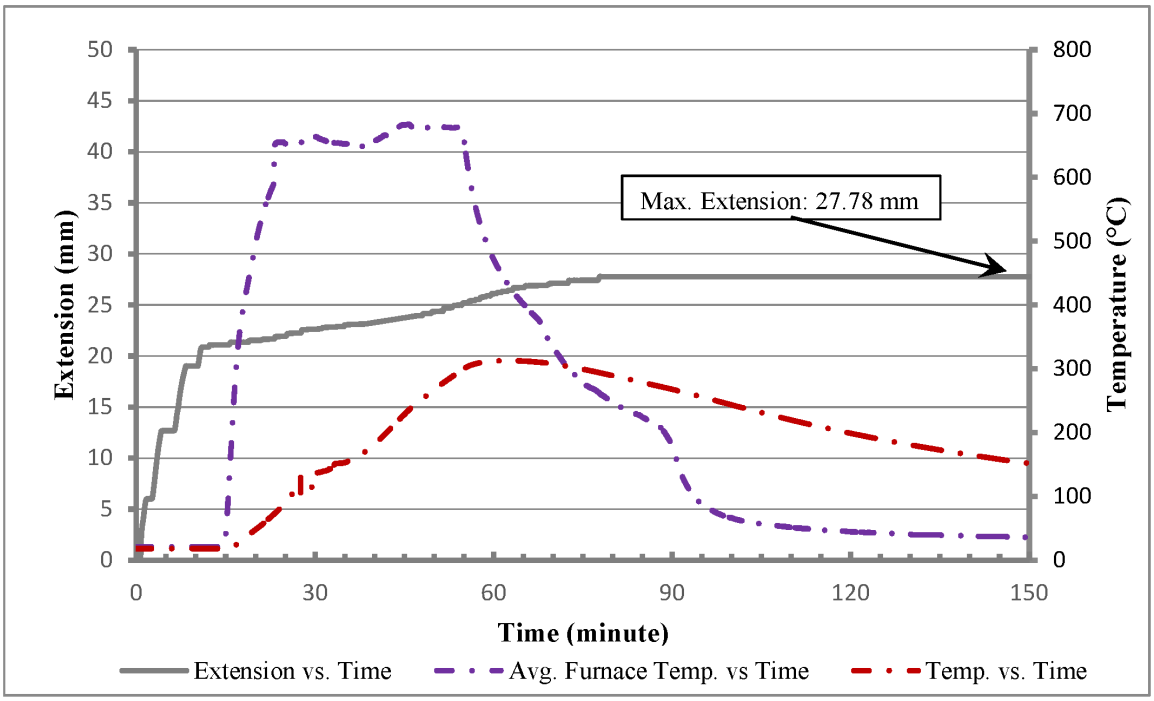

Figure 4.34. Time-history including Extension vs. Time (S5).

4.6.2. Part 2 - Static Test After Cooling

The force-extension relation for the tensile test is shown in below Figure 4.35. The maximum load the cable reached is 682.06 kN which is 94.48% of MUTS. The displacement corresponding to the maximum load is 160.99 mm, which is 4.05% of the cable length between the bearing plates. The static loading test after cooling was terminated when there was a wire break just before the cable reached the target load which is 686 kN (95% of MUTS). The cable was not passed the acceptance criteria.

The strand ruptured at around 57 cm next to the dead end socket and ruptured section located very close to TC3 position inside the furnace zone. Ruptured section position is presented in Figure 4.36. For fire test, TC3 maximum temperature was measured 313^{o}C shown in Figure 4.31.

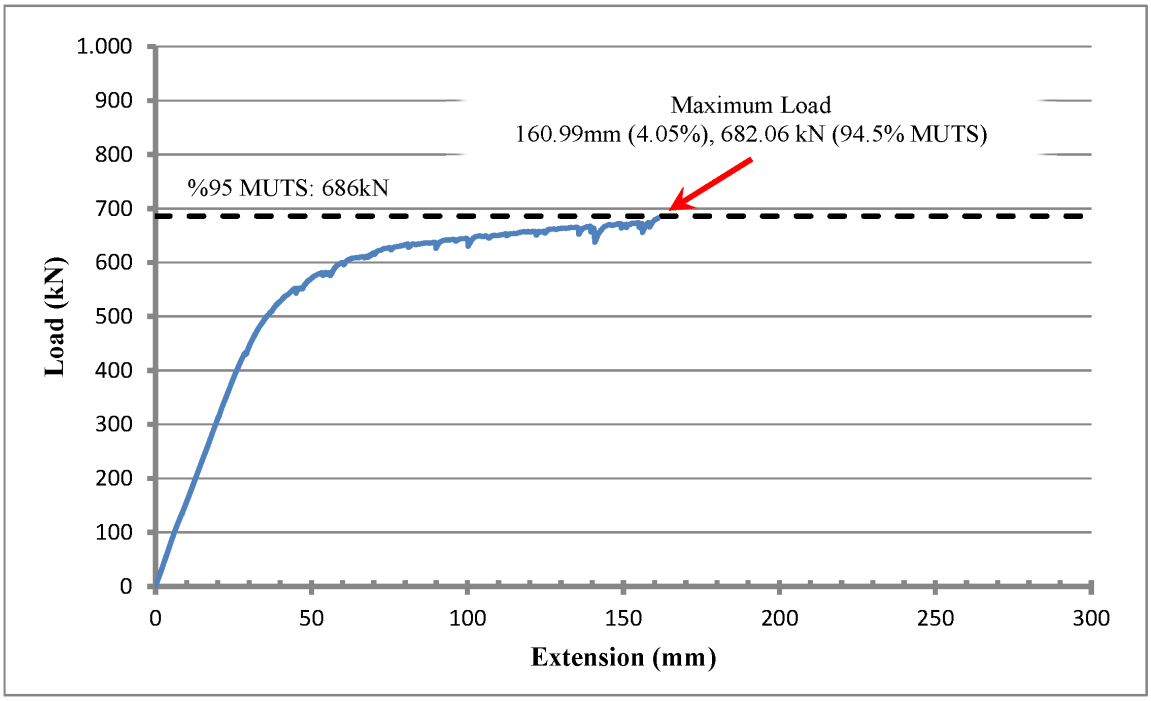

Figure 4.35. Force-extension relation in the tensile test (S5).

After static test, the specimen S5 was removed from the steel test frame. The conditions of a dead end and an active end of the socket heads were visually inspected as shown in Figure 4.37 and Figure 4.38. The sockets were not dissected. There were

no visible cracks or damage on the socket material. Figure 4.39 shows a typical wire breaks for S5. The failure was accompanied by a load "bang" and the potential energy was released in violent recoil of the cable upon rapture. Even though the specimen S5 was protected and passed the transient fire test, the wires showed same signs of discoloration as S3 and S4 as presented Figure 4.36.

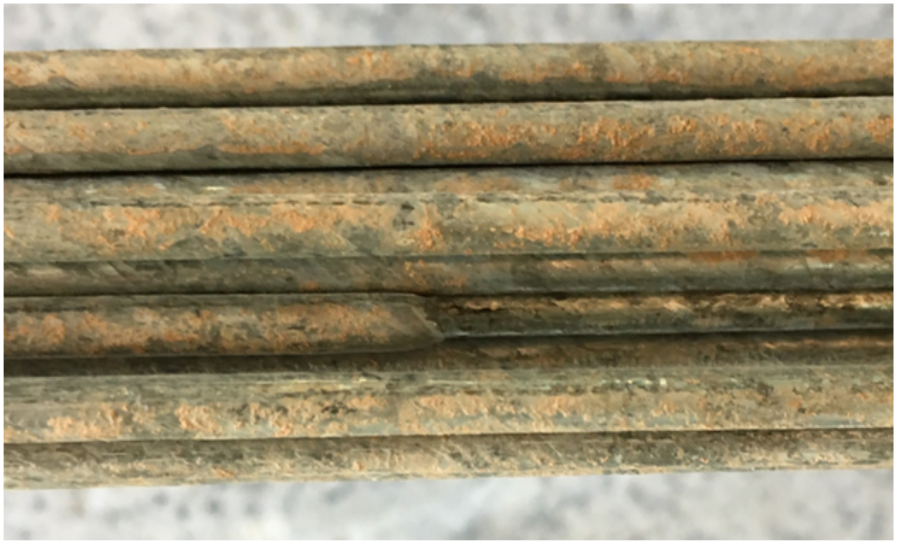

Figure 4.36. S5 discoloration and internal ruptured wire.

Figure 4.37. Condition both ends of the specimen S5.

Figure 4.38. Condition of dead end socket after fire Test 5.

Figure 4.39. A wire fracture for S5.

4.7. Summary

This chapter provided the observations and test data from the experimental testing. Two types of tests were conducted including static loading tests at ambient temperature and rapid rise fire tests including both standard fire curve (hydrocarbon fire UL1709) and a realistic fire curve. Observations were made regards to the type of failure, cable behavior at failure, and any visually noticeable changes in cable properties. Load-extension curves, extension-time-temperature and load-time-temperature history curves were included in this chapter along with photos of the failed cable section. Static test criteria and a summary of the static test results for the 5-19 PWS specimens S1, S2 and S5 are presented in the Table 4.2 and Table 4.3, respectively.

Table 4.2. Cable static test criteria.

Item	**5-19 PWS**
Nominal diameter of wire	5.1 mm
Number of wires	19 ea.
Cable MUTS	721.94 kN
Cable AUTS	742.33 kN
Load required in static test	685.84 kN
Load required in tensile test (% of MUTS)	95%

Table 4.3. Summary of the static test results for Test 1, Test 2 and Test 5 (Part-2).

STATIC TESTS			
Static Test No:	**Test 1**	**Test 2**	**Test 5 (Part 2)**
Date for static test	18.04.2018	19.04.2018	03.05.2018
Max.load reached (kN)	704	695	682
Max.load reached (% of MUTS)	97.5%	96.4%	94.5%
0.2% Offset Yield Load	523	515	580
Max. Estimated Avg. Wire Stress (Mpa)	1813	1792	1757
# of wire breaks (ea.)	1	2	1
Max. extension (mm)	205.62	190.66	160.99
Active end socket avg. Pull-out Length (mm)	4.4	8.5	-
Dead end socket avg. Pull-out Length (mm)	6.53	8.2	-
Wire Failure Type (Fracture)	Shear	Shear	Cup & Cone
Static test (Pass/Fail)	Pass	Pass	Fail
Conclusion	Pass	Pass	Fail

The 5-19 parallel wire strand specimens S1 and S2 satisfied the acceptance criteria and therefore, the other specimens which were exposed to fire test were provide reliable and accurate data for rest of the project. A summary of the transient elevated test results for the 5-19 PWS specimens S3, S4 and S5 are presented in the Table 4.4.

Table 4.4. Summary of the fire test results for Test 3, Test 4 and Test 5 (Part-1).

FIRE TESTS			
Rapid Rise Fire Test No:	**TEST 3 Hydrocarbon fire (UL-1709)**	**TEST 4 Pool Fire Scenario**	**TEST 5 Pool Fire Scenario Pool (Part 1)**
Date for fire test	24.04.2018	30.04.2018	02.05.2018
Initial Constant Holding Load (kN)	325	325	325
MUTS	45%	45%	45%
Full Insulation Installed (Y/N)	N	N	Y
Initial Load Extension	19.35	19.05	21.09
During Fire Test Extension	11.85	13.49	6.07
Total Extension (mm)	31.2	25.34	27.16
Failure Time (sec.)	188	364	-
TC Rupture Temp. (^{o}C)	608	485	-
Furnace Avg. Temp. at Rupture (^{o}C)	592	527	-
TC Max. Temp. (^{o}C)	-	-	313
Max. Furnace Avg. (^{o}C)	-	-	683
Discoloration (Y/N)	Y	Y	Y

The rapid rise temperature testing showed that the rupture temperature of the thermocouples on S3 and S4 were 608^{o}C and 485^{o}C, respectively which are within the predicted range as it mentioned in Chapter 3. Protected specimen S5 passed the fire test and yet it failed to meet the acceptance criteria of static test when exposed to static test after cooling.

There were no visible cracks or damage found in the socket heads after static and fire tests. No failure and no corrosion were observed in the anchor heads.

5. TEST RESULTS AND DISCUSSION

Chapter 5 presents the evaluation and interpretation of the laboratory test results. Experimental findings on the yield strength (0.2% offset yield load), tensile strength and elongation at rupture were determined for specimens including both static test and transient elevated temperature tests at constant load.

As a reminder, the mechanism of the bonding between galvanized wires and a Zn-Cu alloy medium in the socket terminations of a PWS system used for the suspender cable of a suspension bridge is discussed in Chapter 2.1.3. It was decided not to test the cold socketing compound in the fire test programme because it is flammable, although it is recently used for suspender cable applications in suspension bridges. Therefore, cold socketing compound (Wirelock^{TM}) medium in the socket terminations was used for only static loading test.

Note that only for S5 exposed to static test after cooling when its temperature was dropped to the ambient temperature, other specimens which were S1 and S2 were conducted static tests at ambient temperature and they were assembled with hot casting and cold casting method, respectively.

To verify the ultimate tensile strength of the 5-19 parallel wire specimens and to determine bonding strength between galvanized wires and the casting medium, static loading (pullout) tests were conducted on two specimens. In other words, the purpose of these static loading tests was to verify the tensile strength results for the PWS system prior to fire tests.

The specimens S1, S2 and S5 were investigated and their tensile properties were determined experimentally. Figure 5.1 shows the force-extension curves and the variation in the elongation at rupture for the S1 and S5 cable specimens. Note that S1 and S2 force-extension relation is almost same and therefore, S2 is not plotted in this graph. All the three specimens failed by wire breakage.

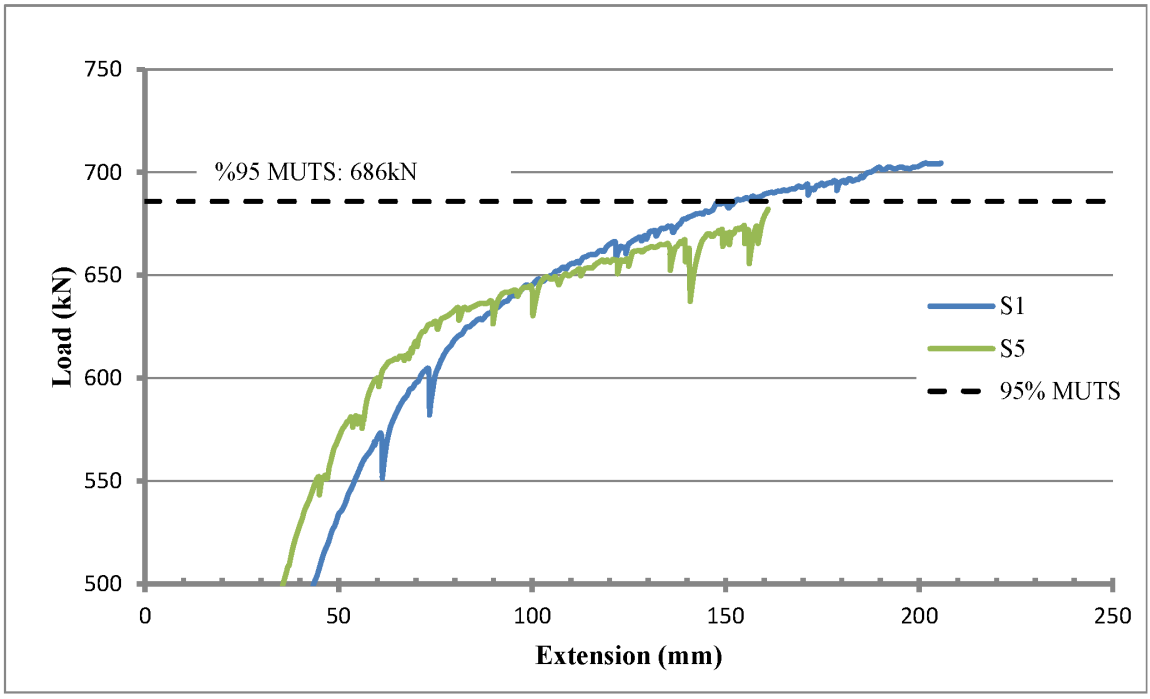

Figure 5.1. Force-extension comparison for S1 and S5.

The ultimate tensile strength for the specimens S1, S2 and S5 shows similar tendencies which were 704kN, 695kN and 682kN as shown in Figure 5.1. The cable specimens S1 and S2 withstood loads beyond 95% of the MUTS of the strand and therefore, the specimens S1 and S2 satisfied the acceptance criteria and ultimate strength values were found as expected. According to static test after cooling (Test 5 - Part 2) results, the specimen S5 was reached 94% of the MUTS which was very close to 95% of the MUTS, and yet it did not satisfied the acceptance criteria.

According to static test results, although the specimens did not fail by complete pullout out from the sockets, a little pullout of the strand from the socket basket was observed. It is actually inevitable that a certain amount of pullout would occur during the cable static test because the magnitude of the load applied to the strand was high (∼700kN, ∼70tonf) resulting in deformation of individual wires in the casting medium during the tests. The final pullout length of the specimens S1 and S2 from the socket head were indicated in summary part of the Chapter 4.7. The final pullout length of the S5 could not obtain due to discoloration. These pullout values are negligible being less than 5% of the socket basket length. In brief, both of the Zn-Cu alloy and cold

socketing compound showed satisfactory pullout performance at ambient temperature even for after cooling test performance.

The breakage of all the bridge wires were expected to characterized by typical cup-and-cone failure which is generally observed in tensile tests of ordinary ductile materials., however, the failure type of S1 and S2 wires were observed shear failure. This undesirable failure type may related with manufacturing errors such as carbon ratio, drawing velocity or the testing system errors such as dissymmetry of the steel plates of the test frame. On the other hand, S3, S4 and S5 wires failure type were characterized typical cup-and-cone failure as expected.

Furthermore, S5 shows a considerable decrease in the elongation which was 160.99 mm due to its increased core temperature which was measured 313°C at fire test. On the other hand, the wire specimens S1 and S2 used for the tensile test at ambient temperature showed that their maximum elongations reached 205.62 and 190.66, respectively. In comparison, the specimen S5 becomes more brittle which decreasing the 20% strain at rupture while slightly decreasing in the tensile strength. As a result, the temperature of 313°C causes approximately 20% strain loss for the S5.

For after cooling test showed that the elevated temperature on 5-19 parallel wire strand causes vital brittleness, making plastic deformation more difficult, besides, the ultimate tensile strength values of the strand is slightly decreases.

The static loading results verified that the ultimate tensile strength and the yield strength (0.2% offset yield load) performance of the PWS specimens were satisfied the acceptance criteria and therefore the specimens were ready to subjected transient elevated temperature tests.

The author has demonstrated the effects of a pool fire on a nineteen parallel wire strand system. Once the governing design fire scenarios were identified, the specimens exposed to designed fire load. The extension-temperature test data for S3 and S4 presented in Figure 5.2 shows that the specimen S3 heated at a higher heating rate

(UL 1709) ruptured at 608^{o}C in 188 seconds. When that heating rate was decrease (pool fire), the specimen S4 ruptured at 485^{o}C in 364 seconds.

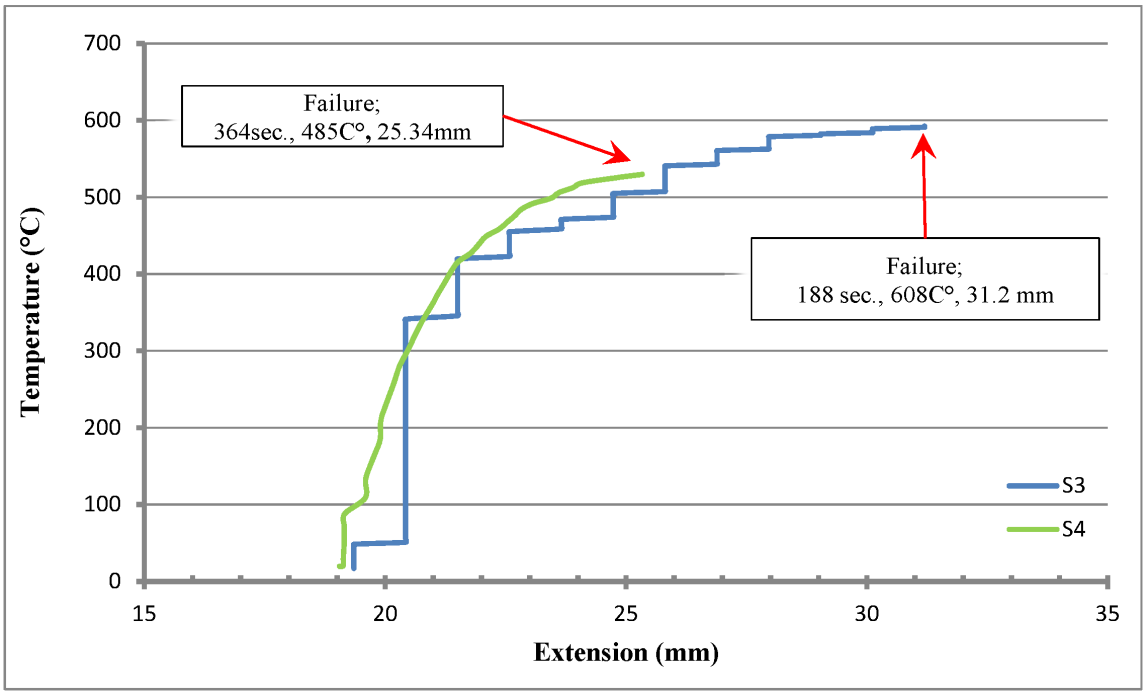

Figure 5.2. Extension-temperature comparison for S3 and S4.

Thus, the rupture temperatures of the average furnace for Test 3 and Test 4 were measured 592°C, and 527^{o}C, respectively. Note that both of the specimens S3 and S4 were not insulated and held at 45% of MUTS which is 325kn or 33tonf. Therefore, the faster heating rate lead to higher rupture temperature, when compared to the rupture temperature which was a slower heating rate. Rapid rise fire tests presented in this thesis are an example of those that can be used to assess the vulnerability of bridge cables to the effects of fire.

The tests equipment's and therefore the specimens presented here is a simplified version, and cannot easily be extended to complex bridge structures, due to factors such as redundancy, redistribution of moments, and geometric, etc. Furthermore, the failure limit states adopted from the test results based on critical cold-drawn high-strength wire temperatures may not be applicable for complex structures.

The application of a ceramic fiber blanket insulation material, even for the most severe scenarios, will maintain structural adequacy until exhaustion of fuel or effective firefighting can take place. However, a ceramic fiber blanket application for fire protection is not practical or realistic fire protection solution for suspender cables due to environmental factors such as rain, wind, intense heat, UV radiation. Therefore, applicable insulation materials for suspender cable should be extensively and experimentally investigated.

When comparing Test 3 and Test 4, the specimens failed almost as soon as the temperature was increased from 485^{o}C to 608^{o}C. It is appears that the critical temperature under this load is at 485^{o}C. In general, the values of the elongation at rupture for the specimens S3, S4, S5 decrease as their temperature increases. The decrement was extremely larger for unprotected specimens which were S3 and S4 relatively protected specimen S5. For all the specimens the approximate elongations at rupture were 205mm, 190mm, 31mm, 25mm, and 160mm respectively. In brief, the elongation at rupture significantly decreases around 85% when the temperature exceeding beyond the 485^{o}C. As noted before, creep strain is not expected to have contributed significantly to the overall strain for the unprotected specimens due to the short duration of the tests.

The outcomes demonstrate that up to temperatures of 313^{o}C, there is certainly not important loss in ultimate strength. However, when the specimen temperature increasing over 485^{o}C, there is a vital reduction in ultimate strength which means that recrystallization of the steel microstructure occurs and the advanced properties produced throughout the cold-working process are completely lost.

Two possible explanations to the dependency on heating rate:

(i) The mechanical property degradation is a time-dependent function for cold-drawn wires,
(ii) Faster heating rates lead to a non-uniform temperature gradient across the strand cross section. In regards to the mechanical property being time-dependent, Callis-

ter, and Rethwisch (2011) discuss recovery (the process of removing the properties gained through cold-working) as a time-dependent process.

When the strand is heated at a faster heating rate, the recovery is incomplete and the material is thus able to withstand a higher rupture temperature. This suggests that the time-dependency of recovery is the primary factor contributing to the increase in strength for the transient tests. However, not enough data was created to suggest a certain correlation between the mechanical property and time-dependency.

The outcomes verified that the spheroidization of the pearlite lamellae microstructure may occur above the temperature of 313^{o}C and this manner can occur within minutes. This phenomenon is crucial for bridge wires since the high-strength properties of cold-drawn steel are a function of the lamellar pearlite structure. Once spheroidization occurs, the pearlite loses its lamellar structure as the lamellae of cementite form into globules. Moreover, the original microstructure is completely changed from the initial cold-drawn state when the steel is heated above 485^{o}C.

As it is mentioned in Chapter 2.1.2.2, PWS system typically protected by an extruded high density polyethylene (HDPE) sheath. It is also known that the HDPE sheath used to prevent from external factors such as humidity, rain, UV light ignites at 330^{o}C. When the sheath starts to burn, there is an impulsive rise in cable temperature. Thus, according to evaluation of the test results and considering the HDPE flammable condition the critical temperature of a parallel wire strand for suspender cable is about 300^{o}C.

In conclusion, an appropriate fire protection to suspender (hanger) cables should be applied in order to hold the PWS wires at temperatures below its critical temperature that is 300^{o}C, and therefore using protection material on PWS suspender cables in suspension bridges can minimize the adverse effects of fire hazard to a great extent.

6. CONCLUSIONS, RECOMMENDATIONS AND FUTURE WORK

After providing an outline of the experimental set-up, parallel wire strand and socket assembly and loading procedures, a detailed account of the test results is presented. Apart from the evaluation of load-extension response and strength properties, particular emphasis is given to assessing the influence of temperature on enhancing the ductility of 5-19 parallel wire strand (Grade 1860). The findings of this study have implications on procedures used for predicting the ultimate behavior of PWS system during, and following, exposure to rapid rise fire (elevated) temperatures. This chapter gives an overview of the laboratory test results performed at TSE Laboratory Complex. Conclusions are drawn from the test program and recommendations are made as long with future work.

This study contributes to the knowledge of tensile properties and the effect of the rapid rise fire on PWS system. The Zn-Cu alloy and cold socketing compound showed satisfactory pullout performance at ambient temperature even for after cooling test performance. S1 and S2 satisfied the acceptance criteria while S5 was very close to reach 95% of the MUTS yet it did not satisfy the acceptance criteria.

The transient test results show that the elevated fire has a major influence on the tensile properties in two specimens which were not insulated. It was found that a faster heating rate which was hydrocarbon standard fire curve (UL-1709) can lead to a higher rupture temperature relative to a slower heating rate which was pool fire scenario. The yield strength, ultimate tensile strength and elongation at rupture were dreadfully affected by the rapid rise fire scenario as shown in Chapter 3.3.

For after cooling test showed that the elevated temperature at 313°C on 5-19 parallel wire strand causes vital brittleness, making plastic deformation more difficult, besides, the ultimate tensile strength values of the strand is slightly decreases.

6.1. Conclusions

Based on the results of the static tests, the following conclusions are obtained:

(i) A different bonding mechanism, namely, the wedging action, which is produced by the conical shape of the casting medium, considerably raises the bonding strength between the wire and the casting medium.

(ii) The efficiency of the mechanism of the bonding between the galvanized wires and epoxy resin-based casting medium (cold casting) is comparable to that of the traditional combination of galvanized wire and the Zn-Cu casting medium. Both of the cable specimens sufficiently withstood the 95% of MUTS which is 686 kN without complete pullout of the strand from the socket termination. Therefore both abovementioned casting mediums were valid for the socket terminations of a PWS specimen.

It is concluded that the phenomenon of lamella collapse (as it mentioned above Chapter 2.4) occurred within 10 minutes if the wires core temperature reach at temperature of 485^oC, and therefore instantaneous failure was observed. While the critical member of the system is the cold-drawn wires by comparison with sockets if the socket is filled with Zn-Cu alloy. At 608^oC all of the advanced properties produced throughout the cold-drawing process of high-strength wires are completely lost. Lastly, the after cooling test data showed that the strength is relatively unaffected until the temperature of 313^oC, however, at that temperature the PWS specimen was became more brittle that is approximately 20% strain loss was observed. Thus, according to evaluation of all test results and considering the HDPE flammable condition the critical temperature of a parallel wire strand for suspender cable is about 300^oC.

The effects of the pool fires were studied and the obtained results from fire tests can be summarized as follows:

(i) The ultimate strength is slightly influence on the whole capacity of PWS, which can be ignored until the temperature of 310^oC.

(ii) The instantaneous failure by strand rupture can be expected between the temperatures of 485^{o}C and 610^{o}C for PWS system which subject to in-service load.

(iii) The mechanical properties of cold-drawn high-strength galvanized wires are significantly affected by increased temperature even if the wire temperature drops to ambient temperature.

(iv) The cold-drawing process gives the wires high-strength properties at room temperature; however, that same process makes the strand more susceptible when exposed to high temperature than mild steel.

(v) In case of a pool fire, the PWS wires cannot expand more than a typical expansion at ambient temperature. Therefore, the fire load will cause brittle failure of the PWS system which is an undesirable failure type.

(vi) When the PWS suspender cable is exposed to substantially large fire load, the increasing level of axial load may eventually lead a catastrophic failure of PWS cable. Therefore, the pool fires can lead to structural damage, rupture of suspender cables and therefore, partial collapse, as well as interruption of traffic flow in the bridge vicinity.

These abovementioned critical temperatures are unfortunately well below those that can occur within the exposure to a tanker pool fire. They are closer to temperatures that can occur adjacent to suspender cables, and care should be taken in those circumstances to assess the risk of premature failure in service. Indeed on bridges close to a suspender cable, the critical temperatures are likely to be reached rapidly in an unprotected condition, although the rupture/time criteria used in the tests reported here are rather progressive if the codified time requirements for structural stability of suspension bridges are considered.

In other words, analysis of the exposure to a tanker pool fire or an LPG fire could result in high temperatures within relatively short times. As far as the suspender cables are concerned, the exposed cold-drawn wires could lose significant strength in a short time if exposed to the serious fire scenarios such as direct exposure to an LPG jet or exposure to the flames from a pool fire. This may not lead to failure of the suspender cable since it is composed of other cooler bridge members. If these other members are

not capable of providing the necessary capacity then it may be necessary to protect the suspender cables.

This research has produced some practical results for beginning to understand how to design a suspender cables against a fire in such a pool fire event.

6.2. Recommendations

Based on the results of the study the following recommendations are made:

(i) Since the PWS cables fall under "critical" risk category, fire proofing of suspender (hanger) members would enhance the fire performance of the suspension bridge.
(ii) The required insulation material thickness and limiting the height to which the mitigation needs to be identified by taking into consideration that the critical temperature of 300°C and fire resistance time of 45 minutes (the possible difficulty of firefighting access). Mitigation and cost savings are also achieved if the required insulation material thickness and limiting the height of PWS cable is reduced.
(iii) Possible post-fire assessment and repair strategies for PWS suspender cables need to be investigated.

6.3. Future Work

The current study has also demonstrated need for further work:

- Conduct a microstructure analysis on the transient test and after cooling test specimens which were S3, S4, and S5.
- Inspect the condition of the casting medium by dissecting all the sockets and measure the exact pullout length of the strand.
- Measure the elastic modulus of the strand during the transient and constant temperature testing.
- Investigate a high-temperature strain gauge that will work for multi-wire steel strand.

- Test the fatigue resistance performance of an insulated 7-19 parallel wires strand specimens including socket heads filled with a resin compound medium while expose to rapid rise realistic fire scenarios.
- Investigate, design, manufacture and test (under fatigue load) an applicable fire insulation material for suspender cables.
- Test the different size of a PWS cable-whether it is 61, or 127 wires under both thermal and mechanical loading will serve to reveal the heat transfer and load redistribution.
- Repeat the current study using other types of bridge cables, such as newly used CFRP stay cables.

REFERENCES

Abrams, M.S. and C.R. Cruz, "The Behavior at High Temperature of Steel Strand for Prestressedconcrete", *Journal of Popular Culture is a peer-reviewed journal and the official publication of the Popular Culture Association*, Research and Development Laboratories, Vol. 3, No. 3, pp. 8-19, 1961.

Alampalli, S. and W.J. Moreau, Inspection, "Evaluation and Maintenance of Suspension Bridges", *Taylor and Francis Group*, May 2016.

American Society for Testing and Materials (ASTM), "Standard Test Methods for Fire Tests of Building Construction and Materials", E119-14, *American Society for Testing and Materials International*, USA, 2014.

American Society for Testing and Materials (ASTM), "Standard Test Methods for Determining Effects of Large Hydrocarbon Pool Fires on Structural Members and Assemblies", ASTM E119-14, *American Society for Testing and Materials International*, USA, 2004.

Andra, W. and W. Zellner, "Zugglieder aus Parallel-Drahtbündeln Und Ihre Verankrung Bei Hoher Dauerschwellbelastung", Die Bautechnik, *Die Verankerung von Drahtseilen*, Der Bauingenieur, Vol. 5, No. 6, 1969.

Astaneh-Asl, A., C. Noble, J. Son, A. Wemhoff, M. Thomas, and L. McMichael, "Fire Protection of Steel Bridgesa and the Case of the Macarthur Maze Fire Collapse", Proc. American Society of Civil Engineers Technical Council on Lifeline Earthquake Engineering Conference, Vol. 1 No. 12, 2009.

Atienza, J. and M. Elices, "Behavior of Prestressing Steels after a Simulated Fire: Fire-Induceddamages", *Construction and Building Materials*, Vol. 23, No. 8, pp. 2932-2940, 2009.

Bai, Y., W. Burkett, and P. Nash, "Rapid Bridge Replacement under Emergency Situation: Case Study", *Journal of Bridge Engineering*, Vol. 11, pp. 266-73, 2006.

Barber, C., A. Gardiner, and M. Law, "Structural fire design of the Qresund Tunnel", *Proceedings of the International Conference on fires in Tunnels*, Boras, Sweden, 295-316, 1994.

Bennets, I. and K. Moinuddin, "Evaluation of the impact of potential fire scenarios on structural elements of a cable-stayed bridge", *Journal of Fire Protection Engineering*, 19, 85-106, 2009.

Betti, R., A.C. West, G. Vermaas, and Y. Cao, "Corrosion and Embrittlement in High-Strength Wires of Suspension Bridge Cables", *Journal of Bridge Engineering*, Vol. 10, No. 2, pp. 151-162, 2005.

Betti, R. and B. Yanev, "Conditions of Suspension Bridge Cables: New York City Case Study", *Transportation Research Record Journal of the Transportation Research Board*, Vol. 1654, No. 1, pp. 105-112, 1998.

British-Adopted European Standard (BS EN)1774:1998 "Zinc and zinc alloys-Alloys for foundry purposes-Ingot and liquid", *British Standards Institution*, ISBN: 058028-9435.

Bulwa, D. and P. Fimrite, "Tanker Fire Destroys Part of MacArthur Maze/ 2 freeways closed near Bay Bridge", April 2007, https://www.sfgate.com/ bayarea/article / Tanker-fire-destroys-part-of- MacArthur-Maze-2575285.php, accessed at May 2018.

California Department of Transportation, "Caltrans Traffic Volumes 2012", https:// data. ca.gov/dataset/caltrans-traffic- volumes/resource/ c8ace60f-c95d-415a-bc3b-19a5395595e2, accessed at May 2018.

Callister, W. and D. Rethwisch, "Fundamentals of materials science and engineering", *3rd Ed, Wiley, Hoboken*, N.J, 2008.

Chung, P., R.W. Wolfe, T. Ostrom, and S. Hida, "Accelerated bridge construction applications in California - a lessons learned report", *Technical report, California Department of Transportation* (CALTRANS), USA, 2008.

Davis, M., P. Tremel, and A. Pedrego, A., 2008, "Bill Williams river concrete bridge fire damage assessment, structure", *a joint publication of*, USA, Vol. 1, pp. 30-32, 2008.

DeGarmo, E., J. Black, and R. Kohser, "Materials and processes in manufacturing", *Macmillan Pub. Co.*, New York, 1988.

Dotreppe, J.C, S. Majkut, and J.M. Franssen, "Failure of a Tied-arch Bridge Submitted to a Severe Localized fire, Structures and Extreme Events", IABSE Symposium, 272-273, 2006.

Durkee L. Jackson, "Advancements in suspension bridge cable construction", *Proceding International Symposium on Suspension Bridges*, Lisbon, 1966.

European Committee for Standardization (CEN), "Eurocode 2: Design of Concrete Structures - Part 1-2: General rules - Structural fire design", *British Standards Institution*, 2004.

European Committee for Standardization (CEN), 2003, "Eurocode 1: Actions on Structures - Part 2: General Actions - Actions on bridges", *Technical report, European Committee for Standardizatio*n (CEN), Brussels, Belgium.

European Committee for Standardization (CEN), "Eurocode 1 Actions on Structures, Part 1-2: General Actions - Actions on Structures Exposed to fire", *Brussels*, Belgium, 2002.

Falbe-Hansen, K. and J. Nissen, "The Qresund Bridge Completion, *Arup Journal*, Vol.

3, pp. 20-7, 2000.

Franssen, J.M. and R. Zaharia, "Design of Steel Structures subjected to Fire", *Background and Design Guide to Eurocode 3*, University of Liege, Belgium, 2005.

Federal Motor Carrier Safety Administration, 2004, "Comparative Risks of Hazardous Materials and Non-Hazardous Materials Truck Shipment Accidents/Incidents", *Technical Report March*, Columbus, OH.

Garlock, M., I. Paya-Zaforteza, V.K.R. Kodur, and L. Gu, "Fire Hazard in Bridges: Review, Assessment and Repair Strategies", *Engineering Structutes*, Vol. 35, pp. 89-98, 2012.

Gross, J.L. and S.A. Cauffman, "Bridges: The Next Generation of Experimental Research in Structural Fires", *Proceedings of the 27th US-Japan Bridge Engineering Workshop*, 2011.

Guthrie, D., V. Goodwill, and M. Hicks, "Tanker Fire Shuts Down I-75, Collapses Nine Mile Bridge", *The Detroit News*, 2009.

Haight, R.Q., D.P. Billington, and D. Khazem, 1997, "Cable Safety Factors for Four Suspension Bridges", *Journal of Bridge Engineering*, Vol. 2, pp. 157-167.

Harmathy, T.Z. and W.W. Stanzak, "Elevated-Temperature Tensile and Creep Properties of Some Structural and Prestressing Steels", *International has published Standard Standard conditions for temperature and pressure -464: Fire Test Performance*, Vol. 1, pp.186-208, 1970.

Hertz, K., "Reinforcement Data for Fire Safety Design", *Magazine of Concrete Research*, Vol. 56, No. 8, pp. 453-459, 2004.

Hobbs, R.E. and B.W. Smith, "Fatigue Performance of Socketed Terminations to Structural Strands", *Processing Institution Civil Engineers*, Vol. 2, No. 75, pp. 35-48, 1983.

Holmes, M., R.D. Anchor, G.M.E. Cook, and R.N. Crook, "The Effects of Elevated Temperatures on the Strength Properties of Reinforcing and Prestressing Steels", *The Structural Engineer*, Vol. 60, No. 1, pp. 7-13, 1982.

Hoon Y., L. Sung-Hyung and L. Jun-Kyung, "Mechanism of Bonding Between Zn-Al-Coated Wires and Zn-Cu Alloy Casting Medium in Hot Casting Socket Terminations for Large Bridge Cables", *Construction and Building Materials*, Vol. 76, No.1, pp. 396-403, 2015.

Hirakida, K. and K. Onomichi, "Steel Structure Architecture by the First Japanese Design and Construction", *Journal Architical Planing*, Vol. 63, No. 628, pp. 1349-1354, 2008.

International Code Council (ICC), "Steel Construction Manual 14th Edition", *American Institute of Steel Construction*, Chicago, 2012.

Isabel, M. L. Ridge and R.E. Hobbs, "The Behaviour of Cast Rope Sockets at Elevated Temperatures", *Journal of Structural Fire Engineering*, Vol. 3, No. 2, pp. 155-168, 2012.

Iqbal, N., M.H. Salley, and S. Weerakkody, "Fire Dynamics Tools Quantitative Fire Hazard Analysis Methods for the US Nuclear Regulatory Commission Fire Protection Inspection Program (NUREG-1805)", Washington, 2004.

Kodur, V.K.R., E. Aziz, and M. Dwaikat, "Evaluating of Fire Resistance of Steel Girders in Bridges", *Journal of Bridge Engineering*, Vol. 18, No. 7, pp. 633-643, 2013.

Kodur, V.K.R., M.Z. Naser, "Importance Factor for Design of Bridges against Fire Hazard", *Engineering Structures*, Vol. 54, pp. 207-220, 2013.

Kanno, R., "Advances in Steel Materials for Innovative and Elegant Steel Review", *Structural Engineering International*, Vol. 3, pp. 242-253, 2016.

Kilic, S.A., H.J. Raatschen, B. Körfgen, N.M. Apaydın, and A. Astaneh-Asl, "FE Model of the Fatih Sultan Mehmet Suspension Bridge Using Thin Shell Finite Elements", *Arabian Journal for Science and Engineering*, Vol. 42, No. 3, pp. 1103-1116, 2017.

Lykke, S., E. Skotting, J. Ebben, and M. Braestrup, "Fire Hazard Mitigation for the Qresund Link Immersed Tunnel", *Proceedings of the IABSE Colloquium*, Vol. 1, pp. 251-62, 1998.

MacLean, K.J.N., L.A. Bisby, and C.C. MacDougall, "Post-fire Deterioration and Prestress Loss Insteel Tendons used in Post-tensioned Slabs", A*irport Council International SP-255: Designing Concrete Structures for FireSafety*, Vo. 1, pp. 147-174, 2008.

Main, J.A. and W.E. Luecke, "NIST Technical Note 1678, Safety Assessment of Parallel Wire Suspension Bridge Cables Under Thermal Effects", Technical Report, *National Institute of Standards and Technology*, 2010.

Mayrbaurl, R. and S. Camo, "National Cooperative Highway Research Program Report 534 - Guidelines for Inspection and Strength Evaluation of Suspension Bridge Parallel Wire Cables", Washington DC: *Transportation Research Board*, 2004.

Mendes, P.A., J.C. Valente, and F.A. Branco, "Simulation of ship fire under Vasco da Gama Bridge", *Airport Council International Structural Journal*, Vol. 97, No. 2, pp. 285-290, 2000.

Modak, A.T., "Thermal Radiation from Pool Fires", *Combust Flame*, Vol. 29, pp. 177-92, 1977.

Mudan. K.S., "Thermal Radiation Hazards From Hydrocarbon Pool Fires", *Program Energy Combust Scienty*, Vol. 10, pp. 59-80, 1984.

National Fire Protection Association "NFPA 502: Standard for Road Tunnels, Bridges,

and other Limited Access Highways", Technical Report, *National Fire Protection Association*, Quincy, MA, 2008.

National Fire Protection Association "NFPA 502: Standard for Road Tunnels, Bridges, and other Limited Access Highways", Technical Report, *National Fire Protection Association*, Quincy, MA, 2011.

Neves, I., J. Rodrigues, and A. Loureiro, "Mechanical Properties of Reinforcing and Prestressing Steels after Heating", *Journal of Material Science and Civil Engineering*, Vol. 8, No. 4, pp. 189-194, 1996.

Oplatka, G. and K. Feyrer, "Temperaturverhalten von Seilvergüssen Teil 1: Dynamische Versuche, Teil 2: Statische Versuche Schritenreihe der Bundesanstalt für Arbeitsschutz Forschung Fb 460", Dortmund, 1986.

Paya-Zaforteza, I. and M.A. Garlock, "Numerical Investigation on the fire Response of a Steel Girder Bridge", *Journal Construct Steel Resistance*, Vol. 75, pp. 93-103, 2012.

Post-Tensioning Institute, "Recommendations for Stay Cable Design, Testing, and Installation", *Post-Tensioning Institute*, Phoenix, AZ, 2012.

Ridge, I. and R.E. Hobbs, "The Behaviour of Cast Rope Sockets at Elevated Temperatures", *Journal of Structural Fire Engineering*, Vol. 3, No. 2, pp. 155-168, 2012.

Ridge, I. and R. Verreet, "Wire Rope end Connections: an Overview", *Proceeding OIPEEC Conference 'Rope Terminations and Fittings*, Vol. 1, pp.1-29, 2001.

Selamet, S., "Thermal Gradient Estimation due to Surface" *Heat Exchange in Steel I-Sections*, 2017.

Shi, Y., G. Deodatis, and R. Betti, "Random Field-Based Approach for Strength Evaluation of Suspension Bridge Cables", *Journal of Structural Engineering*, Vol. 133,

No. 12, pp. 1690-1699, 2007.

Stoddard, R., "Inspection and Repair of a Fire Damaged Prestressed Girder Bridge", Report IBC-04-17, Olympia, *Washington State Department of Transportation*, 2004.

Science Applications International Corporation, Transportation Policy and Analysis Center, 7990 Science Applications Court, "A guide to highway vulnerability assessment for critical asset identification and protection", VA 22182, 2002.

Shutt, A., "Protecting against fire", The Atlas of Social Protection Indicators of Resilience and Equity magazine, *Spring*, Vol. 1, pp. 18-22, 2008.

Tarui, T., N. Maruyama, T. Eguchi, and S. Konno, "High Strength Galvanized Steel Wire for Bridge Cables", *Structural Engineering International*, Vol. 12, No. 4, pp. 209-213, 2002.

Takahashi, T., T. Tarui, and S. Konno, "Development of High Tensile Strength Wire of 180kgf/mm2 for Bridge Cable", *Japan Society of Steel Construction*, Vol. 1, No. 4, pp. 119-126, 1994.

Türkiye Standartları Enstitüsü 1363-1, "Fire resistance- Tests- Part 1: General Requirements", Brussels, *European Committee for Standardization.*

Türkiye Standartları Enstitüsü 1363-2, "Fire Resistance Tests"- Part 2: "Alternative and Additional Procedures", Brussels, *European Committee for Standardization.*

Türkiye Standartları Enstitüsü 1991-1-2, Eurocode 1: "Actions on Structures" - Part 1-2: General actions "Actions on Structures Exposed to Fire", Brussels, *European Committee for Standardization.*

Türkiye Standartları Enstitüsü 1993-1-2, Eurocode 3: "Design of Steel Structures" - Part 1-2: "General Rules -Structural Fire Design", Brussels, *European Committee for Standardization.*

Tarui, T., T. Takahashi, S. Ohashi, and R. Uemori, "Effect of Silicon on the Age Softening of High Carbon Steel Wire", *Iron and Steelmaker*, Vol. 25, pp. 25-30, 1994.

Quiel, S., T. Yokoyama, K. Mueller, L. Bregman, and S. Marjanishvili, "Mitigating the Effects of a Tanker Truck Fire and a Cable-Stayed Bridge", *2nd International Conference on Performance-based and Lifecycle Structural Engineering*, Queensland, Australia, 2015.

Van Horn, J. and Crews Reopen, "Fire-Closed I-95 in Six Days", *Construction Equipment Guide, 470 Maryland Drive*, Fort Washington, 2012.

US Department of Transportation, "Federal Highway Administration, 2012, Highway Statistics, 1995?2010: Ibid.", Highway Statistics (Washington, DC: Annual Issues), table VM-1; March 8, 2012.

Woodworth, M., E. Hansen, C. McArthur, and N. Abboud, "Protection of Cable-Stay Bridges From Accidental and Man-Made Fire Hazards: A Rational Physics-Based Approach to Analysing Vulnerabilities And Mitigations", *Procceeding of the 2015 The American Society of Civil Engineers Structures Congress*, Vol. 1, pp. 23-25, 2015.

Zoli, T.P. and J. Steinhouse, "Some considerations in the design of long span bridges against progressive collapse", *Proceedings of the 23th*, 2007.

APPENDIX A: COLD-DRAWN WIRE SPECIMENS

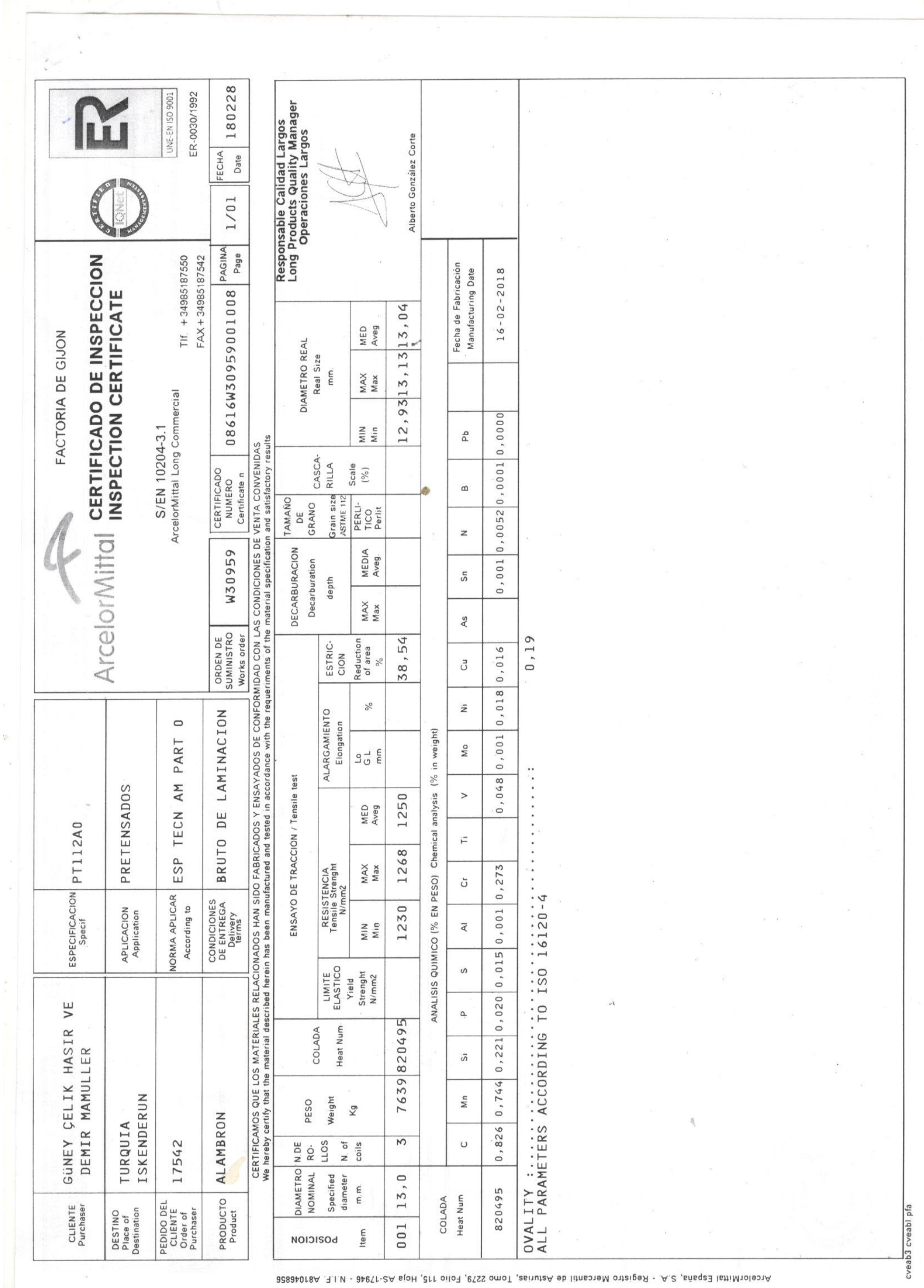

ArcelorMittal — FACTORIA DE GIJON

CERTIFICADO DE INSPECCION / INSPECTION CERTIFICATE

S/EN 10204-3.1

ArcelorMittal Long Commercial — Tlf +34985187550 — FAX +34985187542

UNE-EN ISO 9001 — ER-0030/1992

CLIENTE Purchaser	GÜNEY ÇELIK HASIR VE DEMIR MAMULLER	ESPECIFICACION Specif	PT112A0
DESTINO Place of Destination	TURQUIA ISKENDERUN	APLICACION Application	PRETENSADOS
PEDIDO DEL CLIENTE Order of Purchaser	17542	NORMA APLICAR According to	ESP TECN AM PART 0
PRODUCTO Product	ALAMBRON	CONDICIONES DE ENTREGA Delivery terms	BRUTO DE LAMINACION
ORDEN DE SUMINISTRO Works order	W30959	CERTIFICADO NUMERO Certificate n	08616W30959001008
PAGINA Page	1/01	FECHA Date	180228

CERTIFICAMOS QUE LOS MATERIALES RELACIONADOS HAN SIDO FABRICADOS Y ENSAYADOS DE CONFORMIDAD CON LAS CONDICIONES DE VENTA CONVENIDAS
We hereby certify that the material described herein has been manufactured and tested in accordance with the requirements of the material specification and satisfactory results

ENSAYO DE TRACCION / Tensile test

POSICION Item	DIAMETRO NOMINAL Specified diameter mm	N DE ROLLOS N. of coils	PESO Weight Kg	COLADA Heat Num	LIMITE ELASTICO Yield Strenght N/mm2	RESISTENCIA Tensile Strenght N/mm2 MIN Min	MAX Max	MED Aveg	ALARGAMIENTO Elongation Lo G.L. mm	%	ESTRICCION Reduction of area %	DECARBURACION Decarburation depth MAX Max	MEDIA Aveg	TAMAÑO DE GRANO Grain size ASTME 112 PERLITICO Perlit	CASCARILLA Scale (%)	DIAMETRO REAL Real Size mm MIN Min	MAX Max	MED Aveg
001	13,0	3	7639	820495		1230	1268	1250			38,54					12,93	13,13	13,04

ANALISIS QUIMICO (% EN PESO) Chemical analysis (% in weight)

COLADA Heat Num	C	Mn	Si	P	S	Al	Cr	Ti	V	Mo	Ni	Cu	As	Sn	N	B	Pb	Fecha de Fabricación Manufacturing Date
820495	0,826	0,744	0,221	0,020	0,015	0,001	0,273		0,048	0,001	0,018	0,016		0,001	0,0052	0,0001	0,0000	16-02-2018

OVALITY : 0,19

ALL PARAMETERS ACCORDING TO ISO 16120-4

Responsable Calidad Largos
Long Products Quality Manager
Operaciones Largos

Alberto González Corte

ArcelorMittal España, S.A. - Registro Mercantil de Asturias, Tomo 2279, Folio 115, Hoja AS-17946 - N.I.F. A81046856

cveab3 cveabl pla

Figure A.1. Inspection certificates for wire rod.

KALİTE KONTROL LABORATUVARI

ÇEKME DENEY RAPORU

NUMUNE BİLGİLERİ

Müşteri		Tarih	03/04/18
Standart	Extansometreli çekme	Malzeme	
Dosya no	D_0304_142552	Numune cinsi	
Seri No		Kesit alanı	20.424mm²
İş emri	NUMUNE1	Çap	5.100mm
Döküm No		A Kesiti	mm
Kaynak mukavemeti		B Kesiti	mm

TEST GRAFİĞİ

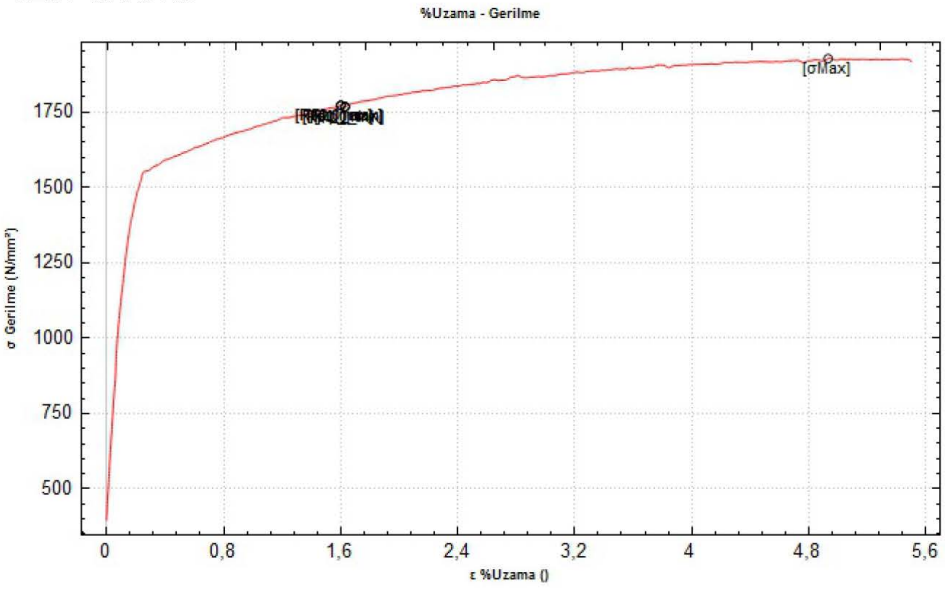

SONUÇLAR

Fm	39.373kN	E modul	638298.00N/mm²
Rm	1927.7N/mm²		
Rp0.1	1766.6N/mm²		
Rp1.0	1766.6N/mm²		
Rp0.2	1766.6N/mm²		
Uzama%	%5.5		

Test sorumlusu xxxxxx Test onaylayan

Figure A.2. Tensile test result #1 for high-strength wire specimen.

KALİTE KONTROL LABORATUVARI

ÇEKME DENEY RAPORU

NUMUNE BİLGİLERİ

Müşteri		Tarih	03/04/18
Standart	Extansometreli çekme	Malzeme	
Dosya no	D_0304_143220	Numune cinsi	
Seri No		Kesit alanı	20.424mm²
İş emri	numune 2	Çap	5.100mm
Döküm No		A Kesiti	mm
Kaynak mukavemeti		B Kesiti	mm

TEST GRAFİĞİ

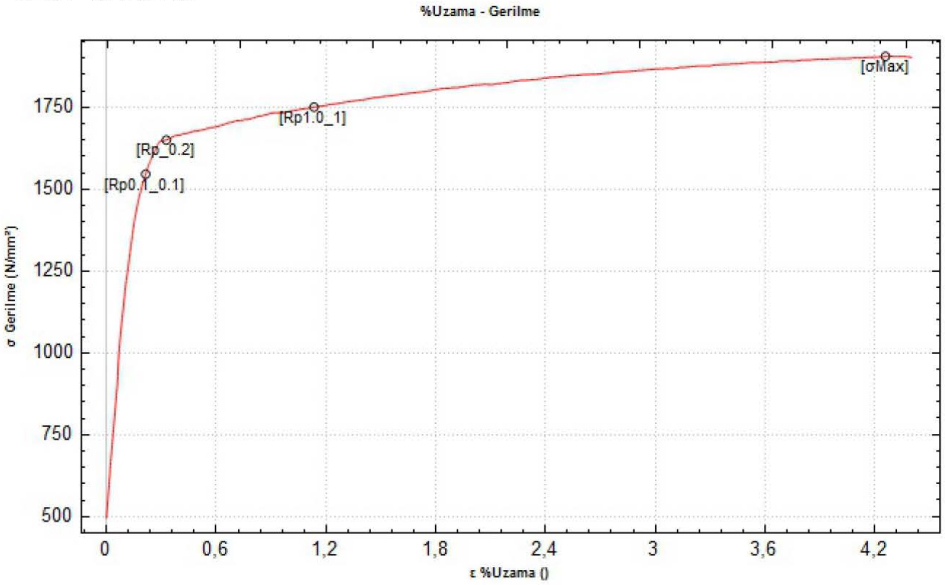

SONUÇLAR

Fm	38.923kN	E modul	8944.54N/mm²
Rm	1905.7N/mm²		
Rp0.1	1548.3N/mm²		
Rp1.0	1750.8N/mm²		
Rp0.2	1653.1N/mm²		
Uzama%	%4.4		

Test sorumlusu xxxxxx Test onaylayan

Figure A.3. Tensile test result #2 for high-strength wire specimen.

KALİTE KONTROL LABORATUVARI

ÇEKME DENEY RAPORU

NUMUNE BİLGİLERİ

Müşteri		Tarih	03/04/18
Standart	Extansometreli çekme	Malzeme	
Dosya no	D_0304_143743	Numune cinsi	
Seri No		Kesit alanı	20.424mm²
İş emri	NUMUNE 3	Çap	5.100mm
Döküm No		A Kesiti	mm
Kaynak mukavemeti		B Kesiti	mm

TEST GRAFİĞİ

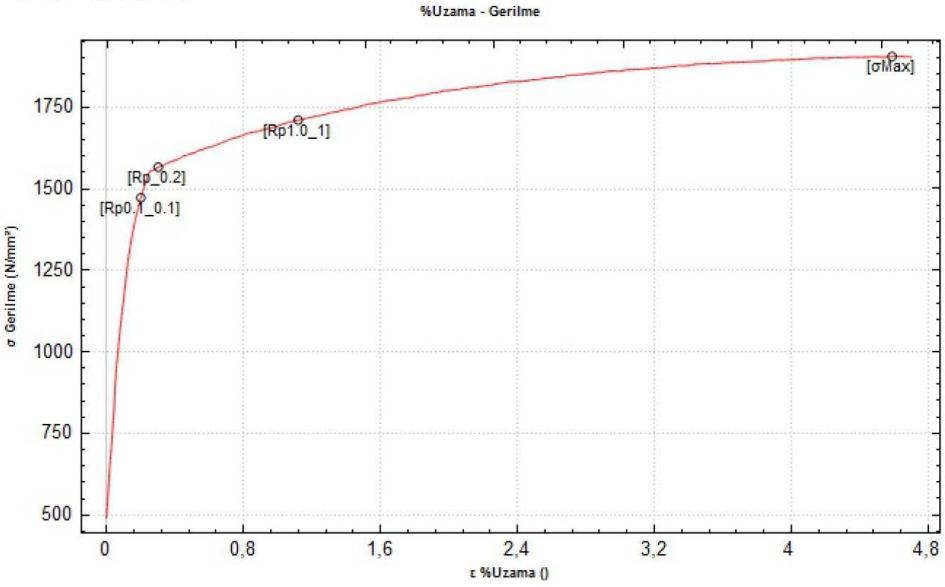

SONUÇLAR

Fm	38.930kN	E modul	12500000.00N/mm²
Rm	1906.0N/mm²		
Rp0.1	1475.2N/mm²		
Rp1.0	1711.3N/mm²		
Rp0.2	1567.8N/mm²		
Uzama%	%4.7		

Test sorumlusu xxxxxx Test onaylayan

Figure A.4. Tensile test result #3 for high-strength wire specimen.

APPENDIX B: WIRELOCK^{TM} (COLD SOCKETING COMPOUND)

DNV·GL

Certificate No:
K-6332
File No:
332.28
Job Id:
262.1-010575-2

TYPE APPROVAL CERTIFICATE

This is to certify:

That the Rope Socketing Compound

with type designation(s)
Wirelock®

Issued to
Millfield Enterprises (Manufacturing) Limited
NEWBURN, NEWCASTLE, United Kingdom

is found to comply with
Det Norske Veritas' Offshore Standards, DNV-OS-E304 Offshore Mooring Steel Wire Ropes
Det Norske Veritas' Type Approval Programme 1-501.18, 2009, Pourable Compound for Rope Socketing

Application :

For socketing wire rope terminations.

This Certificate is valid until **2019-06-30**.
Issued at **Høvik** on **2015-05-28**

DNV GL local station: **Newcastle-upon-Tyne**

Approval Engineer: **Gisle Hersvik**

for **DNV GL**

Digitally Signed By: Strande, Martin
Location: DNV GL Høvik, Norway
Signing Date: 2015-06-11

Martin Strande
Head of Section

This Certificate is subject to terms and conditions overleaf. Any significant change in design or construction may render this Certificate invalid.
The validity date relates to the Type Approval Certificate and not to the approval of equipment/systems installed.

Form code: TA 1411a Revision: 2014-11 www.dnvgl.com Page 1 of 3
© DNV GL 2014. DNV GL and the Horizon Graphic are trademarks of DNV GL AS.

Figure B.1. Type approval certificate.

Certificate No: **K-6332**
File No: **332.28**
Job Id: **262.1-010575-2**

Product description

Wirelock®: Unsaturated polyester resin, dissolved in styrene, for socketing wire rope terminations.

The following properties have been verified by Type Testing of cured resin:

Property	Test Method	Results		
Compressive Strength	ISO 604	156	MPa	msv (mean)
Compressive Strength	ISO 604	147	MPa	msmv
Compressive Modulus	ISO 604	13 766	MPa	msv (mean)
Barcol Hardness	ISO 75-2	42	-	msv (mean)
Density	ISO 3838	1.85	g/m^3	msv (mean)
Density	ISO 3838	1.81	g/m^3	msmv
Curing procedure used for Type Testing		Min. 12 hrs at room temperature, followed by 2 hrs at 70°C and 1 hr at 120°C		

Legend:
mean: Mean of Type Test results
msv: Manufacturer's Specified Value (mean of Type Test results)
msmv: Manufacturer's Specified Minimum Value (to be below mean minus 2 standard deviations)

Type Approval documentation

1. Previous Type Approval Certificate No. K-4599.
2. Letter from Millfield Enterprises (Manufacturing) Limited of 2015-04-15.
3. Periodical Assessment Report from DNV GL Newcastle of 2015-05-20.
4. Survey Report from DNV Newcastle of 2011-03-17.
5. Email from DNV Newcastle-upon-Tyne of 2006-08-01, including further test results.
6. Letter from DNV Newcastle-upon-Tyne of 2006-05-30, including DNV test report of 2006-03-14, test results from Doncaster Analytical Services, and Wirelock® Technical Data Manual.

Tests carried out

Type Testing carried out in accordance with **Type Approval documentation**.

Marking of product

Product/package shall be marked with *manufacturer's name*; **Millfield Enterprises (Manufacturing) Limited, UK** and *type designation*; **Wirelock**.

The marking is to be carried out in such a way that it is visible, legible and indelible. The marking of product is to enable traceability to the DNV GL Type Approval Certificate.

Periodical assessment

The scope of the Periodical Assessment is to verify that the conditions stipulated for the Type Approval is complied with and that no alterations are made to the product design or choice of materials.

Periodical Assessment to be performed after two (2) years (Certificate Retention) and at renewal after four (4) years (Certificate Renewal).

Figure B.2. Product description (p1).

Certificate No: **K-6332**
File No: **332.28**
Job Id: **262.1-010575-2**

The main elements of the Periodical Assessment are to:

- Ensure that **Type Approval documentation** is available.
- Review design, materials, production process, and performance with respect to possible changes, in order to ensure compliance with **Type Approval documentation** and/or referenced material specifications.
- **Ensure traceability between manufacturer's product marking and the DNV GL Type Approval Certificate.**

END OF CERTIFICATE

Figure B.3. Product description (p2).

Section 17: Properties of **WIRELOCK®**

WIRELOCK® in its liquid state is flammable. Flash point 31°C (88°F). **Please note:** flash point is not the auto ignition (spontaneous combustion) temperature, but the temperature above which the material will give off a significant amount of vapour.

Performance criteria

Compressive strength	Min. 100 N/mm2
Modulus of elasticity	Min. 6000 N/mm2
Barcol hardness	Min. 36
Specific gravity	1.55 - 1.95

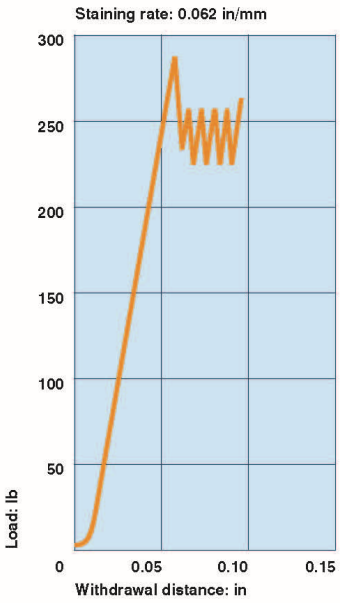

Figure 13: Pull out characteristic for single wire embedded in polyester resin/ silica.

The individual wires of the rope are retained by a combination of bonding and frictional forces. The frictional forces are the result of:

- Shrinkage during the curing of the resin.
- Coefficient of friction between the resin and the individual wires.

The particle size of the silica has been carefully selected to maximise the frictional grip. This is illustrated in figure 13, where it is shown that when the bonds strength has been exceeded the frictional grip continues to hold the load.

Additional forces develop due to the wedging action within the socket as the rope is loaded.

As **WIRELOCK®** cures, it shrinks by between 1.5% and 2.5% (**WIRELOCK®** High Volume by less than 0.5%) and with the introduction of a hard inert filler of specific grain size, a high coefficient is obtained.

WIRELOCK® has excellent penetrating qualities and can flow through the densest wire rope broom, which would impact the flow of zinc.

The **WIRELOCK®** system is designed to have a minimal amount of creep, which ceases once the wedging and frictional forces develop for any given load.

WIRELOCK® excels in its ability to resist the action of fatigue in a wire rope assembly, which is normally prevalent in the rope close to the neck of the socket. **WIRELOCK®** will minimize such problems.

See **www.wirelock.com** for information on:

- **WIRELOCK®** testing documents
- **WIRELOCK®** SDS part A & B
- **WIRELOCK®** training aid – film outlining the correct socketing procedure when using standard taper sockets.

Figure B.4. Technical data sheet for Wirelock^{TM} (p1).

Section 15: Approvals & NATO numbers

Approvals

To maintain **WIRELOCK's** premier position in the marketplace we continually strive to refine and improve the product. We operate a monitoring programme to ensure that the quality of **WIRELOCK®** never varies.

WIRELOCK® is manufactured under ISO 9001 accreditation.

WIRELOCK® meets the requirements of ISO 17558 and DNV-OS-E304.

WIRELOCK® has Type Approval from Lloyds, DNV and ABS.

NATO numbers

100cc	8030-21-902-1823
250cc	8030-21-902-1824
500cc	8030-21-902-1825
1000cc	8030-21-902-1826

Figure B.5. Technical data sheet for Wirelock^{TM} (p2).

APPENDIX C: STEEL TEST FRAME AND TEST SYSTEM

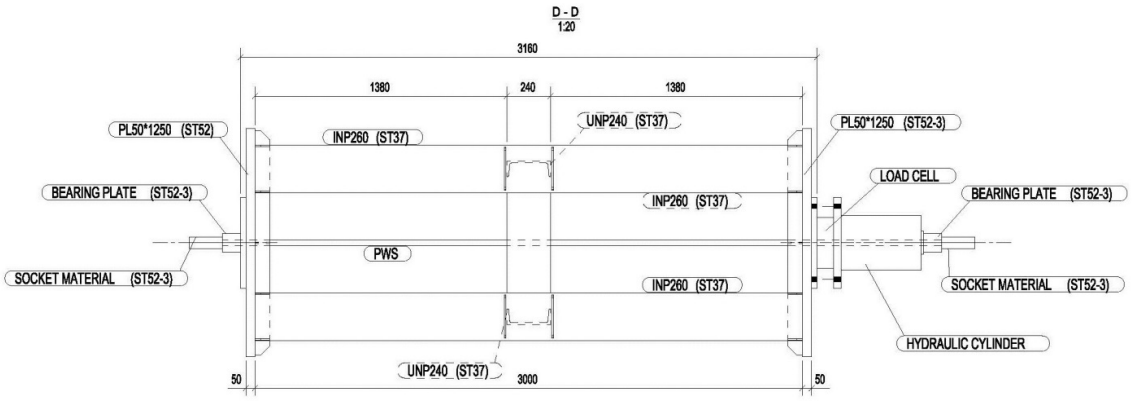

Figure C.1. Steel test frame plan.

Table C.1. Steel test frame part list.

PartPos	**Profile**	**No.**	**Material**	**Length**	**Area (m2)**	**Weight (kg)**
1001	PL50*1250	2	ST52	1250	3.4	613.3
1002	PL8*80	24	ST37	80	0	0.3
1003	PL8*80	8	ST37	820	0.1	4.1
1004	PL8*80	8	ST37	242	0	1.2
1005	PL30*500	1	ST37	500	0.6	58.9
1006	PL10*50	8	ST37	237	0	0.9
1007	PL8*80	4	ST37	552	0.1	2.8
1008	PL8*80	4	ST37	85	0	0.4
1009	PL8*80	8	ST37	550	0.1	2.8
1010	PL30*500	1	ST37	500	0.6	58.9
b/1	UNP240	2	ST37	550	0.4	18.3
b/2	UNP240	2	ST37	924	0.7	30.7
c/2	INP260	4	ST37	3000	2.7	125.5
Total for 76 members:					24.3	2036.8

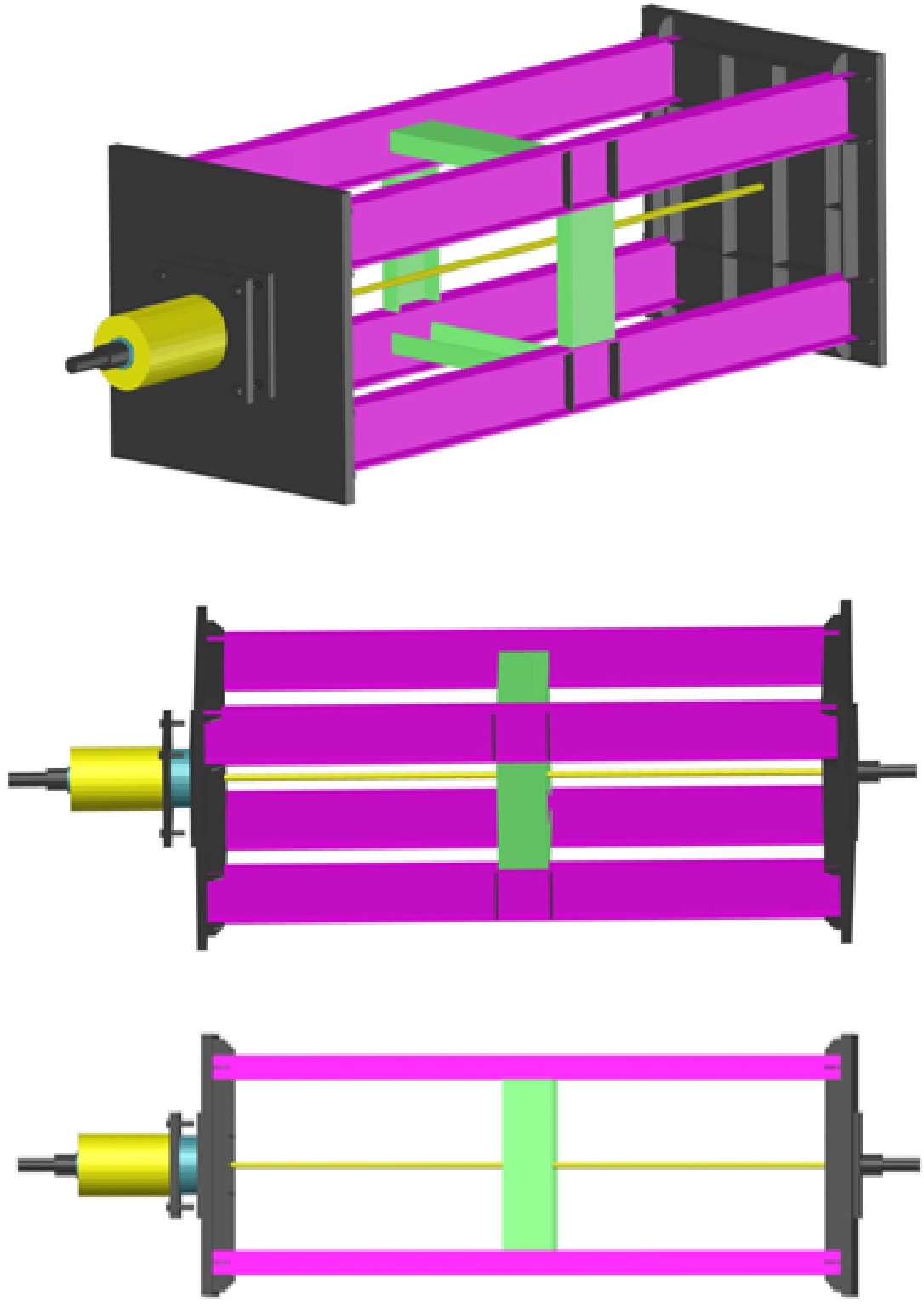

Figure C.2. 3D views of the test system design.

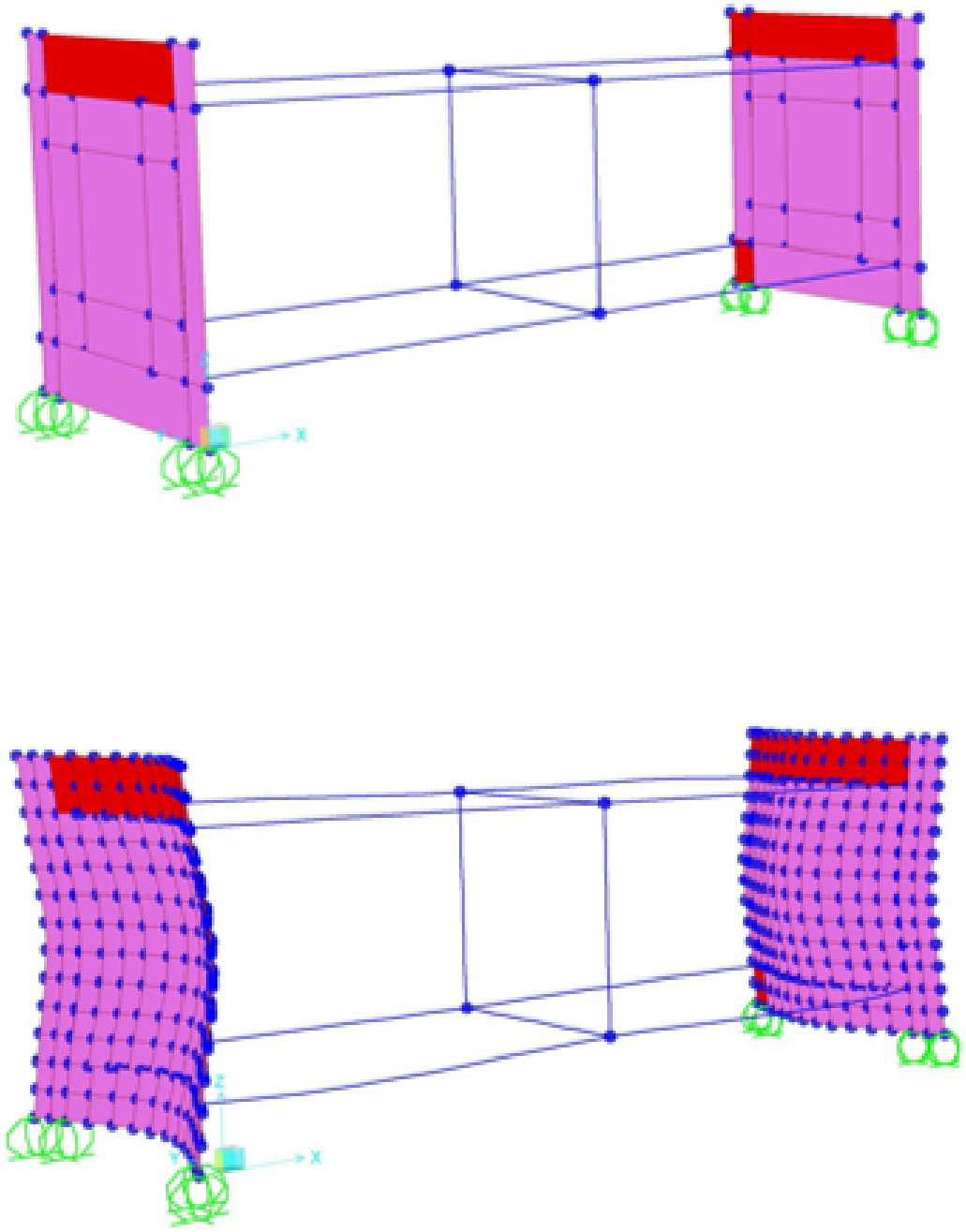

Figure C.3. Design 3D view and deformed shape (SAP 2000).

APPENDIX D: SOCKET LOCKERS

ASİL ÇELİK
SANAYİ ve TİCARET A.Ş.
http://www.asilcelik.com.tr

KALİTE BELGESİ
QUALITY CERTIFICATE /MILL TEST CERTIFICATE

Döküman No / Document Number	Tarih / Date	Sayfa /Page
1507665	01.06.2015	1

Müşteri /Customer	Müşteri Sip. No./ Your Order No	Sip.No./ Our Order No.	Belge Norm/Document Norm	Sip. Miktarı / Order (Kg)
NİHAT UYAR DEMİR ÇELİK SAN.TİC		1711507198	EN 10204/3.1	31000

Kalite / Quality	Kesit / Dimension	Döküm No./ Heat No.	Ağırlık / Weight (Kg)	Adet/Number of pieces
SAE 1045	Y/Rd 150 mm	151702	31200	30

Malzeme / Product

Onaylayan / Approved By
Subutay SEZGİN

VAKUM UYGULAMASI YAPILMIŞTIR.
SICAK BİÇİMLENDİRİLMİŞTİR.
MALZEMELER TAMAMLAMASIZ ÜRETİLMİŞTİR.

Çelik Yapım Metodu / Steelmaking Process : Ark Ocağı / EAF, Pota Fırını / LF, Vakumda Gaz Alma / VD

Pota Kimyasal Analizi / Ladle Chemical Composition (%)

C	Si	Mn	P	S	Cr	Mo	Ni	Al	Cu	Sn
.49	.29	.64	.006	.003	.11	.02	.10	.023	.31	.019

Mekanik Özellikler / Mechanical Properties

Sertlik Hardness
223 HB

H = MAX.2.0 ppm GARANTİ EDİLMİŞTİR.
% 100 KARIŞIKLIK TESTİ YAPILMIŞTIR.
YÜZEY ÇATLAK TESTİ VE ULTRASONİK HATA GARANTİSİ VERİLMEMEKTEDİR.
MALZEMELERE EXPLORIUM AT 900 CİHAZI İLE RADYASYON TESTİ UYGULANMIŞTIR.

KALİTE GÜVENCE
QUALITY ASSURANCE

YUKARIDA BELİRTİLEN MALZEMELERİN TEST EDİLDİĞİ VE SİPARİŞ ŞARTLARINA UYGUN OLDUĞU ONAYLANIR.
WE HEREBY CERTIFY, MATERIAL DESCRIBED ABOVE HAS BEEN TESTED AND COMPLIES WITH THE TERMS OF ORDER CONTRACT.

33.23.169.A4 (1)

Santral / Central
Tel. : +90 224 280 61 00
Faks : +90 224 280 62 00
Fabrika /Head Office & Plant
Gemiç Köyü Mevkii 16800 Orhangazi / BURSA

Satınalma / Purchasing
+90 224 280 61 20
+90 224 280 61 30
Çelik Servis Merkezi / Steel Service Center
TOSB Organize San. Bölg. 13. Sok. No:3 41420
Şekerpınar/KOCAELİ

İç Satış / Domestic Sales
+90 262 781 60 00
+90 262 781 60 05

Dış Satış / Export
+90 262 781 60 00
+90 262 781 60 05

Vergi Dairesi : Büyük Mükellefler Vergi Dairesi Başkanlığı
Vergi No : 0860052518 Ticaret Sicil: 125642 / 72672

Figure D.1. Mill test certificate for socket lockers.

SAKA
KURTULUŞ MAHALLESİ
SANAYİ BÖLGESİ
78200 KARABÜK / TURKEY
Tel:+90 370 413 02 33(Pbx)
Faks: +90 370 424 73 59
e-mail:sakadc@sakadc.com.tr

KALİTE BELGESİ

(QUALITY CERTIFICATE)
www.sakadc.com.tr

TSE TÜV NORD EN ISO 9001:2008

Rapor No : 019330
Report No
Sayfa No :
Page No

MÜŞTERİ / Customer : ÇINARLAR METAL
SEVK / Sending :
TARİH / Date : 17.09.2015

	Kalite (Quality)	Miktar(KG) (Quantity)	Dök.No (Heat Number)	Kimyasal Analizi (Chemical Analysis) , % C	Mn	Si	S	P	Pb	Ni	Mo	Cu	V
26 ÇELİK	1050		524526	,52	,71	,18	,034	,027				,048	
30 ÇELİK	1050		523288	,52	,65	,15	,035	,020				,04	
32 ÇELİK	1050		523288	,52	,65	,15	,035	,020				,04	
35 ÇELİK	1050		514069	,53	,73	,25	,026	,018				,027	
40 ÇELİK	1050		514069	,53	,73	,25	,026	,018				,027	
45 ÇELİK	1050		524526	,52	,71	,18	,034	,027				,048	
55 ÇELİK	1050		524526	,52	,71	,18	,034	,027				,048	
60 ÇELİK	1050		524526	,52	,71	,18	,034	,027				,048	
65 ÇELİK	1050		533892	,49	,74	,20	,039	,030				,035	
70 ÇELİK	1050		533892	,49	,74	,20	,039	,030				,035	
80 ÇELİK	1050		534629	,52	,68	,20	,033	,024				,052	
85 ÇELİK	1050		534629	,52	,68	,20	,033	,024				,052	
90 ÇELİK	1050		534629	,52	,68	,20	,033	,024				,052	
95 ÇELİK	1050		513018	,54	,77	,26	,035	,017				,046	
100 ÇELİK	1050		510976	,48	,69	,22	,025	,021				,044	

1-Bu rapor (iki) 2 nüsha olarak düzenlenmiştir
2-Saka D.Ç A.Ş'nin izni olmadan çoğaltılamaz
3-Bu rapor hukuki işlemlerde kullanılamaz
4-Orijinal kalite belgesi baz alınmıştır.
FR4.04.10 Rev.:1

Kalite Kontrol Müdürü (Y)
Quality Control Manager

Figure D.2. Quality certificate for socket lockers.

APPENDIX E: HOLLOW HYDROLIC CYLINDER

RRH-Series, Hollow Plunger Cylinders

ENERPAC
POWERFUL SOLUTIONS. GLOBAL FORCE.

▼Shown from left to right: **RRH-3010, RRH-1001, RRH-6010**

Versatility in Testing, Maintenance and Tensioning Applications

- **Relief valves prevent damage in case of over-pressurization**
- **Baked enamel finish for increased corrosion resistance**
- **Collar threads enable easy fixturing (except RRH-1001 and RRH-1508)**
- **Double-acting operation for fast retraction**
- **Nickel-plated, floating center tube increases product life**
- **Hollow plunger allows for both pull and push forces**
- **CR-400 couplers and dust caps included on all models**
- **Plunger wiper reduces contamination, extending cylinder life**

Pump Selection
A double-acting cylinder must be powered by a pump with a 4-way valve.
Page: 57

Gauges
Minimize the risk of overloading and ensure long, dependable service from your equipment. Refer to the System Components section for a full range of gauges.
Page: 113

Saddles
All RRH-Series cylinders are equipped with smooth saddles. See table on next page for optional threaded saddles and all dimensional information.
Page: 29

▼*Double-acting hollow plunger cylinders are applied for bridge launching systems.*

Cylinder Capacity (ton)	Stroke (in)	Model Number	Max. Cylinder Capacity (ton)		Cylinder Effective Area (in²)		Oil Capacity (in³)	
			Advance	Retract	Advance	Retract	Advance	Retract
30	7.00	RRH-307	36	24	7.22	4.71	50.55	32.99
	10.13	RRH-3010	36	24	7.22	4.71	73.12	47.71
60	3.50	RRH-603	64	42	12.73	8.37	44.57	29.21
	6.50	RRH-606	64	42	12.73	8.37	82.77	54.24
	10.12	RRH-6010	64	42	12.73	8.37	128.94	84.49
100	1.50	RRH-1001	103	68	20.63	13.54	30.94	20.32
	3.00	RRH-1003	103	68	20.63	13.54	61.88	40.64
	6.00	RRH-1006	103	68	20.63	13.54	123.76	81.29
	10.13	RRH-10010	103	68	20.63	13.54	208.84	137.17
150	8.00	RRH-1508	158	80	31.62	15.91	252.97	127.23

Figure E.1. Technical specifications for hydrolic cylinder (pg1).

Double-Acting, Hollow Plunger Cylinders

Hoses

Enerpac offers a complete line of high quality hydraulic hoses. To ensure the integrity of your system, specify only Enerpac hydraulic hoses.

Page: 114

RRH Series

Capacity:
30-150 tons

Stroke:
1.50-10.13 inches

Center Hole Diameter:
1.31-3.13 inches

Maximum Operating Pressure:
10,000 psi

Optional Heat Treated Saddles						
Saddle Type	Cylinder Model Number	Saddle Model No.	Saddle Dimensions (in) A	B	C	
Threaded Hollow	RRH-307, 3010	HP-3015	2.49	1¼"-7	.38	
	RRH-603, 606, 6010	HP-5016	3.61	1⅝"-5½	.50	
	RRH-1001, 1003, RRH-1006, 10010	HP-10016	4.97	2½"-8	.51	

Smooth hollow saddles are standard on all RRH-models.

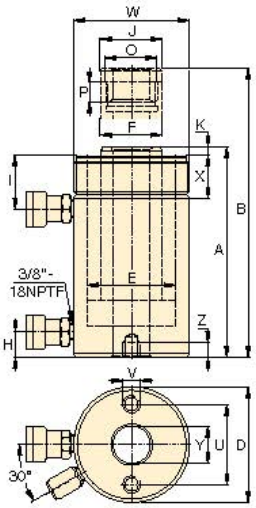

Base Mounting Hole Dimensions (in)			
Model Number	Bolt Circle U	Thread V	Thread Depth Z
RRH-307	3.63	⅜"- 16	.62
RRH-3010	3.63	⅜"- 16	.62
RRH-603	5.12	½"- 13	.55
RRH-606	5.12	½"- 13	.55
RRH-6010	5.12	½"- 13	.55
RRH-1001	7.00	⅝"- 11	.75
RRH-1003	7.00	⅝"- 11	.75
RRH-1006	7.00	⅝"- 11	.75
RRH-10010	7.00	⅝"- 11	.75
RRH-1503	–	–	–

	Collap. Height A (in)	Ext. Height B (in)	Out. Diam. D (in)	Cyl. Bore Diam. E (in)	Plngr. Diam. F (in)	Cyl. Base to Adv. Port H (in)	Cyl. Top to Return Port I (in)	Saddle Diam. J (in)	Saddle Protrusion from Plngr. K (in)	Thread O (in)	Plunger Thread Length P (in)	Collar Thread W (in)	Collar Thread Length X (in)	Center Hole Diam. Y (in)	Wt. (lbs)	Model Number
	13.00	20.00	4.50	3.50	2.50	1.00	2.38	2.50	.38	1⅝"-16	.88	4½"-12	1.66	1.31	48	RRH-307
	17.00	27.13	4.50	3.50	2.50	1.00	2.38	2.50	.38	1⅝"-16	.88	4½"-12	1.66	1.31	60	RRH-3010
	9.75	13.25	6.25	4.88	3.63	1.25	2.63	3.61	.50	2¾"-16	.75	6¼"-12	1.91	2.13	62	RRH-603
	12.75	19.25	6.25	4.88	3.63	1.25	2.63	3.61	.50	2¾"-16	.75	6¼"-12	1.91	2.13	78	RRH-606
	17.25	27.38	6.25	4.88	3.63	1.25	2.63	3.61	.50	2¾"-16	.75	6¼"-12	1.91	2.13	101	RRH-6010
	6.50	8.00	8.38	6.50	5.00	1.50	1.75	4.97	.50	4"-16	1.00	–	–	3.13	85	RRH-1001
	10.00	13.00	8.38	6.50	5.00	1.50	3.38	4.97	.50	4"-16	1.00	8⅜"-12	2.38	3.13	135	RRH-1003
	13.50	19.50	8.38	6.50	5.00	1.50	3.38	4.97	.50	4"-16	1.00	8⅜"-12	2.38	3.13	175	RRH-1006
	18.13	28.25	8.38	6.50	5.00	1.50	3.38	4.97	.50	4"-16	1.00	8⅜"-12	2.38	3.13	235	RRH-10010
	13.75	21.75	9.75	7.50	6.00	1.50	2.38	5.00	.19	4¼"-12	1.00	–	–	3.13	245	RRH-1503

Figure E.2. Technical specifications of hydrolic cylinder (pg2).

APPENDIX F: PAN CAKE LOAD CELL (100TF)

LS / LSU Pan cake load cell, 1tf - 100tf

Load Cell

FEATURES

- Hermetically sealed
- High reliability against fatigue and side force

OPTIONS

- High accuracy grade

SPECIFICATIONS

Max. capacity	tf	1,2,3,5,10,20,30,50(LSU),100(LSU),200(LSU)	
Rated output	mV/V	2.0 ±0.005	
Zero balance	mV/V	0 ±0.02	
Accuracy class		A	B
Combined error	%	0.02	0.05
Repeatability	%	0.01	0.02
Creep for 30min.	%	0.03	0.03
Temperature effection			
Zero Value	%/10℃	0.03	0.03
Output value	%/10℃	0.03	0.03
Excitation			
Recommended	V	10	
Maximum	V	15	
Resistance			
Input	Ω	350 ±3.5	
Output	Ω	350 ±3.5	
Insulation	MΩ	> 2000	
Compensated temperature range	℃	-10 to +40	
Operating temperature range	℃	-20 to +80	

DIMENSIONS

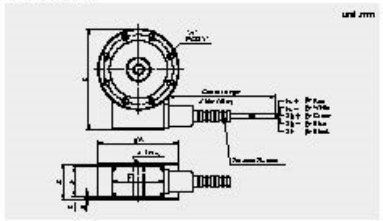

Material
Palt finished steel

Cable
Braided shield 4-wire round cable with P.V.C-jacket

Model	Capacity	A	B	C	D	E	F	G	H	I	J	K
LS-1	1tf	112	ø6	4	1	38	68	141.5	8 - ø5.6	57.2	M16 ×2.0	9m
LS-2	2tf											
LS-3	3tf	112	ø6	4	1	38	68	141.5	8 - ø5.6	57.2	M16 ×2.0	
LS-5	5tf	120	ø6	4	1	38	68	149.5	8 - ø9	103.2	M18 ×1.5	
LS-10	10tf	138	60	11	1	38	68	167.5	8 - ø11	117.6	M24 ×2.0	
LS-20	20tf	184	80	21	1	38	68	213.5	8 - ø14	157.6	M39 ×2.0	10m
LS-30	30tf											
LSU-50	50tf	200	60	11	1	38	68	229.5	12 - ø14.3	170	M45 ×3.0	
LSU-100	100tf	278	90	31	1	38	68	307.5	16 - ø16.3	229	M70 ×3.0	
LSU-200	200tf	366	108	36	1	38	68	394.5	12 - ø35	298	M90 ×3.0	

Figure F.1. Technical specifications for load cell.

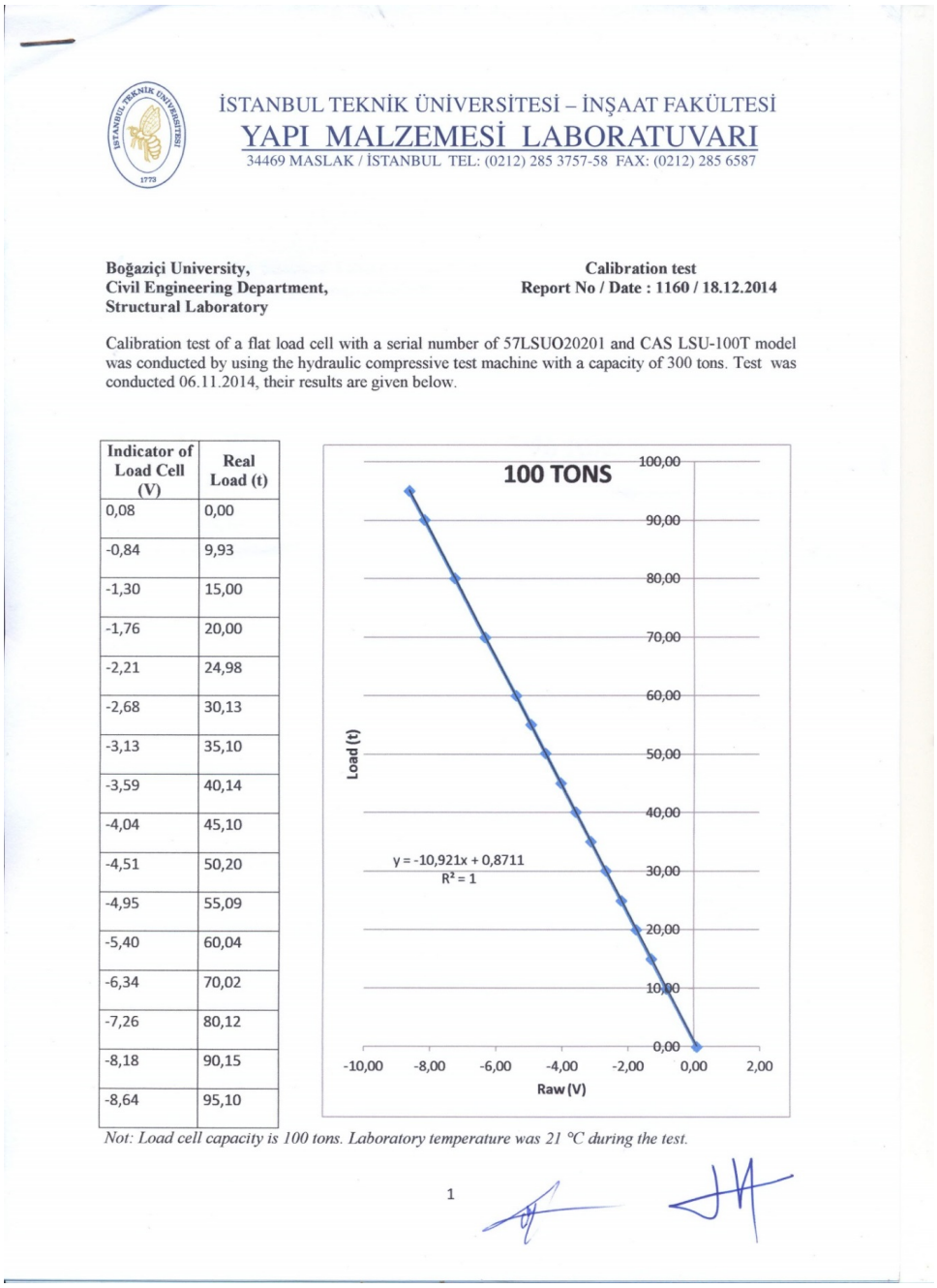

İSTANBUL TEKNİK ÜNİVERSİTESİ – İNŞAAT FAKÜLTESİ
YAPI MALZEMESİ LABORATUVARI
34469 MASLAK / İSTANBUL TEL: (0212) 285 3757-58 FAX: (0212) 285 6587

Boğaziçi University,
Civil Engineering Department,
Structural Laboratory

Calibration test
Report No / Date : 1160 / 18.12.2014

Calibration test of a flat load cell with a serial number of 57LSUO20201 and CAS LSU-100T model was conducted by using the hydraulic compressive test machine with a capacity of 300 tons. Test was conducted 06.11.2014, their results are given below.

Indicator of Load Cell (V)	Real Load (t)
0,08	0,00
-0,84	9,93
-1,30	15,00
-1,76	20,00
-2,21	24,98
-2,68	30,13
-3,13	35,10
-3,59	40,14
-4,04	45,10
-4,51	50,20
-4,95	55,09
-5,40	60,04
-6,34	70,02
-7,26	80,12
-8,18	90,15
-8,64	95,10

Not: Load cell capacity is 100 tons. Laboratory temperature was 21 °C during the test.

1

Figure F.2. Calibration test report for load cell.

APPENDIX G: LINEAR POTENTIOMETER

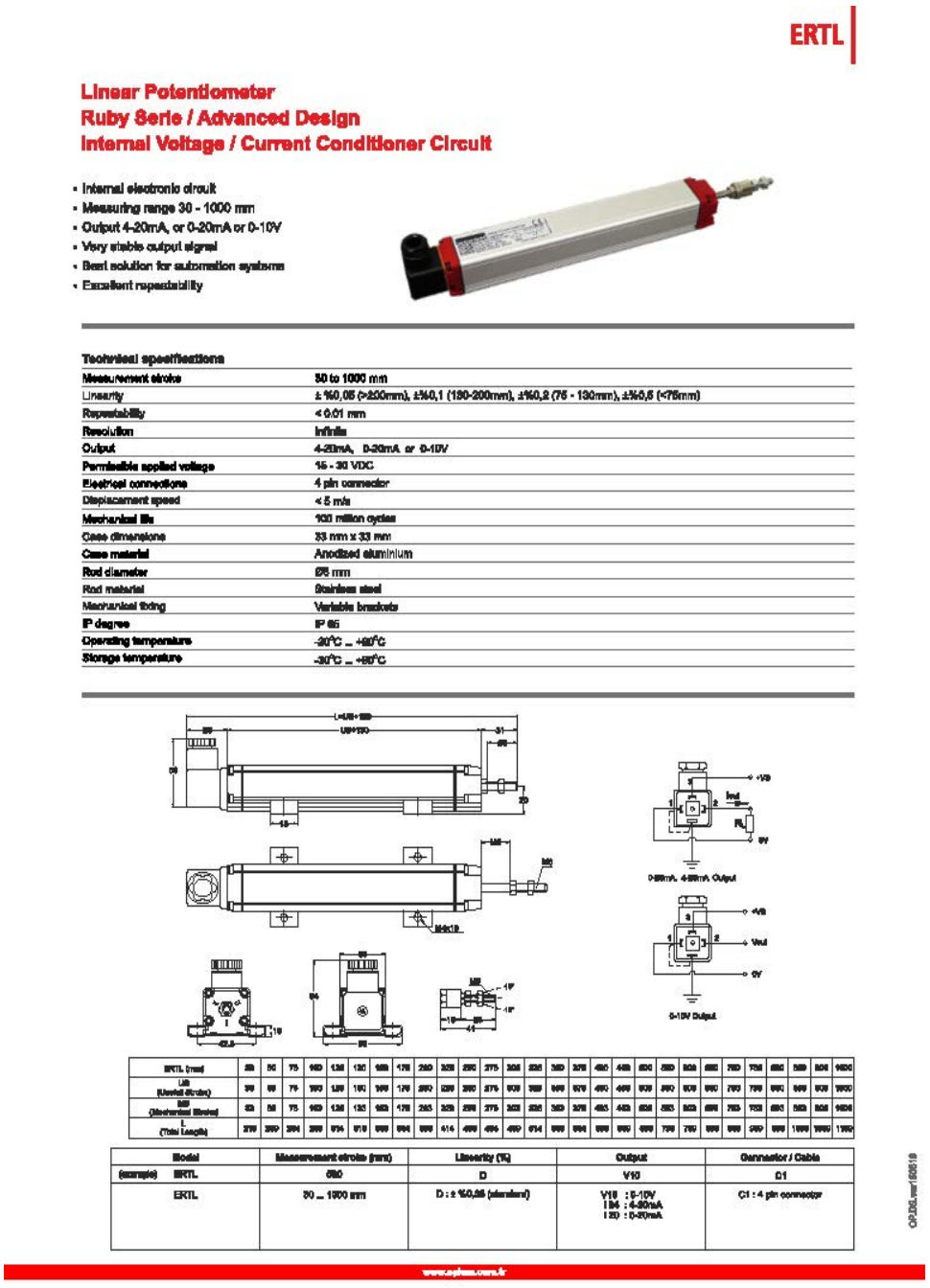

ERTL

Linear Potentiometer
Ruby Serie / Advanced Design
Internal Voltage / Current Conditioner Circuit

- Internal electronic circuit
- Measuring range 30 - 1000 mm
- Output 4-20mA, or 0-20mA or 0-10V
- Very stable output signal
- Best solution for automation systems
- Excellent repeatability

Technical specifications	
Measurement stroke	30 to 1000 mm
Linearity	± %0,05 (>200mm), ±%0,1 (130-200mm), ±%0,2 (75 - 130mm), ±%0,5 (<75mm)
Repeatability	< 0.01 mm
Resolution	Infinite
Output	4-20mA, 0-20mA or 0-10V
Permissible applied voltage	15 - 30 VDC
Electrical connections	4 pin connector
Displacement speed	< 5 m/s
Mechanical life	100 million cycles
Case dimensions	33 mm x 33 mm
Case material	Anodized aluminium
Rod diameter	Ø6 mm
Rod material	Stainless steel
Mechanical fixing	Variable brackets
IP degree	IP 65
Operating temperature	-20°C ... +80°C
Storage temperature	-30°C ... +85°C

ERTL (mm)	30	50	75	100	125	150	175	200	225	250	275	300	325	350	375	400	425	450	475	500	525	550	575	600	625	650	675	700	725	750	775	800	825	850	875	900	925	950	975	1000
LM (Useful Stroke)	50	60	75	100	125	150	175	200	225	250	275	300	325	350	375	400	425	450	475	500	525	550	575	600	625	650	675	700	725	750	775	800	825	850	875	900	925	950	975	1000
MM (Mechanical Stroke)	60	80	75	100	125	150	175	200	225	250	275	300	325	350	375	400	425	450	475	500	525	550	575	600	625	650	675	700	725	750	775	800	825	850	875	900	925	950	975	1000
L (Total Length)	270	290	304	329	354	379	404	429	454	479	504	529	554	579	604	629	654	679	704	729	754	779	804	829	854	879	904	929	954	979	1004	1029	1054	1079	1104	1129	1154	1179	1204	1229

Model	Measurement stroke (mm)	Linearity (%)	Output	Connector / Cable
(example) ERTL	500	D	V10	C1
ERTL	30 ... 1000 mm	D : ± %0,05 (standard)	V10 : 0-10V I04 : 4-20mA I20 : 0-20mA	C1 : 4 pin connector

www.ertlsensors.ir

Figure G.1. Technical specifications for linear potentiometer.

APPENDIX H: TECHNICAL DATA SHEET FOR FILAMENT TAPE

Scotch® **3M**

Bi-Directional Filament Tape

8959

Technical Data **March, 2003**

Product Description

Scotch® Filament Tape 8959 is a bi-directional specialty packaging tape reinforced with continuous glass yarns in both the longitudinal and transverse direction along with a biaxially oriented polypropylene backing. The polypropylene backing provides good abrasion, moisture and scuff resistance. The adhesive is specifically formulated to provide good adhesion to a wide variety of surfaces including metallic, plastic, and fiberboard.

Construction

Backing	Adhesive	Reinforcement	Backing Color
3M™ Scotchpro™ film	Pressure sensitive synthetic rubber resin	Bi-directional glass yarn	Clear

Typical Physical Properties

Note: The following technical information and data should be considered representative or typical only, and should not be used for specification purposes.

		ASTM Test Method
Adhesion to Steel:	100 oz./in. width (109 N/100 mm width)	D-3330
Tensile Strength:	150 lbs./in. width (2600 N/100 mm width)	D-3759
Elongation at Break:	6%	D-3759
Total Thickness:	5.7 mil (0.14 mm)	D-3652

Features

- High cross-direction tensile strength.
- Allows printing and illustrations to be seen through the tape.
- Excellent shear and initial adhesion.
- Excellent aging.
- Protection of filaments and adhesive to provide longer package life.
- Performs better than paper backings when exposed to outdoor and humid environments.
- Resists center seams slitting in both machine and cross direction, increasing the performance of the tape.
- Excellent holding power under wide range of application conditions with minimum amount of tape.
- Hold with minimum rubdown, doesn't require water to activate.
- Boxes remain closed for long periods of time.

Figure H.1. TDS for filament tape (pg1).

Scotch® Bi-Directional Filament Tape
8959

Available Sizes	Standard Widths:	.75 in. (19 mm), .98 in. (25 mm), 2.0 in. (50 mm), 3.0 in. (75 mm)
	Core Size (ID):	3 in. (76.2 mm)
	Lengths:	60 yds. (50 m)

Application Techniques

An extensive line of application equipment is available including portable hand-held dispensers and stationary definite-length dispensers. Application of Scotch® Filament Tape 8959 is most easily accomplished at room temperature. At colder tempertures, approaching 32°F (0°C), the adhesive becomes firm. Once applied, Scotch® Tape 8959 performs well throughout the normal temperature ranges typically encountered by packaged products in shipping and storage environments.

Storage Conditions

Store behind present stock. Store in a clean, dry place. Temperature of 40-80°F (4-26°C) and 40-50% relative humidity are recommended. Rotate your stock.

Precautionary Information

Refer to Product Label and Material Safety Data Sheet for health and safety information before using this product. For additional health and safety information, call 1-800-364-3577 or (651) 737-6501.

For Additional Information

To request additional product information or to arrange for sales assistance, call toll free 1-800-362-3550 or visit www.3M.com/packaging. Address correspondence to: 3M Industrial Adhesives and Tapes Division, Building 21-1W-10, 900 Bush Avenue, St. Paul, MN 55106. Our fax number is 651-733-9175. In Canada, phone: 1-800-364-3577. In Puerto Rico, phone: 1-787-750-3000. In Mexico, phone: 52-70-04-00.

Important Notice

3M MAKES NO WARRANTIES, EXPRESS OR IMPLIED, INCLUDING, BUT NOT LIMITED TO, ANY IMPLIED WARRANTY OF MERCHANTABILITY OR FITNESS FOR A PARTICULAR PURPOSE. User is responsible for determining whether the 3M product is fit for a particular purpose and suitable for user's application. Please remember that many factors can affect the use and performance of a 3M product in a particular application. The materials to be bonded with the product, the surface preparation of those materials, the product selected for use, the conditions in which the product is used, and the time and environmental conditions in which the product is expected to perform are among the many factors that can affect the use and performance of a 3M product. Given the variety of factors that can affect the use and performance of a 3M product, some of which are uniquely within the user's knowledge and control, it is essential that the user evaluate the 3M product to determine whether it is fit for a particular purpose and suitable for the user's application.

Limitation of Remedies and Liability

If the 3M product is proved to be defective, THE EXCLUSIVE REMEDY, AT 3M'S OPTION, SHALL BE TO REFUND THE PURCHASE PRICE OF OR TO REPAIR OR REPLACE THE DEFECTIVE 3M PRODUCT. 3M shall not otherwise be liable for loss or damages, whether direct, indirect, special, incidental, or consequential, regardless of the legal theory asserted, including, but not limited to, contract, negligence, warranty, or strict liability.

ISO 9002

This Industrial Adhesives and Tapes Division product was manufactured under a 3M quality system registered to ISO 9002 standards.

3M

Industrial Business
Industrial Adhesives and Tapes Division
3M Center, Building 21-1W-10, 900 Bush Avenue
St. Paul, MN 55106

Recycled Paper
40% pre-consumer
10% post-consumer

Printed in U.S.A.
 70-0710-0233-4 (3/03)

Figure H.2. TDS for filament tape (pg2).

APPENDIX I: KLEBEPASTE SB (CERAMIC FIBRE BLANKET ADHESIVE)

PRODUCT INFORMATION

ADHESIVES	KLEBEPASTE SB

Product Description

Klebepaste SB is an all-purpose, cold-setting adhesive based on aluminum silicates and waterglass, and exhibits outstanding long-term adhesion and high strength.

Applications

Klebepaste SB is used to bond cold or hot core and mold halves, to assemble complex core packets, and to repair broken pieces of cores and molds. After standing for two to three hours, parts assembled with this adhesive automatically develop an excellent bond. Post-drying is unnecessary. The adhesive bonds reach their peak strength levels after approx. 24 hours.

Typical Data

Viscosity	**(20 °C)**	**:**	**68 - 76 Pa . s**
Tensile strength		**:**	**> 500 N/cm^2**
Test pieces		**:**	**DIN 52404**
Storage life		**:**	**Six months when protected against frost and exposure to air**
Delivery form		**:**	**In tubular bags, tubes, pails and small drums**

Processing

Klebepaste SB is applied manually, from tubular bags, or mechanically. Tubular bags have the advantage that they permit sparing use of the product, and simultaneously keep it fresh, thus preventing crusting of the adhesive.

17 2 / 0798

Figure I.1. Product information for Klebepaste SB (ceramic fibre adhesive).

APPENDIX J: CERAMIC FIBRE BLANKET (TR)

ravaber	TEKNİK BİLGİ DÖKÜMANI			
	RAVABER SERAMİK YÜNÜ BATTANİYE			
ÖZELLİKLER	SEMBOL	BİRİM	TOLERANSLAR	
Malzeme	MW			SERAMİK YÜNÜ
Yoğunluk	d	kg/m³	(+,-)% 10	**128**
Uzunluk Toleransı	l	mm	(+,-) %2	7200
Genişlik Toleransı	b	mm	(+,-) %1,5	610
Kalınlık	d_N	mm	(- 1, +3)	**25**

Kimyasal Analizleri:	RAVABER 1260 STD	ÜRÜN ÖZELLİKLERİ	
Na_2O (Sodyum Oksit)	**%1.38**	Maksimum Kullanım Sıcaklığı	1260 °C
MgO (Magnezyum Oksit)	**%0.69**	Elyaf Uzunluğu (mm)	13-100
Al_2O_3 (Aluminyum Oksit)	**%41.42**	400°C ısı iletkenlik (W/m.K)	0,090
SiO_2 (Silisyumdi Oksit)	**%52.19**	500°C ısı iletkenlik (W/m.K)	0,119
ZrO_2 (Zirkonyum Oksit)	**% 0.13**	600°C ısı iletkenlik (W/m.K)	0,152
CaO (Kalsiyum Oksit)	**1%**	Renk	Beyaz
Sertifikalar	**ISO 9001,ISO 14001,ISO 18001,ISO 50001,ISO10002 sertifiklarına sahip tesislerde üretilmiştir.**		
Ürün anahtarı	Ürünümüz RoHS belgesine saahiptir.		

Figure J.1. TDS for ceramic fibre blanket (turkish version).